

# «ELECTRICAL ENGINEERING & ELECTROMECHANICS»

SCIENTIFIC & PRACTICAL JOURNAL

Journal was founded in 2002 by

National Technical University «Kharkiv Polytechnic Institute»

Co-Founder – State Institution «Institute of Technical Problems of Magnetism of the NAS of Ukraine»



## INTERNATIONAL EDITORIAL BOARD

- Klymenko B.V.** Editor-in-Chief, Professor, National Technical University "Kharkiv Polytechnic Institute" (NTU "KhPI"), Ukraine  
**Sokol Ye.I.** Deputy Editor, Professor, Corresponding member of NAS of Ukraine, rector of NTU "KhPI", Ukraine  
**Rozov V.Yu.** Deputy Editor, Professor, Corresponding member of NAS of Ukraine, Director of State Institution "Institute of Technical Problems of Magnetism of the NAS of Ukraine"(SI "ITPM NASU"), Kharkiv, Ukraine
- Batygin Yu.V.** Professor, Kharkiv National Automobile and Highway University, Ukraine  
**Bíró O.** Professor, Institute for Fundamentals and Theory in Electrical Engineering, Graz, Austria  
**Bolyukh V.F.** Professor, NTU "KhPI", Ukraine  
**Doležel I.** Professor, University of West Bohemia, Pilsen, Czech Republic  
**Féliachi M.** Professor, University of Nantes, France  
**Gurevich V.I.** Ph.D., Honorable Professor, Central Electrical Laboratory of Israel Electric Corporation, Haifa, Israel  
**Kildishev A.V.** Associate Research Professor, Purdue University, USA  
**Kuznetsov B.I.** Professor, SI "ITPM NASU", Kharkiv, Ukraine  
**Kyrylenko O.V.** Professor, Member of NAS of Ukraine, Institute of Electrodynamics of NAS of Ukraine, Kyiv, Ukraine  
**Podoltsev A.D.** Professor, Institute of Electrodynamics of NAS of Ukraine, Kyiv, Ukraine  
**Rainin V.E.** Professor, Moscow Power Engineering Institute, Russia  
**Rezynkina M.M.** Professor, SI "ITPM NASU", Kharkiv, Ukraine  
**Rozanov Yu.K.** Professor, Moscow Power Engineering Institute, Russia  
**Shkolnik A.A.** Ph.D., Central Electrical Laboratory of Israel Electric Corporation, member of CIGRE (SC A2 - Transformers), Haifa, Israel  
**Yufarov V.B.** Professor, National Science Center "Kharkiv Institute of Physics and Technology", Ukraine  
**Vinitzki Yu.D.** Professor, GE EEM, Moscow, Russia  
**Zagirnyak M.V.** Professor, Corresponding member of NAES of Ukraine, rector of Kremenchuk M.Ostrohradskyi National University, Ukraine  
**Zgraja J.** Professor, Institute of Applied Computer Science, Lodz University of Technology, Poland

## НАЦІОНАЛЬНА РЕДАКЦІЙНА КОЛЕГІЯ\*

- Клименко Б.В.** головний редактор, професор, НТУ "ХПІ"  
**Сокол Є.І.** заступник головного редактора, член-кор. НАНУ, ректор НТУ "ХПІ"  
**Розов В.Ю.** заступник головного редактора, член-кор. НАНУ, директор ДУ "ІТПМ НАНУ"  
**Гречко О.М.** відповідальний секретар, к.т.н., НТУ "ХПІ"  
**Баранов М.І.** д.т.н., НДПКи "Молнія" НТУ "ХПІ"  
**Боев В.М.** професор, НТУ "ХПІ"  
**Веприк Ю.М.** професор, НТУ "ХПІ"  
**Гриб О.Г.** професор, НТУ "ХПІ"  
**Гурин А.Г.** професор, НТУ "ХПІ"  
**Данько В.Г.** професор, НТУ "ХПІ"  
**Жемеров Г.Г.** професор, НТУ "ХПІ"  
**Клепиков В.Б.** професор, НТУ "ХПІ"  
**Кравченко В.І.** професор, директор НДПКи "Молнія" НТУ "ХПІ"  
**Міліх В.І.** професор, НТУ "ХПІ"  
**Михайлов В.М.** професор, НТУ "ХПІ"  
**Омельяненко В.І.** професор, НТУ "ХПІ"  
**Пуйло Г.В.** професор, ОНТУ, Одеса  
**Резинкін О.Л.** професор, НТУ "ХПІ"  
**Сосков А.Г.** професор, ХНУМГ імені О.М. Бекетова, Харків  
**Ткачук В.І.** професор, НУ "Львівська Політехніка"  
**Шинкаренко В.Ф.** професор, Національний технічний університет України "Київський політехнічний інститут"

\* Члени національної редакційної колегії працюють у провідних українських наукових, освітніх та дослідницьких установах

## NATIONAL EDITORIAL BOARD\*

- Klymenko B.V.** Editor-in-Chief, professor, NTU "KhPI"  
**Sokol Ye.I.** Deputy Editor, corresponding member of NAS of Ukraine, rector of NTU "KhPI"  
**Rozov V.Yu.** Deputy Editor, corresponding member of NAS of Ukraine, Director of SI "ITPM NASU"  
**Grechko O.M.** Executive Managing Editor, Ph.D., NTU "KhPI"  
**Baranov M.I.** Dr.Sc. (Eng.), NTU "KhPI"  
**Boev V.M.** Professor, NTU "KhPI"  
**Vepryk Yu.M.** Professor, NTU "KhPI"  
**Gryb O.G.** Professor, NTU "KhPI"  
**Guryn A.G.** Professor, NTU "KhPI"  
**Dan'ko V.G.** Professor, NTU "KhPI"  
**Zhemerov G.G.** Professor, NTU "KhPI"  
**Klepikov V.B.** Professor, NTU "KhPI"  
**Kravchenko V.I.** Professor, NTU "KhPI"  
**Milykh V.I.** Professor, NTU "KhPI"  
**Mikhaylov V.M.** Professor, NTU "KhPI"  
**Omel'yanenko V.I.** Professor, NTU "KhPI"  
**Puilo G.V.** Professor, Odessa National Polytechnic University  
**Rezynkin O.L.** Professor, NTU "KhPI"  
**Soskov A.G.** Professor, O.M. Beketov National University of Urban Economy in Kharkiv  
**Tkachuk V.I.** Professor, Lviv Polytechnic National University  
**Shynkarenko V.F.** Professor, National Technical University of Ukraine "Kyiv Polytechnic Institute"

\* Members of National Editorial Board work in leading Ukrainian scientific, educational and research institutions

## Адреса редакції / Editorial office address:

Кафедра "Електричні апарати", НТУ "ХПІ", вул. Кирпичова, 21, м. Харків, 61002, Україна  
Dept. of Electrical Apparatus, NTU "KhPI", Kyrpychova Str., 21, Kharkiv, 61002, Ukraine

тел. / phone: +380 57 7076281, +380 67 3594696, e-mail: a.m.grechko@gmail.com (Гречко Олександр Михайлович / Grechko O.M.)

ISSN (print) 2074-272X

© National Technical University «Kharkiv Polytechnic Institute», 2016

ISSN (online) 2309-3404

© State Institution «Institute of Technical Problems of Magnetism of the NAS of Ukraine», 2016

Printed 24.10.2016. Format 60 x 90 1/8. Paper – offset. Laser printing.

Edition 200 copies. Order no.66/172-05-2016.

Design of cover by Vyrovets L.P. e-mail: vsv\_2007@ukr.net

Printed by Printing house «Madrid Ltd» (11, Maksymilianivska Str., Kharkiv, 61024, Ukraine)



---

**2016/5**

**TABLE OF CONTENTS**

***Electrical Engineering. Great Events. Famous Names***

**Baranov M.I.** An anthology of the distinguished achievements in science and technique. Part 34: Discovery and study of quantum-wave nature of microscopic world of matter ..... 3

***Electrical Machines and Apparatus***

**Milykh V.I.** The numerical-field analysis of the magnetic field and the electrical quantities in the turbogenerator stator under autonomous unbalanced loading ..... 16

***Electrotechnical Complexes and Systems. Power Electronics***

**Polyakov M.A., Larionova T.Y.** Efficiency evaluation technique of the semiconductor DC-DC converter application in the power-supply system ..... 23

***Theoretical Electrical Engineering and Electrophysics***

**Baranov M.I., Rudakov S.V.** Average geometrical features of the electron wave packages distribution in metallic conductors with pulsed axial current of high density ..... 29

***High Electric and Magnetic Field Engineering. Cable Engineering***

**Batygin Yu.V., Chaplygin E.A., Sabokar O.S.** Magnetic pulsed processing of metals for advanced technologies of modernity – a brief review ..... 35

**Beliaev V.K., Panenko H.N.** Determination of insulation parameters of current transformers at multiple measurements in monitoring systems under working voltage..... 40

**Golik O.V.** Statistical procedures for two-sided limit of a controlled parameter in the process of production of cable and wire products..... 47

**Rudakov V.V., Korobko A.A.** A high sensitive microwave measuring device of the moisture content in the non-polar dielectric liquids based on an inhomogeneous step coaxial resonator..... 51

**Shalamov S.P.** An induction sensor for measuring currents of nanosecond range ..... 57

***Power Stations, Grids and Systems***

**Voloshko A.V., Bederak Ya.S.** A method of automatic determination of the number of the electrical motors simultaneously working in group ..... 61

**Olszowiec P.** Low voltage networks insulation monitoring with two and three voltmeter readouts methods ..... 64

**Rudenko S.S.** Requirements for devices for vertical electrical sounding of soil at diagnostics of grounding devices..... 68

M.I. Baranov

**AN ANTHOLOGY OF THE DISTINGUISHED ACHIEVEMENTS IN SCIENCE AND TECHNIQUE. PART 34: DISCOVERY AND STUDY OF QUANTUM-WAVE NATURE OF MICROSCOPIC WORLD OF MATTER**

*Purpose. Implementation of brief analytical review of the basic distinguished scientific achievements of the world scientists-physicists in area of discovery and study of quantum-wave nature of physical processes and phenomena flowing in the microscopic world of circumferential people matter. Methodology. Scientific methods of collection, analysis and analytical treatment of scientific and technical information in area of theoretical and experimental physics, devoted the results of researches of quantum and physical processes flowing in nature on atomic and subatomic levels. Results. The brief scientific and technical review of the basic scientific discovery and achievements of scientists-physicists is resulted in area of structure of atom of matter, generation, radiation, distribution and absorption of physical bodies of short-wave hertzian waves, indicative on a dominating role in the microscopic financial world of positions and conformities to the law of wave (by quantum) mechanics, carrying especially probabilistic character a microstructure. Originality. Systematization is executed with exposition in the short concentrated form of the known materials on the quantum theory (electromagnetic) of caloradiance, quantum theory of atom, electronic waves, quantum theory of actinoelectricity, quantum statistics of microparticless, quantum theory of the phenomenon superfluidity of liquid helium, quantum electronics and quantum-wave nature of drift of lone electrons in the metal of explorers with an electric current. Practical value. Popularization and deepening of fundamental physical and technical knowledges for students and engineer and technical specialists in area of classic and quantum physics, extending their scientific range of interests, and also support a further scientific study by them surrounding nature and to development of scientific and technical progress in society. References 27, figures 15.*

*Key words: quantum theory of thermal radiation, quantum theory of atom, electron waves, quantum theory of photoelectric effect, quantum statistics of microparticles, quantum theory of the phenomena of superfluidity of helium, quantum electronics, quantum wave nature of the drift of electrons in metal, review.*

*Приведен краткий аналитический обзор основных научных достижений ученых в области открытия и изучения квантово-волновой природы физических процессов и явлений, протекающих в микромире окружающей нас материи. В число таких достижений вошли как ставшие классическими квантовые теории теплового излучения абсолютно черного тела, атома, фотоэлектрического эффекта и явления сверхтекучести жидкого гелия, так и современные открытия в области квантовой электроники и новейшие квантовомеханические результаты для дрейфа свободных электронов и их волновых распределений в проводниках электрических цепей с током. Библ. 27, рис. 15.*

*Ключевые слова: квантовая теория теплового излучения, квантовая теория атома, электронные волны, квантовая теория фотоэффекта, квантовая статистика микрочастиц, квантовая теория явления сверхтекучести гелия, квантовая электроника, квантово-волновая природа дрейфа электронов в металле, обзор.*

**Introduction.** In the process of cognition of the surrounding nature people accumulate a certain «baggage» (margin) of scientific and technical knowledge, we have understood that humanity is interesting and important for their life living on Earth, and the constant time-development of industrial production and a variety of advanced technologies not only the macrocosm but microcosm defining occurrence in nature the various physico-chemical and biological processes and the macroscopic properties of matter. It is necessary to remind the reader that, according modern ideas about the structure of matter at the microcosm is understood as set placed in a vacuum of material objects (bodies) with linear dimensions of 10 nm or less [1]. Therefore, practically since the end of the 19th century, physicists and chemists in the extent of its theoretical possibilities and means at their disposal physical and chemical tools have been actively engaged in the study of microscopic properties of matter and at the same time opening new physical and chemical phenomena. The first in a series of similar discoveries was the discovery of outstanding

German experimental physicist Wilhelm Roentgen (1845-1923) in 1895 receiving in the near future the name «X-rays» and marked one of the first Nobel Prizes in physics for 1901 [2, 3]. Then, in 1896 the eminent French physicist Henri Becquerel (1852-1908) discovered the phenomenon of «radioactivity» named in 1898 to study its outstanding French physicists and chemists Marie Sklodowska-Curie (1867-1934) and Pierre Curie (1859-1906) and for which in 1903 Becquerel and M. Sklodowska-Curie and Pierre Curie who discovered at that time, such as a radioactive chemical elements polonium *Po* and radium *Ra* were awarded the Nobel Prize in physics [2, 3]. We mention the fact that for the release of radioactive radium *Ra* in pure metallic form, and a comprehensive study of it as a chemical element in the periodic system of elements of D.I. Mendeleev [4] M. Sklodowska-Curie was awarded the [2, 3] for the second time the Nobel Prize in chemistry for 1911. Today such an honor is not honored more than any woman in the world. In 1935, the eldest daughter of M. Sklodowska-

© M.I. Baranov

Curie and Pierre Curie Irène Curie (1897-1956) and her husband Frederic Joliot-Curie (1900-1958) became prominent French scientists-physicists, for the discovery of a fundamental phenomenon of «*artificial radioactivity*» won the Nobel Prize in chemistry [2, 3]. Returning again to the end of the 19th century, we note that in 1897, an outstanding British physicist Joseph John Thomson (1856-1940) elementary carriers of electricity (a kind of «*quanta of electricity*») were open - electrons [2, 3]. During this scientific discovery J.J. Thomson was awarded the Nobel Prize in physics for 1906 [3, 5]. The quantitative value of the negative charge of an electron  $e_0=1.602\cdot 10^{-19}$  K is a global constant has been determined empirically with a surprisingly high degree of accuracy (with measurement errors of up to 1%) in 1917 by outstanding American experimental physicist Robert Millikan (1868-1953) [2]. The results of these experimental studies R. Millikan was highly appreciated by the international scientific community and awarded the Nobel Prize in physics for 1923 [3, 5].

To the above it should be added that in fact even in 1886 by the German physicist Eugen Goldstein (1850-1930) who first introduced to electrophysics in 1876 the term «*cathode rays*» in a two-electrode discharge tube filled with the most abundant naturally occurring isotope of hydrogen protium  ${}_1^1\text{H}$  were opened «*canal rays*» and the elementary particles such as protons are present in them having a positive electric charge [3, 6]. At that time the values of their charge or their weight are not yet known. It is much later experimental physicists significantly, it was found that the modulus of the charge is equal to the module of the electron charge  $e_0$  and their mass  $m_p$  about 1836 times more the mass of the rest electron  $m_e$  [1, 4]. In physics, it is considered, however, that the proton as an elementary particle, «embossed» by alpha-particle of the atomic nucleus opened in the period 1914-1919 by a group of talented British atomic physicists including E. Rutherford, E. Marsden and J. Nuttall [3, 4]. It is necessary to specify the fact that this is extremely important for the understanding of the structure of a microcosm of the earth and nature of our universe as a whole electrically neutral elementary particle, the neutron was discovered in the course of experimental atomic research with the help of alpha particles in 1932 by a member of the famous school of physics of Ernest Rutherford outstanding British experimental physicist James Chadwick (1891-1974) [3, 5]. The mass of the neutron  $m_n$  with zero total electric charge in accordance with the experimental data of modern nuclear measurements was found to be about 1839  $m_e$  [1, 4].

In the world history of the development of physics teaching on the atom of matter and the structure of the theory is of a special place. The reason for that is the fundamental nature of these issues, the underlying structure of matter. By 1913, thanks to the results of experimental research using the «*X-ray*» a talented young British physicist Henry Moseley (1887-1915) who was

tragically killed on the battlefields of World War I was installed one of the main physical characteristics of the substance of the atom - the value of positive charge its nucleus, located in the center of this microformations [2, 5]. This value is later called «*the number of Mendeleev*» corresponds to the sequence number  $Z$  of the chemical element in the periodic system of the fundamental elements of the D.I. Mendeleev [4]. Using the experimental results of his student an outstanding British physicist Ernest Rutherford (1871-1937) in 1913, after years of deliberation and searching proposed to scientific world known *planetary-nuclear model of the atom* [3, 4]. It should be noted that the precursor of such a momentous event in the physico-chemical studies of world steel Rutherford and his other young talented student, the British physicist and chemist Frederick Soddy (1877-1956) who became the winner of the Nobel Prize in chemistry for 1921 [3], in the theory and practice of the radioactive decay of chemical elements. For scientific achievements in describing patterns of radioactive transformation of atoms like without external interference, and bombarded emanating from the radioactive source containing a capsule of radium *Ra*, by alpha particles - double ionized helium atoms  ${}_2^4\text{He}$  and in fact by their nuclei, E. Rutherford was awarded the Nobel Prize in chemistry for 1908 [3].

**1. Max Planck - founder of the quantum theory of thermal radiation.** At the turn of the 19th and 20th centuries in physical science, new concepts and theories, significantly changed as a scientific «front», and internal scientific «stuffing» the seemingly immutable «building» of classical physics. In 1897 the talented German physicist Max Planck (Fig. 1) started the theoretical study of the dynamics of thermal radiation of the absolute blackbody (ABB). It is necessary to remind the reader that ABB considered a physical body that absorbs all incident on the surface of the thermal (electromagnetic) radiation, regardless of wavelength and the body temperature [4]. Of course, that ABB is an idealized physical body, absent in nature, but is often used by us as a calculated thermophysical model.

In 1900 Max Planck based on a fundamentally new and revolutionary approach in fact showed that the emission or absorption of the physical body of the thermal radiation, which has, by the way, an electromagnetic nature [4, 7], is not continuous, as anticipated earlier in classical physics and intermittently. And, and, these processes occur individual energy portions, which he called «*quanta of action*» [3, 4]. The value of the photon energy  $E_n$  is a multiplication of the fundamental constant  $h=6.626\cdot 10^{-34}$  J·s later called in physics as the Planck constant [3] on the quantized frequency  $\nu_n$  ( $n=1,2,3, \dots$  - integer quantum number) of radiation waves (absorption) [4, 7]. For the discovery of discrete quanta of energy (action) M. Planck was awarded Nobel Prize in Physics for 1918 [3, 6].



Fig. 1. Prominent German theoretical physicist Max Planck (1858-1947)



Fig. 2. Prominent Danish theoretical physicist Niels Bohr (1885-1962)

**2. Niels Bohr and the creation of a quantum-nuclear model of the atom.** For all its physical and progressive values proposed by E. Rutherford within the framework of classical mechanics and electrodynamics *planetary nuclear model of the atom*, containing in the central part of the positively charged nucleus and around the periphery of a negatively charged electron shell of a sphere-like, had a significant and insurmountable flaw. This theoretical model is electrically neutral atom with rotating around a fixed core bound electrons was unstable electrodynamic system. According to the laws of classical electrodynamics moving electrons in such a model were to continuously radiate electromagnetic energy and eventually «fall» into the nucleus [4, 6]. In nature these subatomic processes are observed. Using quantum theory of the outstanding German theoretical physicist Max Planck, the eminent Danish physicist Niels Bohr (1885-1962) in 1913 to overcome the above-mentioned fundamental lack of *planetary nuclear model of the atom* by Rutherford proposed a new hypothesis (in Greek the word «*hypothesis*» refers to namely «*scientific hypothesis*» [8]) that the atom of matter absorbs and emits electromagnetic energy by individual discrete portions (quanta) [3]. N. Bohr (Fig. 2) at the same time formulated a new physical idea that the atom of substance may be present in a number of discrete stationary energy states are not accompanied by the emission (absorption) of electromagnetic energy by it [3, 4, 7].

Furthermore, according to the hypothesis put forward by N. Bohr atomic transition of a substance from the normal (stationary) to an excited energy state can only occur due to the absorption of its bound electrons, rotating in the area of nuclear power of the skin in circular orbits around the nucleus of an atom, the quantum of energy (light) strictly defined value [2, 4]. In the case of bound electron absorption of the quantum of energy he had to move to a more distant from the nucleus of an atom circular orbit. Radiating in this orbit thus obtained quantized electromagnetic energy before they  $\Delta E_n$  the electron is forced to make an abrupt transition from the core to the remote orbit on its original and located closer to the nucleus orbit radius  $r_n$ , where  $n = 1, 2, 3, \dots$  - integer quantum number equal to the sequence number of the electron orbit in an atom as the distance it from its core [4, 7]. We should not confuse this with the number  $n$  a principal quantum number, corresponding to the number of electron shells in the atom number and the period of the atom in the periodic table of elements by D.I. Mendeleev. Moreover, this transition is bound electron, emitting a quantum of energy with frequency  $\nu_n = \Delta E_n / h$  it had to do without going through all the intermediate and discrete set of the proposed model of circular electron orbits of the atom. That this was the basic idea of developed by N. Bohr *quantum-nuclear model of the atom*. In 1922 N. Bohr for the creation of the model of the atom, which had fundamental importance for the description of subatomic processes, was awarded [3, 5] the Nobel Prize in physics. This model of the atom was successfully used in the description of subatomic processes for the simplest atom of matter - hydrogen isotope protium  ${}^1_1H$  around which a nucleus consisting of one proton  $p^+$ , single electron  $e^-$  moves in a circular orbit. Quantum theory of the Bohr atom fully satisfy the fundamental law of spectroscopy obtained experimentally by physicists and use the Rydberg constant is numerically

equal to  $R=3.289842 \cdot 10^{15} \text{ s}^{-1}$  [4]. It allows with high accuracy to calculate the above-mentioned constant  $R=m_e e_0^4 (8\epsilon_0^2 h^2)^{-1}$  based on the four fundamental values: the electron charge module  $e_0=1.602 \cdot 10^{-19} \text{ C}$ , the rest mass of the electron  $m_e=9.109 \cdot 10^{-31} \text{ kg}$ , the electric constant  $\epsilon_0=8.854 \cdot 10^{-12} \text{ F/m}$  and the Planck constant  $h=6.626 \cdot 10^{-34} \text{ J}\cdot\text{s}$ . This quantum theory of the atom of substance to ensure the correct physical and quantitative interpretation of experimentally observed previously in the laboratory physicists line emission spectra for hydrogen isotope  ${}^1\text{H}$  (protium), including Lyman, Balmer, Paschen, Brackett and Pfund series [4, 7].

Besides, it should be noted, however, that the quantum theory of the atom by Bohr received in 1914 and its direct experimental confirmation in the famous experiments of German experimental physicists James Franck (1882-1964) and Gustav Hertz (1887-1975) for the detection of discrete excited states of a number of atoms (e.g., mercury *Hg*) and determining their ionization energy [2, 4, 6]. Experimental results by J. Franck and G. Hertz significantly indicated that the energy of the atoms changes discretely quantized way with a strictly specific to each type of atom energy portions. So, for mercury atoms *Hg*, this portion of (quantum) of electromagnetic energy, causing their excitation and subsequent emission of a photon of energy out of the transition in the ground state, was about 4.9 eV which corresponds to a photon energy of ultraviolet light with a wavelength of 253.6 nm [4, 6]. For outstanding results of years of nuclear research J. Franck and G. Hertz were awarded the Nobel Prize in physics for 1925 [3, 6].

**3. Albert Einstein and the creation of the quantum theory of the photoelectric effect.** As is known, the phenomenon of the *photoelectric effect* is the change in the electrical properties of a substance by electromagnetic radiation (light, gamma rays, ultraviolet, X-ray, and other rays) [8]. In physics today known [4, 7]: the *external photoelectric effect* (the emission of the substance outside the electrons when exposed to light); *internal photoelectric effect* (change in electrical resistance of matter under the influence of the quanta of the electromagnetic field); *photovoltaic effect* (the appearance of the electromotive force in the matter under the influence of solar radiation); *nuclear photoelectric effect* (the emergence of a nuclear reaction in the material under the action of gamma rays). Next, we will focus on the *external photoelectric effect* or *photoelectric effect*. It is known that this effect was observed in 1887, one of the founders of classical electrodynamics, the eminent German physicist Heinrich Hertz (1857-1894) the first experimentally proved in 1888 the existence of electromagnetic waves [3, 6]. Thus Hertz found that electric discharge in the air between two metal electrodes occurs more rapidly or at a lower voltage between the electrodes in the case of illumination luminous flux of the discharge gap containing ultraviolet rays. The physical explanation of the photoelectric effect from the standpoint

of the emerging quantum mechanics was given in 1906 by the outstanding German theoretical physicist Albert Einstein (1879-1955) shown in Fig. 3.



Fig. 3. Prominent German theoretical physicist Albert Einstein (1879-1955)

Improving the quantum theory by M. Planck, A. Einstein for light emission in 1905 introduced the concept of light as a stream of quanta of the electromagnetic field or the photon flux and developed the photon theory of light [3, 4, 9]. In this theory A. Einstein based on quantum theory of electromagnetic radiation, it showed that not only the emission of light, but its distribution and absorption is performed discretely (in portions) using «*light quanta*». It is a new quantum-mechanical approach allowed him to formulate the law of photoemission (in physics it came as «*Einstein law of the photoelectric effect*») [3, 9]. For the discovering on the basis of the quantum theory of the law of the photoelectric effect, A. Einstein was awarded the Nobel Prize in physics for 1921 [3, 9]. The experiments of the American physicist Robert Millikan performed with high accuracy in 1916 consistent with the photoelectric effect Einstein's theory [9]. A convincing proof of the discreteness of the electromagnetic energy and the existence of the photon were the results of experimental studies of another American physicist Arthur Compton (1892-1962) to change the wavelength of X-rays due to its solid-state electron scattering (*Compton effect*) [4]. In 1927, A. Compton for his discovery and development of the theory of «*Compton quantum phenomena*» was awarded the Nobel Prize in physics [3, 7].

**4. Louis de Broglie and the discovery of the electron waves.** In the history of physics it turned out that Louis de Broglie (Fig. 4) introduced the first scientific idea on the wave properties of the material of the microparticles in modern physics [10]. The starting point in the famous works of outstanding French theoretical physicist Louis de Broglie (1892-1987) dedicated to the

wave properties of material microparticles became brilliant physical idea of the eminent German theoretical physicist Albert Einstein formulated it in 1905-1917 on the quantum structure of light (the «*light quanta*») [3, 11]. He put forward and substantiated the hypothesis of dualism of universality in microcosm [10, 11].



Fig. 4. Prominent French theoretical physicist Louis de Broglie (1892-1987)

In 1923 Louis de Broglie in his three research papers carried a significant development of the idea of Einstein about the dual nature of light. His original approach, he connected with the transfer of wave-particle duality of light (its simultaneous duality of particles and waves) on the microparticle substances with a rest mass. Historically, it turned out that the idea of the wave nature of matter belongs to the talented scientist Einstein once wrote [10]: «... *De Broglie was the first to realize the close physical and formal relationship between quantum states of matter and resonance phenomena in the days when the wave nature of matter was not discovered experimentally*». Each particle of matter has to comply with a wave of matter. This bold and revolutionary idea of Louis de Broglie has allowed him to gain which has now become a classic relationship for  $\lambda_e$  wavelength non-relativistic electrons in the form [4, 7]:  $\lambda_e = h / (m_e v_e)$ , where  $v_e$  is the electron velocity. Young Louis de Broglie supposes that [10]: «... *electron can no longer be regarded as a mere speck of electricity. I wave to be associated with it*». These physical results Louis de Broglie summarized in 1924 in his doctoral thesis on «*Studies on the quantum theory*» which he successfully defended the University of Paris (the famous «*Sorbonne*») [3, 6]. For the discovery of the wave nature of the electron de Broglie was awarded the Nobel Prize in physics for 1929 [3]. During the ceremony of presentation and awarding him the prize they said [10]: «... *De Broglie discovered a completely new aspect of the nature of matter, which previously no one suspected. Brilliant guess*

*de Broglie allowed long-running dispute, finding that there are not two worlds, one - light and waves, the other - matter and corpuscles. There is only one common world*». What a wise and deep philosophical and physical thought!

Experimental confirmation of the hypothesis of de Broglie wave properties of electrons was carried out outstanding Britain experimental physicist George Thomson (1892-1975) - the son of the previously mentioned master of the world of physics Joseph John Thomson, who, irrespective of American experimental physicists Clinton Davisson (1881-1958) and Lester Germer (1896-1971) in 1927 discovered the diffraction of low-energy electrons («*cathode rays*») on a single crystal of nickel *Ni* [3, 4]. During his experiments, J. Thomson revealed that he had received the diffraction pattern is very reminiscent of the already known by the time the diffraction of «*X-rays*». For this remarkable discovery J. Thomson and K. Davisson were awarded the Nobel Prize in physics for 1937 [3, 6].

**5. Erwin Schrödinger and the creation of wave mechanics.** Based on the laws of classical theoretical mechanics, the Austrian theoretical physicist Erwin Schrödinger (Fig. 5) in 1926 published his famous four papers which set out a new approach to solving problems of quantum physics for nuclear facilities [3, 6]. In them, he challenges to quantum theory of the microworld reduced to the problem of mathematical physics at the eigenvalues of some function, which he called «*wave function*» [6, 12].



Fig. 5. Prominent Austrian theoretical physicist Erwin Schrödinger (1887-1961)

For the mathematical obtaining of the wave function ( $\psi$ -function) with respect to the atom of substance, he received the corresponding partial differential equation of the second order (in the history of physics is entered as «*Schrödinger equation*» [3, 6]), which describes the behavior of bound electrons in the well-known to him

planetary-nuclear model of the atom [4, 12, 13]. This is the Schrödinger wave equation turned out to be a generalization and application of these earlier «*wave ideas*» the French theoretical physicist Louis de Broglie to the hydrogen-like atom [4]. The solution of this equation is reduced to a standing electron waves in a specified atom [4, 6].

Creating the wave (quantum) mechanics allowed E. Schrödinger a fresh look at the atomic and subatomic processes theory. Applying the Schrödinger wave equation to describe the quantum mechanical processes in hydrogen atoms of the material showed that the distribution of bound electrons in atomic spherical shell is subject to the respective quantized wave  $\psi_n$ -function describing in three-dimensional space of a standing wave of matter (de Broglie wave). Moreover, in this case, each quantized wave  $\psi_n$ -function matched strictly certain quantized energy of a bound electron, indicating its energy level. With such a quantum-physical approach to the analysis of intra-process it turned out that a bound electron atom considered able to move from one energy state, which corresponds to a quantized wave  $\psi_n$ -function into another energy state described by another quantized wave  $\psi_n$ -function [4, 6]. Moreover, received thus on the basis of exact solutions of the Schrödinger wave equation for the hydrogen isotope  ${}^1_1H$  (protium) the eigenvalues of the energy of its associated  $s$ -electron ( $E_s = -13.6$  eV) and the most probable radius of its orbit ( $r_s = 0,529 \cdot 10^{-10}$  m) fully coincided with calculated results arising from *quantum-nuclear model of the atom by Bohr* [4, 7]. In fact, by E. Schrödinger new quantum mechanical model of the atom (in the history of physics it came as *Schrödinger quantum-wave model of the atom*) has been developed on the basis of the laws of wave mechanics [3, 4, 13]. For the development of new forms of atomic theory (*wave mechanics*) Schrödinger was honored for 1933 the Nobel Prize in physics [3]. According to this model, the atom distribution of electrons in its atomic shell described quantized wave  $\psi_n$ -functions are spatially standing waves [4]. From atomic model by Schrödinger it followed that associated electron in the atomic shell in a stationary orbit can not radiate energy on the grounds that his condition is determined by said electronic standing waves. In theory, Bohr postulated such a position only with no physical explanation. [4] The new atomic theory Schrödinger explained the phenomenon of displacement of the energy levels of the atom under the influence of strong external electric field (Stark effect, opened in 1913 [2, 4, 7]). Quantum theory of Schrödinger correctly explained the spectral lines in the hydrogen atom [4]. This quantum theory was a major scientific discovery of the first half of the 20th century in the field of nuclear physics processes.

American physicists Clinton Davisson and Lester Germer examining at the end of 1927 the scattering of electrons on a single crystal of nickel  $Ni$  and comparing them received experimental data with the calculated

results of the well-known formula in materials by Bragg-Wulf experimentally confirmed the existence of electron waves in the nature of matter. In addition, some of the first experimental evidence of quantum (wave) mechanics also were physical experiences of the German scientist Otto Stern carried out in 1929. These experiments have been associated with the study of the wave nature of neutral atoms and molecules, scattered on the two-dimensional diffraction grating  $LiF$  crystal [4, 6]. O. Stern when it was shown that light atoms  ${}^1_1H$  isotope of hydrogen (protium) and helium  ${}^4_2He$  under these conditions, there is a clear diffraction pattern, and for the heavy atoms of matter having a small «de Broglie» wavelength diffraction picture is fuzzy (vague). Moreover, in the experiments conducted by the physical intensity of the peaks above us on the diffraction patterns observed in places where the waves of matter («de Broglie» wave) going to (interfere) in the same phase [4].

**6. Wolfgang Pauli and the formulation of the «exclusion principle».** Austrian theoretical physicist Wolfgang Pauli (Fig. 6) has made a significant contribution to the development of quantum mechanics as the theory of physical processes and phenomena in the microcosm of nature. In the period 1924-1925 he formulated his famous «*exclusion principle*» (in the history of physics is the concept became a «*Pauli exclusion principle*» [3]). In the words of Wolfgang Pauli [14]: «... *in the atom can be two electrons in which all four quantum numbers would be the same*». This is the essence of this principle. Perhaps the introduction of the physical concept was a major achievement Pauli quantum theory of subatomic processes [3, 14].



Fig. 6. Prominent Austrian theoretical physicist Wolfgang Pauli (1900-1958)

In accordance with the fundamental «*Pauli exclusion principle*» in the atom of substance in its electronic shells can be only one so-called bound electron, characterized by the appropriate only for him to certain

quantitative set of four quantum numbers used in atomic physics [4, 7]: the principal quantum number  $n$ ; orbital quantum number  $l$ ; magnetic quantum number  $m_l$ ; spin quantum number  $m_s$ . It is known that in the atom of matter quantum number  $n$  determines its kinetic and potential energy, the quantum number  $l$  - the shape of the electron orbit, quantum number  $m_l$  - the position of the electron orbit in atomic space and the quantum number  $m_s$  - its direction of circular rotation around its own axis [4, 7]. This physical principle has played a huge role in determining the order of development bound electrons of the atomic shell. For scientific discovery of the «*Pauli exclusion principle*» outstanding theoretical physicist of the 20th century W. Pauli was awarded the Nobel Prize in physics for 1945 [3, 5, 6].

**7. Werner Heisenberg and the formulation of the «uncertainty relations».** Prominent German physicist Werner Heisenberg (Fig. 7) is the author of a number of fundamental scientific results in quantum mechanics. In 1925 he developed a «*matrix mechanics*» which was the one of the theoretical aspects of quantum physics (later this mechanism was perfected by German theoretical physicists Max Born and Pascual Jordan) [3]. The starting «point» when creating this Heisenberg mechanics equivalent to E. Schrödinger's *wave mechanics* and the awarded of the 1932 Nobel Prize in physics [3], it was his fundamental rejection of the classical and the researcher observed subatomic processes concepts of «*position*» and «*impulse*» of the electron in an atom of matter and applying instead the concepts of «*frequency*» and «*amplitude*» of its oscillations, which the researcher can accurately be determined from optical experiment [15]. In quantum mechanics, momentum of microparticles  $p=mv$ , where  $m$  and  $v$  are respectively, the rest mass and the speed of the microparticles, with its wavelength  $\lambda$  associated by de Broglie relation ( $p=h/\lambda$ ) [4]. As is known, the wavelength  $\lambda$  is a function of the waveform and not the spatial coordinates (e.g.,  $z$ ). Therefore the impulse of the microparticles  $p$  will not be a function of the coordinate  $z$ . In this regard, in quantum mechanics it is impossible to simultaneously determine the  $z$  coordinate and impulse  $p$  of the microparticles. In 1927 W. Heisenberg to resolve this paradox formulated the fundamental physical principles of quantum mechanics - the «*uncertainty relation*» named later by his name and having, for example, to conjugate variables «*coordinate-momentum*» form [4]:  $\Delta z \cdot \Delta p \geq h/(4\pi)$ , where  $\Delta z$ ,  $\Delta p$  are the uncertainties in finding the position and momentum of the microparticle.

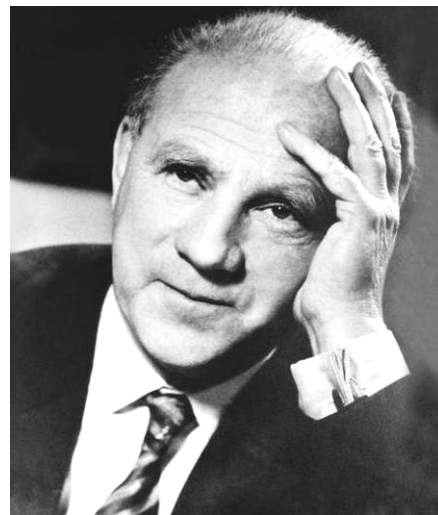


Fig. 7. Prominent German theoretical physicist Werner Heisenberg (1901-1976)

**8. «Bohr's» formulation of the «principles of the relevant and complementarity».** After developing his famous quantum theory of the atom, N. Bohr continued to develop this theory by trying to generalize it to the case of more complex than hydrogen  ${}^1H$  (protium) the many-electron atoms. In 1918 in his paper «*On the Quantum Theory of Line Spectra*» N. Bohr quantitatively formulated the so-called «*principle of correspondence*» linking the quantum theory with classical physics [3, 16]. He also used his idea from 1913 that in the nuclear related shell transitions of electrons between stationary orbits with large quantum numbers should provide radiation at a frequency coinciding with the frequency of revolution of the electron in the atom [16]. In formulating this principle, N. Bohr noted [16]: «... *Each transition between two stationary states associated with a respective harmonic component so that the probability of the transition depends on the amplitude of oscillation. The polarization of the radiation is due to the more detailed properties of fluctuations as well as the intensity and polarization of light in the system of waves emitted by an atom from the classical theory due to the presence of said component fluctuations, determined by the amplitude and other properties of the latter*». This principle has allowed N. Bohr to determine the probability of transitions of electrons and hence the intensity of the spectral lines, as well as obtain the selection rule (in particular, for the harmonic oscillator) and give an interpretation of the number and the polarization component of the «*Stark and Zeeman splitting*» of spectral lines in strong electric and magnetic fields. The «*correspondence principle*» has played a huge role in the construction of a consistent quantum mechanics [16]. According to this principle, the equations of quantum physics for large quantum numbers, or with the involvement in the monitoring process of a large number of photons must coincide with the equations of classical physics to the corresponding averaged physical quantities [4]. Another important for the understanding of the physical principles and interpretation

of the results of quantum mechanics was «*complementarity principle*» proposed by N. Bohr in 1927 [3, 16]. This principle reflects the logical relationship between the two methods of description or set of views for the same events in the microcosm. Indeed, on the one hand, the predictions of quantum mechanics are probabilistic. On the other hand, are used for their interpretation and presentation of the terminology of classical physics. The basis of the interpretation of quantum theory, Bohr put the wave-particle duality of microparticles which first turned his keen and insightful account of Louis de Broglie. The essence of «*subsidiarity principle*» is that the microparticles can not be a physical situation in which the two complementary aspects to it (for a single phenomenon in microcosm) have emerged at the same time and equally clearly [16]. In other words, in the microcosm there are no physical conditions in which micro-object would have the exact same time dynamic characteristics (for example, coordinate, momentum, energy and other values) belonging to two different specific concepts mutually exclusive. It is the scientific position and found its concrete expression in the formulated by W. Heisenberg in 1927 regardless of N. Bohr's «*uncertainty relation*».

**9. The creation of quantum statistics of microparticles.** We begin here with the fact that we point out that in physics at the quantum statistics of mean statistical method for studying systems consisting of a large number of microparticles and obey the laws of quantum (wave) mechanics [7]. Development of this new for the first half of the 20th century physics as quantum mechanics (physics) statistical approach to describe the behavior of systems with identical (identical) microparticles faced serious scientific difficulties when trying to physics scholars of determining the number of energy states in an arbitrary gas (system microparticles) containing such microparticles that can be characterized by their «*degeneracy*». By this for a better understanding of the reader of the composite material should be added that the gas applied to microparticles (e.g., the «*electronic gas*» or so-called «*electronic cloud*» of the metal conductor) is considered «*degenerate*» in the case where the properties described by quantum-physical laws, differ significantly from the usual properties of the gas, obeying the laws of classical physics, and in accordance with laws based on its statistical physics [7]. An important step in overcoming the problems of scientific difficulties in creating quantum gas statistics, consisting of «*degenerate*» microparticles was made by talented theoretical physicists from Asia and Europe in the first quarter of the 20th century [3].

*The quantum statistics of Bose-Einstein.* The famous Indian theoretica; physicist Shatendranat Bose (1894-1974) in 1924 regardless of the outstanding German theoretical physicist Albert Einstein (1879-1955) developed the quantum statistics of identical microparticles with a zero and spin (the concept of «*spin*»

means own mechanical angular momentum of rotating around own axis of the microparticles) received in the physics of elementary particles the name «*bosons*» (these include photons, phonons, and some nuclei of atoms) [3, 4, 7]. This statistics by names of its founders in quantum physics called «*Bose-Einstein statistics*» [7, 16]. We point out that an important feature of *bosons* named after physicist S. Bose (Fig. 8) is their fundamental insubordination «*Pauli exclusion principle*». Therefore for *bosons* there are no restrictions on the number of microparticles that may be present in certain quantized energy state. With regard to the quantum statistics of the microparticles in analytical form have been received  $f_B$  distribution functions of *bosons* (Bose gases) for energy, which in quantum physics became known as the Bose-Einstein distribution functions [4, 7, 17].



Fig. 8. Outstanding Indian theoretical physicist Shatendranat Bose (1894-1974)

*Quantum Fermi-Dirac statistics.* Young and in future outstanding Italian physicist Enrico Fermi (1901-1954) awarded in 1938 the Nobel Prize in physics for their discovery of artificial radioactivity, chemical elements, caused by the bombing of them by «*slow*» neutrons, in 1925 regardless of when also the young and also in future the outstanding British theoretical physicist Paul Dirac in the future (1902-1984) which became in 1933 for the discovery of new productive forms of atomic theory (for the creation of *quantum mechanics*) the Nobel Prize in physics [3] developed a quantum statistics for microparticles with half-integer *spin* (such as electrons, protons, neutrons, and other representatives of the microcosm of matter) [7]. An important feature of these microparticles (in elementary particle physics, such microparticles are now called «*fermions*» [4]) is that they obey the «*Pauli exclusion principle*» in certain quantized energy state of which can be either only one microparticle, or none microparticles. This statistic is named after talented scientists and its developers E. Fermi

(Fig. 9) and P. Dirac (Fig. 10) in quantum physics called «Fermi-Dirac statistics» [7].

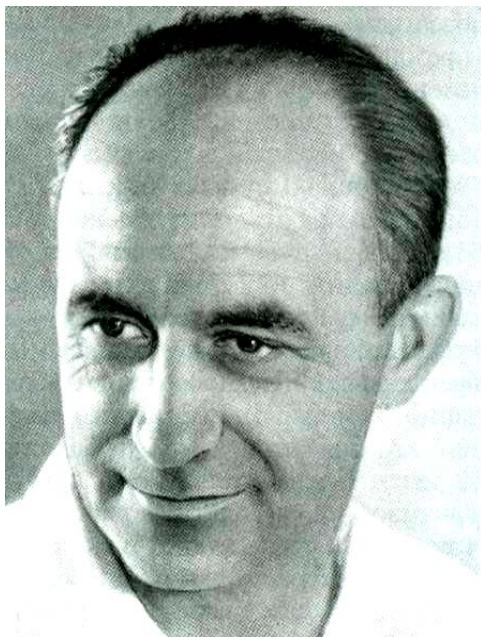


Fig. 9. Outstanding Italian theoretical physicist Enrico Fermi (1901-1954)



Fig. 10. Outstanding British theoretical physicist Paul Dirac (1902-1984)

Co-authors of the quantum statistics in an analytical form were obtained distribution function  $f_F$  of *fermions* (Fermi gases) at energies corresponding to the average number of microparticles in the same energy state [4, 7]. These quantum mechanical functions  $f_F$  in quantum physics have been called the Fermi-Dirac distribution functions [7]. From a comparison of mentioned analytic functions distribution  $f_B$  and  $f_F$  with distribution function  $f_{MB}$  by Maxwell-Boltzmann [4] characteristic of the «old» classical physics (respectively, and classical statistics) and

reflecting the average number of «non-degenerate» microparticles in the same energy state, it follows that no *bosons* or *fermions* do not obey the classical distribution of microparticles in energy (velocity) in ordinary gases described previously received in the 19th century the classical distribution function  $f_{MB}$  by Maxwell-Boltzmann [7]. Taking into account that *fermions* are part of all, without exception, we know atoms and molecules created in the first quarter of the 20th century «Fermi-Dirac statistics» becomes essential scientific and practical value for such rapidly developing worldwide knowledge areas as nuclear physics, elementary particle physics, high-energy plasma and condensed state of any matter [3, 4, 7].

**10. Max Born and the formulation of the statistical interpretation of the wave function of the microparticle.** In 1926, the eminent German theoretical physicist Max Born (1882-1970) Using physical idea of Einstein that light waves characterizes the square of the amplitude probability density  $\rho_F$  of appearance of photons («quanta of the electromagnetic field») [4] He offered to the scientific world the statistical interpretation of the wave  $\psi$ -function by Schrödinger [3, 18]. At the same time M. Born (Fig. 11) postulated that the value of the squared modulus of the quantized wave function  $|\psi_n|^2$  must be a probability density  $\rho_n$  for stay of the microparticle (e.g., electron, proton, neutron, or other particles) in a given volume substance. Expanding physical meaning of the «Schrödinger 's» wave  $\psi$ -function, M. Born swung thus a kind of «bridge» between the wave and corpuscular theory of matter microparticles. Designed by M. Born physical approach was an important «step» on the way «reconciliation» of the old classic presentation «particulates of matter» with the representation of the new quantum-mechanical «waves of matter» [3]. The statistical interpretation in 1926 by M. Born of the wave  $\psi$ -function by Schrödinger was the first «step» on the way scientists study the probabilistic interpretation of quantum mechanics (physics), which determines the behavior of micro-particles of any substance.



Fig. 11. Prominent German theoretical physicist Max Born (1882-1970)

Such an interpretation of the wave  $\psi$ -function by Schrödinger pointed to the fundamental role of probability in the laws of the microcosm of nature around us. A more rapid recognition in the world of such an interpretation of the wave  $\psi$ -function by Schrödinger contributed described earlier by «Heisenberg uncertainty relation» «reconciling» the corpuscular and wave pattern of distribution of the microparticles, explaining the connection of classical mechanics to quantum mechanics and restricting the use of microscopic bodies to the concepts of classical physics. In 1954 Max Born won the Nobel Prize in physics «for outstanding results in the field of quantum mechanics» [3, 18].

**11. Lev Landau and the creation of the quantum theory of the phenomenon of superfluidity of liquid helium.** With the approach of the temperature of the physical body to absolute zero, and a sharp decrease in the velocity of the thermal motion of the atoms, «de Broglie» wavelength of its atoms in accordance with the formula of de Broglie and quantum uncertainty of its atomic coordinates according to the « Heisenberg uncertainty relations» become significantly more of its interatomic distances [6]. Under these conditions, a significant role in condensed matter, quantum effects begin to play and begins to manifest itself through macroscopic quantum wave nature of physical processes in the condensed state of matter («*quantum fluid*»). With such a mysterious manifestation of physical processes encountered physicists who received liquid helium-I with a critical temperature of 4.22 K and liquid helium-II of (for example, a prominent Dutch experimental physicist Heike Kamerlingh Onnes (1853-1926) who in 1911 won the Nobel Prize in physics for the discovery of superconductivity in metals [3, 6]) and studying their physical properties (e.g., the prominent Soviet experimental physicist Pyotr Leonidovich Kapitsa (1894-1984) awarded in 1978 the Nobel Prize in physics for «*fundamental inventions and discoveries in the field of low temperatures*» [3, 6]). Experiments of P.L. Kapitsa at the created by him in 1935 the Institute of Physical Problems (IPhP) of the Academy of Sciences of the USSR ended by the discovering in 1937 the phenomenon of superfluidity of liquid helium-II with a critical temperature of 2.19 K [3, 4, 7]. Many attempts at domestic and foreign theoretical physicists for an explanation of the paradoxical behavior of liquid helium-II for many years remained unsuccessful. After the moving in 1937 from the Ukrainian Physico-Technical Institute (Kharkov) to work at the IPhP, Academy of Sciences of the USSR (Moscow) prominent Soviet theoretical physicist and future Academician of the Academy of Sciences of the USSR (1946) Lev Davidovich Landau (1908-1968) started close to the disclosure of the phenomenon of liquid helium-II. By 1941 L.D. Landau (Fig. 12) concludes that in liquid helium-II phase transition of II-kind not accompanied by the release (or absorption) of heat, unlike the phase

transition of I-type and associated with the appearance of a substance qualitatively new specific properties [4, 19].

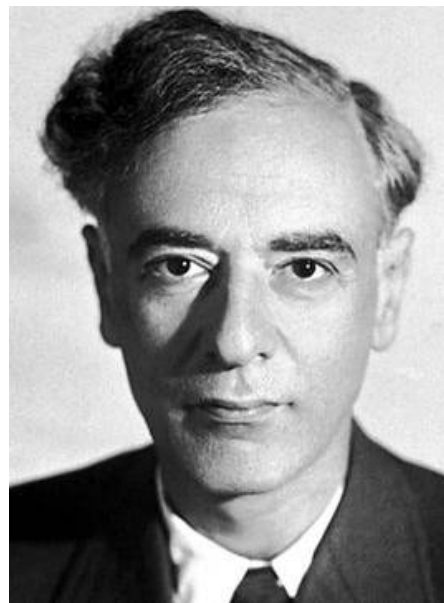


Fig. 12. Prominent Soviet theoretical physicist, Academician of the Academy of Sciences of the USSR Lev Davidovich Landau (1908–1968)

L.D. Landau in the construction of the quantum theory of liquid helium II-type of superfluidity phenomenon took advantage of the concept of «*quasi-particles*» («*like particles*») which are mainly chosen *phonons* (sound quanta of energy, responsible for a potential motion of matter) and *rotons* (quantum elementary pathogens responsible for the eddy motion of matter) [3, 6]. In addition, L.D. Landau thus introduced the concept of the normal and superfluid component of liquid helium of II-kind. These quasi-particles is described by the behavior of the normal component in this helium condensate. This component is moved in it with friction and participated in the transfer of heat. The superfluid component moving in liquid helium II-type of friction-free and was not involved in the transfer of heat in it. These are the main characteristics of the developed by L.D. Landau in 1945 the two-fluid model of quantum liquid helium of II-kind. Completed in 1945 at the IPhP of the Academy of Sciences of the USSR low-temperature experiments involving the future Doctor of Physical and Mathematical sciences E. Andronikashvili confirmed the presence in liquid helium-II of normal and superfluid components, as well as the reliability of the whole of created by L.D. Landau the quantum theory of superfluidity of liquid helium-II [3, 6]. Taking into account the fundamental nature of this achievement, in 1962 L.D. Landau was awarded the Nobel Prize in physics «for his pioneering research in condensed matter theory, especially liquid helium» [3, 19].

**12. Quantum Electronics and the creation of quantum generators of electromagnetic radiation.** The term «*quantum electronics*» refers to a new branch of

physics that studies the methods of amplification and generation of electromagnetic oscillations based on the use of the effect of stimulated (induced) radiation [4, 20]. Recall that in 1905 the eminent German physicist Albert Einstein based on the statistical analysis of energy fluctuations of equilibrium radiation advanced the hypothesis of «*light quanta*» [3]. In 1916 he came to understand the nature of equilibrium radiation in quantum systems that have discrete levels of radiation energy. At the same time by him to similar systems it introduced the concept of «*stimulated emission of radiation*» associated with the energy of a quantum particle transitions included in a single physical ensemble (atoms, molecules, solid, gas, etc.). In this regard, the physical basis for *quantum electronics* [4, 20] consists of the following three fundamental positions. The *first* – the energy of electromagnetic radiation consists of discrete portions of energy («*light quanta*» or «*photons*»). The *second* – emission of light quanta in its high intensity determined by the effect of induced emission. The *third* - quanta of forced and forces of electromagnetic radiation (photons) are identical and are subject to quantum statistics of Bose-Einstein. As a result, the quantum nature of electromagnetic radiation and the quantization of the energy levels of microparticles objectively lead to the existence of physical processes in the microscopic world, accompanied by the generation of identical each other of light quanta («*bosons*»). Bosonity of photons allows you to navigate in quantum electronics from the corpuscular representation of the wave, which is characterized by the principles of superposition and amplification of coherent oscillations [4, 20]. In 1927 the eminent British theoretical physicist Paul Dirac developed a consistent quantum theory of radiation (absorption) of light, the most important result of which was a rigorous justification of «*stimulated emission*» postulated by Albert Einstein, and its coherence [3, 21]. Despite the creation of the above-mentioned physical prerequisites for the emergence in the world of quantum electronics, until the end of 1954 in the field of quantum electronics was created at the same time in the Soviet Union (at the Laboratory of oscillations of the Physical Institute of the Academy of Sciences of the USSR under the supervision of the future Academician Alexander Mikhailovich Prokhorov (Fig. 13) and Nikolai Gennadievich Basov (Fig. 14), Moscow, Russia) and the USA (at the Laboratory of emissions of the Columbia University under the supervision of Professor Charles Townes (Fig. 15), New York city), the first «*molecular quantum generator*» of the microwave-induced radiation («*ammonia maser*») having a narrow beam of radio waves with a length of 1.27 cm wave [5, 21]. In this physical device due to the use of energy physicists sorting and excitation energy ammonia molecules in the active quantum medium with population inversion, placed in the cavity, carried out a quantum jump between discrete energy levels in molecules of ammonia [4, 5]. This gas maser is very stable stimulated coherent radiation.



Fig. 13. Prominent Soviet experimental physicist, Academician of the Academy of Sciences of the USSR Alexander Mikhailovich Prokhorov (1916–2002)



Fig. 14. Prominent Soviet experimental physicist, Academician of the Academy of Sciences of the USSR Nikolai Gennadievich Basov (1922-2001)



Fig. 15. Prominent American experimental physicist Charles Townes (1915-2015)

An important scientific «step» by domestic scientists-physicists in the field of quantum electronics was made in 1955 when N.G. Basov and A.M. Prokhorov proposed a new method of creating radiation in the active medium of inversion and non-equilibrium quantum systems – «*three-level pump method*» widely used in lasers and today [5].

Quantum electronics in the second half of the 20th century was not limited only to the development of microwave amplifiers through stimulated electromagnetic radiation («*masers*»). In 1960 the first solid-state «*optical quantum generator*» («*ruby laser*») was created by the American physicist T. Maiman based on the ruby crystal [5]. Then came gas, semiconductor, chemical, and other «*lasers*» [5, 21]. In 1964 Charles Townes, A.M. Prokhorov and N.G. Basov was awarded the Nobel Prize in physics «*for fundamental work in quantum electronics, which led to the creation of masers and lasers*» [3]. Currently, lasers of varying power output operate in continuous and pulsed modes, over a sufficiently wide frequency range of radiation-induced waves. Now in the world there is a huge variety of «*maser*» and «*lasers*» with various active quantum fluids and systems of excitation («*pumping*») [5, 20].

**13. The quantum wave nature of the drift of the free electrons in metal.** A convincing, clear and accessible to many electrophysicists example of the manifestation of quantum-wave properties of electrons as a microcosm of representatives are set at the macroscopic level recently in Ukraine quantum-physical features of the flow of pulsed conduction current in metals due to drift of the free electrons [22-27]. These features are manifested in the fact that, for example, in the form of aperiodic time shape 9/160 ms of relatively high density conductive structure thin galvanized wire cylindrical configuration with an axial current pulse (till 0.37 kA/mm<sup>2</sup>) for forming quantized through an electronic half-waves de Broglie wave of quantized electronic wave packages (EWP) of macroscopic dimensions there arises a periodic longitudinal thermal macrostructure consisting of alternating between a relatively «*hot*» and «*cold*» longitudinal sections with visual lockable researcher their lengths (widths)  $\Delta z_z$  and  $\Delta z_x$ , respectively. Moreover, the width  $\Delta z_z$  of «*hot*» longitudinal sections EWP of conductor correspond to said previously «*Heisenberg uncertainty relations*», which determines the uncertainty of the longitudinal coordinates  $\Delta z$  drifting electrons with a maximum energy of approaching  $W_F$  Fermi energy the most likely area of their location, the corresponding square module quantized wave function  $|\psi_{en}|^2$  for these electrons. In [22-27] it has been convincingly, both theoretically and experimentally shown to be drifting in a metal conductor with an electrical DC, AC or pulsed current of free electrons («*fermions*») which are quantum objects and obeying «*Pauli exclusion principle*», as well as meet «*quantum statistics of Fermi-Dirac*», because of its wave nature of the length  $l_0$  and the radius  $r_0$  of said

circular cylindrical conductor distributed wave manner so that its length  $l_0$  and radius  $r_0$  always fit an integer quantized electronic half-waves of de Broglie, respectively of length  $\lambda_{ln}/2=l_0/n$  и  $\lambda_{rn}/2=r_0/n$ , where  $n = 1,2,3, \dots$  - integer quantum number. Quantized values  $\lambda_{ln}/2$  and  $\lambda_{rn}/2$  precisely define periodic step structure for the above quantized EWP in the conductors with the electrical current. The research results presented in [22-27], conclusively point to a clear manifestation in the metal conductors with an electric current of high density «*quantum effect periodic macrolocalization free electrons*», which determines the appearance of their conductive structure with EWP inhomogeneous periodic longitudinal and radial temperature fields.

**Conclusion.** The nature of existence and the transition of matter at the atomic and subatomic levels of its one physical state to another, chaotic (directed) motion of microparticles in the fields of physical and leakage caused by their spatial displacement of certain probabilistic micro- and macroevents determined stochastic quantum physical phenomena occurring in the microcosm any material and describes the known laws of quantum, atomic and nuclear physics, as well as the laws of physics of elementary particles, plasma, high energy and condensed state of matter. In this regard, taking into account the currently available theoretical and experimental data in the scientific world, we can confidently state that one fundamentally important scientific position that the known (yes, probably, and even unknown) physical processes and phenomena in the microcosm of matter are quantum-wave and probabilistic nature. Despite this, the quantum-wave processes which characterize the microcosm objects causally linked and determined. They can be described in the relevant differential equations uniquely determines the desired quantized wave  $\psi_n$ -functions and other necessary physical quantities in the study of the behavior and evolution we have examined microscopic representatives of nature.

#### REFERENCES

1. Astafurov V.I., Busev A.I. *Stroenie veshchestva* [Structure of matter]. Moscow, Education Publ., 1977, 160 p. (Rus).
2. Kudryavtsev P.S. *Kurs istorii fiziki* [The course of the history of physics]. Moscow, Education Publ., 1974, 312 p. (Rus).
3. Khramov Yu.A. *Istoriia fiziki* [History of Physics]. Kiev, Feniks Publ., 2006. 1176 p. (Rus).
4. Kuz'michev V.E. *Zakony i formuly fiziki* [Laws and formulas of physics]. Kiev, Naukova Dumka Publ., 1989. 864 p. (Rus).
5. Baranov M.I. *Antologiya vydaishchikhsia dostizhenii v nauke i tekhnike: Monografiia v 2-kh tomakh. Tom 1.* [An anthology of outstanding achievements in science and technology: Monographs in 2 vols. Vol.1]. Kharkov, NTMT Publ., 2011. 311 p. (Rus).
6. Baranov M.I. *Izbrannye voprosy elektrofiziki: Monografiia v 2-h tomakh. Tom 1: Elektrofizika i vydajshhiesja fiziki mira* [Selected topics electrophysics: Monographs in 2 vols. Vol.1: Electrophysics and outstanding physics of the world]. Kharkov, NTU «KhPI» Publ., 2008. 252 p. (Rus).
7. Javorskij B.M., Detlaf A.A. *Spravochnik po fizike* [Handbook of physics]. Moscow, Nauka Publ., 1990. 624 p. (Rus).

8. *Bol'shoj illjustrirovannyj slovar' inostrannyh slov* [Large illustrated dictionary of foreign words]. Moscow, Russkie slovari Publ., 2004. 957 p. (Rus).
9. Available at: [https://ru.wikipedia.org/wiki/Эйнштейн,\\_Альберт](https://ru.wikipedia.org/wiki/Эйнштейн,_Альберт) (accessed 10 April 2014). (Rus).
10. Available at: <http://100v.com.ua/en/node/2822> (accessed 12 May 2011). (Rus).
11. Available at: [https://ru.wikipedia.org/wiki/Де\\_Бройль,\\_Луи](https://ru.wikipedia.org/wiki/Де_Бройль,_Луи) (accessed 18 September 2013). (Rus).
12. Grashin A.F. *Kvantovaja mehanika* [Quantum mechanics]. Moscow, Education Publ., 1974, 207 p. (Rus).
13. Available at: [https://ru.wikipedia.org/wiki/Шрёдингер,\\_Эрвин](https://ru.wikipedia.org/wiki/Шрёдингер,_Эрвин) (accessed 15 June 2012). (Rus).
14. Available at: [https://ru.wikipedia.org/wiki/Паули,\\_Вольфганг](https://ru.wikipedia.org/wiki/Паули,_Вольфганг) (accessed 10 April 2014). (Rus).
15. Available at: [https://ru.wikipedia.org/wiki/Гейзенберг,\\_Вернер](https://ru.wikipedia.org/wiki/Гейзенберг,_Вернер) (accessed 21 May 2012). (Rus).
16. Available at: [https://ru.wikipedia.org/wiki/Бор,\\_Нильс](https://ru.wikipedia.org/wiki/Бор,_Нильс) (accessed 10 May 2013). (Rus).
17. Available at: [https://ru.wikipedia.org/wiki/Бозе,\\_Шатъендранат](https://ru.wikipedia.org/wiki/Бозе,_Шатъендранат) (accessed 22 February 2010). (Rus).
18. Available at: [https://ru.wikipedia.org/wiki/Борн,\\_Макс](https://ru.wikipedia.org/wiki/Борн,_Макс) (accessed 21 April 2008). (Rus).
19. Available at: [https://ru.wikipedia.org/wiki/Ландау,\\_Лев\\_Давидович](https://ru.wikipedia.org/wiki/Ландау,_Лев_Давидович) (accessed 18 September 2013). (Rus).
20. Available at: <http://dic.academic.ru/dic.nsf/bse/94619> (accessed 11 May 2011). (Rus).
21. Available at: [http://edu.sernam.ru/lect\\_qe.php?id=13](http://edu.sernam.ru/lect_qe.php?id=13) (accessed 20 August 2012). (Rus).
22. Baranov M.I. Wave distribution of free electrons in conductor with electric current of the conductivities. *Electrical Engineering*, 2005, no.7, pp. 25-33. (Rus).
23. Baranov M.I. New physical mechanisms and approaches in the study of the formation and distribution of the electric conduction current in the conductor. *Tekhnichna elektrodynamika*, 2007, no.1, pp. 13-19. (Rus).
24. Baranov M.I. Characteristic radial distribution of free electrons in a cylindrical conductor with varying electric current. *Tekhnichna elektrodynamika*, 2009, no.1, pp. 6-11. (Rus).
25. Baranov M.I. Features heating thin bimetallic conductor large pulse current. *Elektrichestvo*, 2014, no.4, pp. 34-42. (Rus).
26. Baranov M.I. Quantum-wave nature of electric current in a metallic conductor and some of its electrophysical macrophenomena. *Electrical engineering & electromechanics*, 2014, no.4, pp. 25-33. (Rus). doi: 10.20998/2074-272X.2014.4.05.
27. Baranov M.I. Main characteristics of the wave distribution of free electrons in a thin metallic conductor with a pulse current of high density. *Elektrichestvo*, 2015, no.10, pp.20-32. (Rus).

Received 21.12.2015

M.I. Baranov, Doctor of Technical Science, Chief Researcher, Scientific-&-Research Planning-&-Design Institute «Molnija» National Technical University «Kharkiv Polytechnic Institute», 47, Shevchenko Str., Kharkiv, 61013, Ukraine, phone +38 057 7076841, e-mail: eft@kpi.kharkov.ua

#### How to cite this article:

Baranov M.I. An anthology of the distinguished achievements in science and technique. Part 34: Discovery and study of quantum-wave nature of microscopic world of matter. *Electrical engineering & electromechanics*, 2016, no.5, pp. 3-15. doi: 10.20998/2074-272X.2016.5.01.

V.I. Milykh

## THE NUMERICAL-FIELD ANALYSIS OF THE MAGNETIC FIELD AND THE ELECTRICAL QUANTITIES IN THE TURBOGENERATOR STATOR UNDER AUTONOMOUS UNBALANCED LOADING

*Purpose. Assessing the impact of load asymmetry of turbogenerator (TG) on the magnetic field distribution, on the electrical and energy processes in it based on the numerical-field analysis within the constraints regulated by the standards. Methodology. The calculation model of TG has been constructed on the method of symmetrical components of the three-phase current system. The formed asymmetric system of the currents is used for multi-position numerical calculations of rotating magnetic fields. The temporal functions of the electromagnetic quantities which are subjected to the harmonic analysis are obtained on this basis. Results. Test calculations are conducted on a three-phase 35 MW TG during his work under autonomous unbalanced loading. The analysis of the temporal functions of the magnetic induction at different points of the TG stator and also similar functions of the magnetic flux linkage, EMF phase stator windings and other variables have been executed. Originality. Problems of exploitation of turbo-generators under unbalanced loading are detected by the consideration of their electromagnetic system on the whole, but not their simplified local parts, as usual. It has been shown that the temporal functions of EMF of the phase stator windings under unbalanced loading significantly differ in shape from sine waves and from each other and contain a number of significant upper harmonics. It has been detected that the phase currents would contain not only the first but also significant upper harmonics under unbalanced loading. Practical value. Analysis of the work of TG under unbalanced loading showed the «top» level of problems of electromagnetic character. It has been established that the function of the magnetic induction at the fixed points of the magnetic system on the whole have been changed but not in principle. The temporal functions of EMF, and, hence, the voltage of the stator phase windings significantly differ in shape from sine waves and from each other, there is a considerable imbalance of active powers generated by the individual phase windings of the stator. The information provided will allow the measures to ensure a durable and reliable operation of turbo-generators. References 14, tables 2, figures 9.*

*Key words: turbo-generator, unbalanced loading, magnetic fields, numerical calculations, electromagnetic processes, temporal functions.*

*На основе численных расчетов вращающегося магнитного поля проведена оценка работы турбогенератора при несимметричной нагрузке. Анализируются временные функции магнитной индукции в неподвижных точках магнитной системы статора, форма и гармонический состав ЭДС его обмоток, их мощности. Результаты расчетов при несимметричной нагрузке сопоставляются с аналогичными результатами при симметричной нагрузке. Библ. 14, табл. 2, рис. 9.*

*Ключевые слова: турбогенератор, несимметричная нагрузка, магнитные поля, численные расчеты, электромагнитные процессы, временные функции.*

**Introduction.** Along with the basic mode of operation of turbo-generators (TG) to the symmetrical loading for which they usually are designed [1], by the interstate standard DSU 533-2000 and long-term operation at unbalanced loading is regulated. And this applies both to an autonomous work of TG, and to work on the power system [2].

Operation at unbalanced load leads to a number of additional problems in the operation of TG which are of electromagnetic nature and result increased thermal and power stresses, vibration problems and poor-quality of the three-phase power supply system.

So, for example, for TG up to 100 MV·A, according to the standard and normal VDE 0530, it is allowed a long-term unbalanced load with the negative sequence current up to 8 % of the rated current. At higher power, due to increased exploitation, the permissible unbalanced load should be reduced.

These limitations are the result of numerous studies of unbalanced modes of turbo-generators [3] which showed that we need to strengthen structures for sufficient thermal stability of the rotor.

Calculations at unbalanced loading conducted earlier by analytical methods could not reach the fullness of the electromagnetic processes in the TG. With the development of numerical methods for the calculation of electromagnetic fields, the possibilities of mathematical model-

ing have increased significantly. However, the attempts to study mainly concern the calculation of eddy currents (EC) in the local conductive elements on the surface of the rotor from the magnetic field of the negative sequence with very serious easy simplifications of the calculated area.

For example, in [4] and [5] computer modeling of electromagnetic processes in the TG of 300 MW in two-dimensional formulation at long-term unbalance loading is carried out. The focus is on the study of EC and additional power losses in the rotor slot wedges. However, such conflicting results in these two works are given that we have to doubt their authenticity: the current density and heat generation differ by several orders of magnitude.

To identify problems of operation of TG at unbalanced loading from different sides, and not only in terms of EC in the rotor wedges, with a sufficient degree of adequacy we can only considering TG in general, not limited to its local simplistic parts. The complete formulation is a task of extreme complexity. So here, keeping the overall structure of the TG electromagnetic system, we consider another extreme case of assumptions – the lack of EC response in the rotor elements.

This makes it possible to identify the «top» level of the problems of the electromagnetic nature which in reality will be smoothed by damping reaction of currents in

© V.I. Milykh

the electrically conductive array of the rotor body and its individual elements.

New opportunities for the study of the problems of the electromagnetic nature at the operation of the TG at unbalanced loads are provided by numerical methods of magnetic fields calculation [6, 7] in conjunction with high-speed computers and efficient software. This contributed to the novelty of the results presented, as TG electromagnetic system as a whole is considered.

**The goal of the work.** This work is devoted to assessing the influence of TG unbalance loading on the distribution of the magnetic field, electrical and power processes in them based on the numerical-field analysis within indicated limitations of Standards. This is carried out through the identification and analysis of temporal functions of the magnetic flux density (MFD) at different points of the TG stator and similar functions of the magnetic flux linkage (MFL) and the EMF of phase stator windings.

Numerical methods for the calculation of the magnetic fields are removed restrictions on the account of actual constructive shapes of electric machines as a whole and their elements, on account of the magnetic saturation. Here, powerful modern computers allow you to do this in the statics and dynamics. Examples of such studies are presented in papers by the author [7, 8] and other researchers, for example, in [9].

**Object of investigations.** Demonstration calculations are carried out on a three-phase two-pole TG, a cross section of the electromagnetic system of which is shown in Fig. 1. It has rated: power  $P_N = 35$  MW, phase voltages  $U_{sN} = 6.3$  kV and current  $I_{sN} = 2315$  A at the stator winding circuit – «triangle»; power factor  $\cos\varphi_{sN} = 0.8$ ; frequency  $f_s = 50$  Hz. Active stator length  $l_a = 2.7$  m; nonmagnetic gap – 27 mm; rotor radius – 0.408 m; on the phase stator winding there are  $N_s = 18$  consecutive turns, its relative shortening  $\beta_s = 22/27$ ; phase winding resistances: active  $R_s = 0.00537 \Omega$ ; reactive from a frontal scattering  $X_s = 0.134 \Omega$ ; in the rotor winding the turns number  $N_r = 224$ .

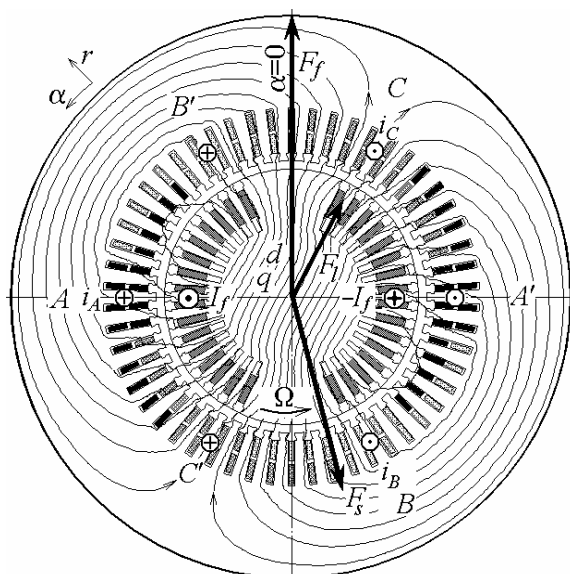


Fig. 1. Calculation model of the turbo-generator with magnetic field distribution at the unbalanced load

**Theoretical basics of the TG unbalanced operation mode analysis.** Unbalanced modes in three-phase TG are results of phase currents difference because of different stator phase windings loadings. These modes are investigated by using the method of symmetrical components [2, 3]. Actually, phase currents of direct  $I_{A1}, I_{B1}, I_{C1}$  and negative  $I_{A2}, I_{B2}, I_{C2}$  sequences as well as resulting currents  $I_A, I_B, I_C$  are considered. Their assumed initial system is presented in Fig. 2 by vector diagram.

In the correspondence with DSU 533-200 RMS of negative sequence currents are assumed  $0.08 \cdot I_{sN}$ . Besides, maximal RMS of all resulting phase currents is limited by rated value  $I_{sN}$ .

On this basis, by calculation it is determined that the phase currents RMS are  $I_A = 2170.2$  A;  $I_B = 2314.7$  A;  $I_C = 2015.3$  A, and more detailed methods of their calculation is presented in [10].

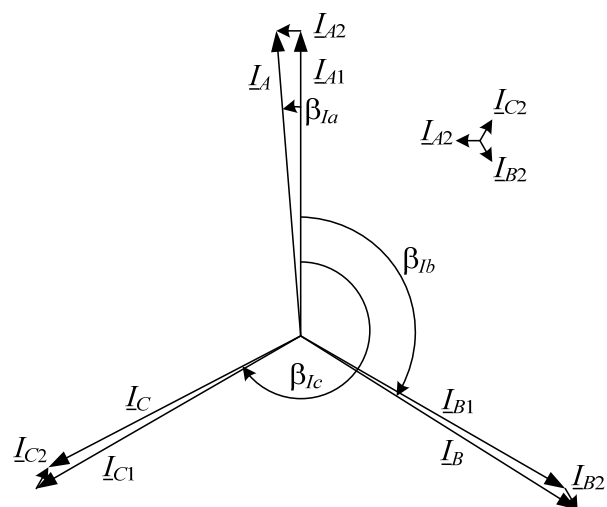


Fig. 2. Phase currents of direct and negative sequence and resulting TG currents

In the calculations of rotating magnetic fields instantaneous values of phase currents are used [7, 8]. In this paper, at unbalanced loading phase currents are defined by their temporal functions:

$$\begin{aligned} i_A &= I_{ma} \cdot \cos(\omega \cdot t + \beta_{Ia} + \beta); \\ i_B &= I_{mb} \cdot \cos(\omega \cdot t + \beta_{Ib} + \beta); \\ i_C &= I_{mc} \cdot \cos(\omega \cdot t + \beta_{Ic} + \beta), \end{aligned} \quad (1)$$

where  $\omega = 2 \pi f_s$  is the angular frequency;  $I_{ma}, I_{mb}, I_{mc}$  are the amplitudes of currents determined by their above-mentioned RMS.

The initial phase of currents  $\beta_{Ia}, \beta_{Ib}, \beta_{Ic}$  determined initially by summing the vectors in Fig. 2 and therefore rigidly connected with each other. They were then turned on all selected by numerical experiments a certain angle so that when  $\beta = 0$  resulting MMF of the stator winding  $F_s$  is directed along the longitudinal rotor axis  $d$  which is shown in Fig. 1. In such a way the necessary initial phase are received:  $\beta_{Ia} = 9.15^\circ$ ;  $\beta_{Ib} = -117.56^\circ$ ;  $\beta_{Ic} = -237.88^\circ$ .

In (1) additional rotation angle  $\beta$  for all currents, respectively, rotates vector  $F_s$  of MMF at the same angle with the proviso that when at predetermined stator currents and excitation current to provide the required output

electric power of TG as presented in [11]. Placed in such a position vector  $F_s$  is shown in Fig. 1. Together with the vector of MMF of field winding  $F_f$  they form a conditional resulting MMF at the load mode  $F_l$ .

The system of phase relationships of electromagnetic quantities in TG is presented in detail in [11] for the mode of its symmetrical loading. This angle  $\beta$  and field current  $I_f$  are determined by a special technique from the condition that they must provide the nominal output data of the TG:  $U_{sN}$  voltage and power factor  $\cos\varphi_{sN}$  which makes at a rated current of the stator  $I_{sN}$  rated active power  $P_N$ . Specifically, for the considered TG at the symmetrical loading  $\beta = -165.12^\circ$  and  $I_f = 632$  A are detected. The RMS of the phase currents were  $I_A=I_B=I_C=2315$  A and in the system (1)  $\beta_{la} = 0$ ;  $\beta_{lb} = -120^\circ$ ;  $\beta_{lc} = -240^\circ$  were adopted.

To adequately reflect changes that occur in the TG at the transition from symmetric to unbalanced loading, it was found that here the control actions on TG absent. That is, from the turbine to the TG shaft the same mechanical power is supplied and excitation current is stored, as that at the symmetrical loading. On this basis by numerical experiments using already called  $\beta$  value as the first approximation, it was found that the rated power at unbalanced loading is obtained at  $\beta = -167.2^\circ$  and presented excitation current  $I_f = 632$  A. The vector diagram of formed asymmetrical current system and obtained as results of computation other electromagnetic quantities calculation is presented below.

For the analysis of electromagnetic processes in the active part of the TG magnetic field at given its winding currents is calculated in 2D formulation in its cross section (Fig. 1). This field is described by the known differential equation

$$\operatorname{rot}\left[\frac{1}{\mu}\operatorname{rot}(\vec{k}A_z)\right]=\vec{k}J_z, \quad (2)$$

where  $A_z$ ,  $J_z$  are axial components of the magnetic vector potential (MVP) and current density;  $\mu$  is the absolute magnetic permeability;  $\vec{k}$  is the ort by axial axis  $z$ .

**Organization of calculation of temporal functions of electromagnetic quantities.** The values stated with the purpose of the work of values of MFD, MFL and EMF are determined based on the calculation of the magnetic field of TG and their temporal functions by such multi-position calculations [7, 8] for time series with step  $\Delta t$ :

$$t_k=\Delta t\cdot(k-1); k=1, 2, \dots, K, \quad (3)$$

at corresponding angular positions of the rotor

$$\alpha_k=\Delta\alpha(k-1); k=1, 2, \dots, K, \quad (4)$$

and with synchronous stator magnetic field rotation by changing of phase currents (1) in its winding in the correspondence with series  $t_k$  (3).

In (3) and (4)  $\Delta\alpha=\Omega\cdot\Delta t$ ,  $\Omega=\omega/p$  are the angular step and the rotor rotation speed;  $p$  is the number of pole pairs.

Symbol  $K$  in (3), (4) denotes the number of positions permitting to adequately form temporal functions on their period  $T$ .

Considered in this work functions have semiperiodic asymmetry with a condition like

$$\Gamma(t_k + T/2) = -\Gamma(t_k), k=1, 2, \dots, K, \quad (5)$$

where  $\Gamma$  is the yet generalized letter.

Therefore, functions of actual quantities taking into account the TG magnetic field periodicity are formed at the rotor rotation from 0 to  $180^\circ$  with angular step of  $1^\circ$ , i.e.  $K$  equals to 180.

The magnetic field based on (2) is calculated by the finite element method taking into account the saturation of the core by the FEMM software [12]. Operations during its work on the calculation of the field, the definition of electromagnetic parameters and the formation of temporary functions are carried out by the control program written on the algorithmic language Lua [13].

Magnetic field distribution at the unbalanced loading mode at initial time is shown in Fig. 1 by magnetic field lines. Note that the structure of the magnetic field corresponds approximately to what was the case in the symmetrical loading.

#### Temporal functions of the magnetic flux density.

The base quantity used in electromagnetic calculations is the magnetic flux density in the form of its radial and angular components as well as its module:

$$B_r = \frac{1}{r} \frac{\partial A_z}{\partial \alpha}; B_\alpha = -\frac{\partial A_z}{\partial r}; B = \sqrt{B_r^2 + B_\alpha^2}. \quad (6)$$

Note that in areas of the laminated cores the FEMM software «outputs» MFD values «smeared» for the whole of their axial length. Therefore, it is necessary to divide these values into  $k_{Fe}$  – filling factor of the core by steel. Then we obtain the MFD values directly for the steel sheets. For the considered TG taking into account laminating and packaging of the stator core, this ratio was 0.78.

In the fixed points of the TG electromagnetic system by already represented principle temporary MFD functions in discrete form are obtained:

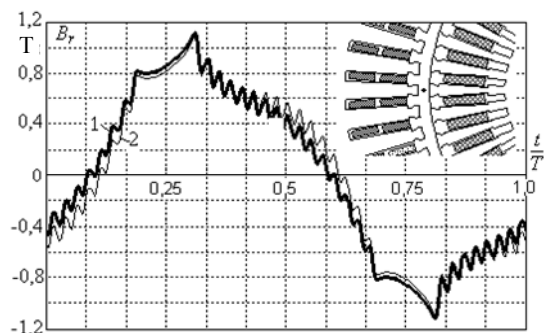
$$B_r(t_k), B_\alpha(t_k), B(t_k), k=1, 2, \dots, K. \quad (7)$$

Note that at the expansion of the values obtained to the second half period by the condition (5) for the module of  $B$  it is not necessary to change the sign.

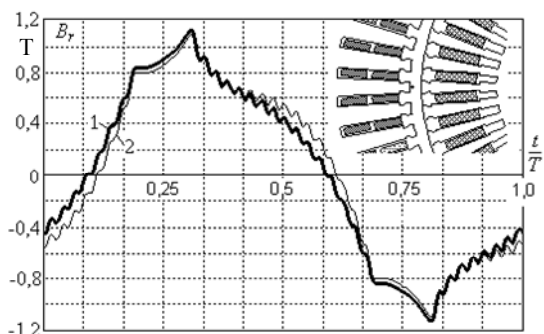
Distributions of temporal functions (7) for two fixed points in the gap are shown in Fig. 3 where time is given in relative units. Variant  $a$  corresponds to the point in the middle of the gap,  $b$  – on the bore of the stator core.

The presented functions are far from sinusoidal. In these charts there are clear zones of influence of the large rotor teeth and claw tooth pulsations from the rest of its teeth. The pulsations are amplified as they approach the surface of the rotor (from Fig. 3b to Fig. 3a). In temporary functions in fixed points tooth pulsation from the stator core are not shown as it is presented more in [8].

Fig. 4 shows the temporal function of the radial component of the magnetic flux density in the tooth of the stator core in the indicated on the fragment of the Figure points  $z1$  and  $z2$  – in its crown and the base. Functions  $B_r(t)$  again far from sinusoidal, and substantially are formed by toothed rotor structure, although with some damping of tooth pulsations compared to what it was in the gap (Fig. 3). Obtained charts indicate that adopted in the design of TG sinusoidal character of the magnetic flux density in the teeth is a very rough approximation.



a



b

Fig. 3. Temporal functions of the MFD radial component in the indicated points in the gap on the stator core tooth:  
1 – asymmetry; 2 – symmetry

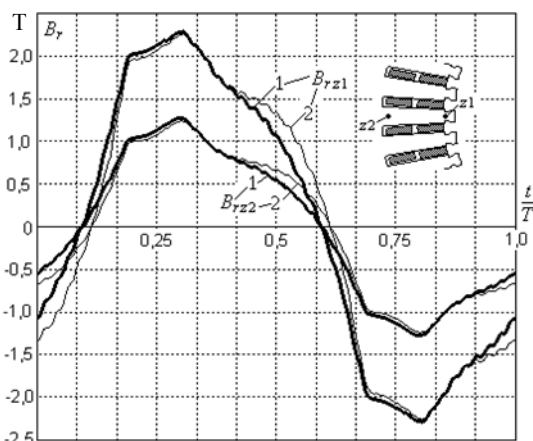


Fig. 4. Temporal functions of the radial component  $B_r$  of the magnetic flux density in the stator core tooth:  
1 – asymmetry; 2 – symmetry

Fig. 5 shows the temporal functions of the angular component  $B_\alpha$  and the MFD module  $B$  in the indicated point at the back of the stator core. Functions  $B_\alpha(t)$  are close to sinusoidal, although experiencing some distortions, reaching from the functions already present in the gap and teeth.

In general, in Fig. 3 – 5 differences for various types of the TG loading though are noticeable but not fundamental. A general interest is the nature of these functions the obtaining of which is, in principle, it has been possible on the basis of multiposition calculations of the magnetic fields. This is a non-trivial approach to electric machines in general.

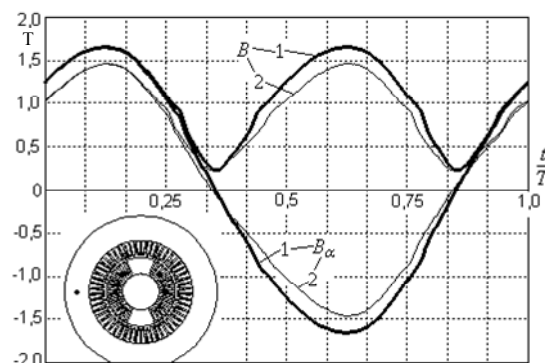


Fig. 5. Temporal functions of the angular component  $B_\alpha$  and module  $B$  of the magnetic flux density in the stator core:  
1 – asymmetry; 2 – symmetry

**Magnetic flux leakage and EMF of stator phase windings.** As it was already presented in [7] the base of the EMF is the temporal MFL function of the stator phase winding.

MFL is obtained by the MVP distribution. For example, for each of the six phase zones (Fig. 1) MFL is determined by the formula

$$\Psi = \frac{N_s I_a}{S_\phi} \int_{S_\phi} A_z dS, \quad (8)$$

there  $S_\phi$  is the sectional area by conductive phase zone's elements.

Determination of the MFL by the formula (8) is not difficult since to determine  $S_\phi$  and the integral in the integrated in the FEMM software Lua script there are appropriate procedures [14].

For all phase winding, for example for the phase  $A$ , MFL is obtained by the formula

$$\Psi_A = \Psi_{sA} - \Psi_{sA'}, \quad (9)$$

there  $\Psi_{sA}$  и  $\Psi_{sA'}$  are the MFL in the phase zones  $A$  and  $A'$  (Fig. 1) determined by formula (8).

On this base in the process of already described calculation of the rotating magnetic field the discrete temporal MFL function is formed

$$\Psi_s(t_k), k=1,2,\dots,K, \quad (10)$$

where the index  $s$  is the generalized letter of any phase windings:  $A, B, C$ .

The function  $\Psi_s(t_k)$  is decomposed as in [7, 8] according to known rules in the cosine harmonic series of odd harmonics taking into account the condition (5)

$$\Psi_s = \sum_{\nu=1,3,5\dots}^{N_g} \Psi_{m,\nu} \cos(\nu \omega t + \gamma_\nu), \quad (11)$$

where the summation over harmonics numbers  $\nu$  is possible until  $N_g$  number which, in principle, is limited by accepted in (5, 10) value of  $K$ .

Based on the law of electromagnetic induction a transition from (11) to the phase winding EMF is carried out:

$$e_s = -\frac{d\Psi_s}{dt} = \sum_{\nu=1,3,5\dots}^{N_g} \nu \omega \Psi_{m,\nu} \cos(\nu \omega t + \gamma_\nu - \pi/2), \quad (12)$$

from here amplitudes of harmonics  $E_{m,\nu} = \nu \omega \Psi_{m,\nu}$  are obtained.

Temporary functions of MFL (11) and EMF (12) were determined for each of the phase windings and at the unbalanced loading were, of course, different. They are shown in their full period of the change in Fig. 6.

For comparison, calculations were carried out using the same procedure and under TG symmetric load. The corresponding results are shown in Fig. 7.

Obviously, at the symmetric loading the temporal MFL functions are close to sinusoidal, but in the nature of the EMF a marked influence of the higher harmonics has shown, which, unlike similar MFL harmonics multiplied by their numbers.

At the unbalanced load EMF functions difference of different phases and how they differ from regular sine waves appeared a much greater extent, and the distortions and the differences are already noticeable and for source for EMF the MFL functions.

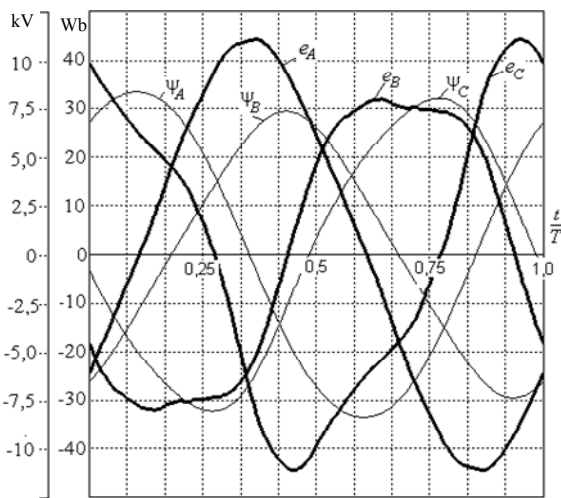


Fig. 6. Temporal functions of the phase MFL and EMF at the TG unbalanced loading

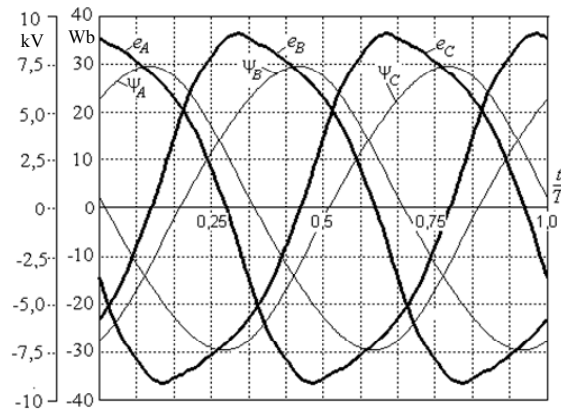


Fig. 7. Temporal functions of the phase MFL and EMF at the TG symmetric loading

Sense shown «top» level of the electromagnetic nature of the problems is that understood: for their «anti-aliasing» to an acceptable level requires an adequate response these currents, which actually transports them to a problem with the current, which is also a serious problem with asymmetrical operation TG load. Table 1 shows the numerical data for the phase EMF at the TG unbalanced loading. Here, the amplitude of the first EMF harmonic  $E_{m,1}$  and its RMS  $E_{s,1}$  are given in absolute terms, and the

amplitude of the higher harmonics – in the relative form  $E_{m,v,*} = E_{m,v} / E_{m,1}$ . In general, the influence of higher harmonics is estimated by the distortion coefficient

$$d_{dist} = \frac{E_{m,1}}{\sqrt{\sum_{v=1}^{N_g} E_{m,v}^2}} \quad (13)$$

Table 1

Harmonic composition of the stator winding EMF				
Phase	$E_{m,1}, V$	$E_{s,1}, V$	$E_{m,3,*}$	$E_{m,5,*}$
A	10702	7568	0.043	0.007
B	8865	6268	0.144	0.018
C	10071	7121	0.183	0.015
Phase	$E_{m,7,*}$	$E_{m,9,*}$	$E_{m,11,*}$	$d_{dist}$
A	-	0.005	0.003	0.999
B	0.003	0.007	0.003	0.990
C	0.004	0.008	0.004	0.983

The large proportion of the third harmonic is obvious which at the «triangle» scheme will also create a problem of significant parasitic circulating currents in the three phase windings [5].

In addition to the already mentioned values of phase relations in (1), from the expansion type (11) for each phase winding by the argument  $\gamma_v$  the initial phases of the MFL  $\gamma_{\psi a}, \gamma_{\psi b}$  and  $\gamma_{\psi c}$  for the first harmonics are determined. Phase EMF behind their MFL for  $\pi/2$  or  $90^\circ$ , respectively (12). Then the initial phases of the EMF are  $\gamma_{Ea} = \gamma_{\psi a} - 90^\circ$ ;  $\gamma_{Eb} = \gamma_{\psi b} - 90^\circ$ ;  $\gamma_{Ec} = \gamma_{\psi c} - 90^\circ$ . Determined are the phase shifts of the EMF with respect to currents of their phase windings:

$$\varphi_{IEa} = \gamma_{Ea} - \beta_{Ia}; \varphi_{IEb} = \gamma_{Eb} - \beta_{Ib}; \varphi_{IEc} = \gamma_{Ec} - \beta_{Ic} \quad (14)$$

All these phase relationships and relationships of values of the phase currents, MFL, EMF and voltages are represented in scale in Fig. 8 by means of the vector diagram. This corresponds to the first harmonics of the electromagnetic quantities of the TG at unbalanced loading for all the phase windings.

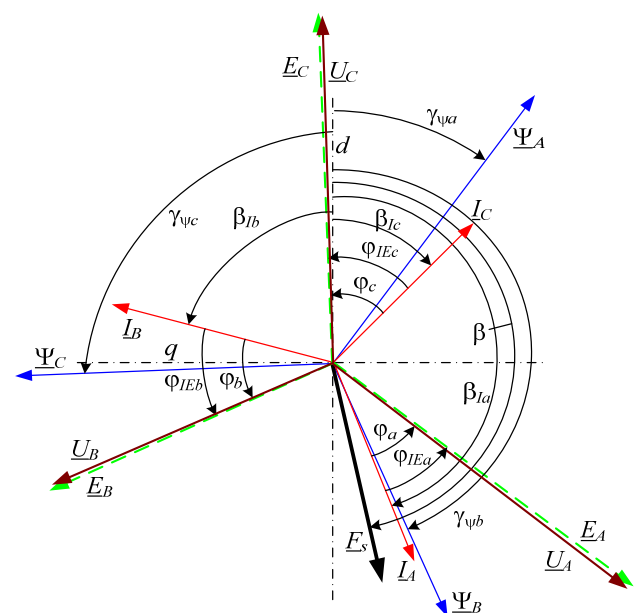


Fig. 8. Vector diagram of the electromagnetic quantities at the TG unbalanced loadings

The definition of the phase voltage we conduct on an example of the phase winding  $A$ . Necessary for this fragment to the vector diagram of Fig. 8 is shown in Fig. 9a in original and with the increase of the scale, and in the rotated view without observing the proportions is shown in Fig. 9b. Here, in addition the voltage drop on the active resistance of  $\underline{U}_R=R_s \underline{I}_A$  as well as EMF from the flow of frontal scattering  $\underline{E}_v=-jX_v \underline{I}_A$  are shown.

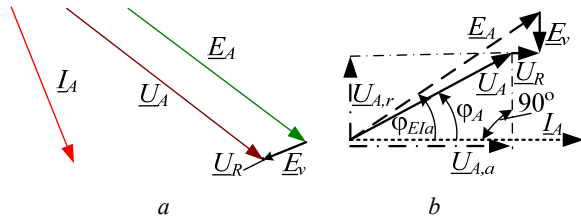


Fig. 9. Fragments of the vector diagram

From geometrical relations in Fig. 9b active and reactive voltage components, its RMS and phase shift from the vector of current, as well as active power are obtained:

$$U_{A,a} = E_A \cos \varphi_{IEa} - U_R; \quad U_{A,r} = E_A \sin \varphi_{IEa} - E_v; \quad (15)$$

$$U_A = \sqrt{U_{A,a}^2 + U_{A,r}^2}; \quad \varphi_{SA} = \arctg(U_{A,r} / U_{A,a}); \quad (16)$$

$$P_{aA} = U_A I_A \cos \varphi_{SA}. \quad (17)$$

Similarly, all done for the other phase windings and calculation results with the generalizing index  $s$  are presented in Table 2. Obviously, the total active power of the TG was 34.90 MW, i.e. almost nominal power is generated. At the reduced stator currents but at rated excitation current this was due to the increase in EMF and voltage due to the increase of the MFL with reduced armature reaction.

Table 2

Calculation data at the unbalanced loading					
Phase	$I_s$	$U_s$	$\cos \varphi_s$	$\varphi_s$ , grad	$P_{as}$ , MW
A	2170	7489	0.861	30.55	14.00
B	2315	6174	0.785	38.28	11.22
C	2015	7029	0.684	46.86	9.69

In Table 2 we should pay attention to the difference of the phase windings loadings – by active power and the nature set by specified power factor. This means that one of the reasons of the specifically considered unbalance is different nature and value of the phase resistances of the three-phase loading.

The value of the phase voltages in Table 2 is not very different from the phase EMF in Table. 1. Therefore, the voltages have approximately the same harmonic composition as EMF. So, the phase currents will have the similar composition. Thus, the unbalanced loading is always accompanied by not sinusoidal and more complicated functions as harmonic series of about the same composition as in Table. 1.

From all of this it follows that the adopted sinusoidal character of currents here (1) and in the Standard is another major assumption of the calculation method adopted in this paper and in the calculations of the unbalanced loading in the mentioned [4, 5] and other similar works.

Apparently, the more precise formulation of the problem of calculation of unbalanced modes of operation

is to harmonize the temporal function of the phase currents and EMF – perhaps by the iterative way or another effective technique.

Defined in [10] and continued here research theme does not exhaust the possibilities of the developed method of analysis of the TG unbalanced operation mode. This method allows you to continue the study started, and, above all, the consideration of the electromagnetic processes in the rotor and force actions in the entire electromagnetic system of the TG.

### Conclusions.

1. Problems of exploitation of TG at asymmetrical loading it is possible to fully identify in quite considering the TG as a whole, and not its local simplified parts. Here, to analyze a wide range of problems of the electromagnetic nature an effective base is the multiposition numerical calculations of rotating magnetic fields allowing to form temporal functions of the considered quantities.

2. An extremely difficult problem of analyzing the electromagnetic phenomena in the overall structure of the TG electromagnetic system is just solved under the assumption of lack of response of the EC in the rotor design elements, as well as how it was identified, sinusoidal nature of the TG phase currents. It is possible to reveal the ultimate level of the problems of the electromagnetic nature which in reality will be smoothed by the damping reaction of indicated currents.

3. By the considered complex of the electromagnetic phenomena within standard limits of the TG unbalanced mode it was found that:

- functions of the magnetic flux density in the fixed points of the magnetic system in general have changed, but not the principle, in the gap and the teeth of the stator core they are far from sinusoidal and in addition they even have a tooth pulsations due to the rotor core, in the back of the stator it is close to sinusoids;

- temporal EMF functions and, hence, the stator windings phase voltages by the shape are significantly different from sine waves and each other, differences of such EMF are obvious by values, too;

- there is a significant imbalance of active powers generated by the individual stator phase windings.

4. Sense shown «top» level of the problems of the electromagnetic nature is that understood: for their «smoothing» to the acceptable level an adequate reaction of indicated currents is required which actually transports problems from them to these currents that is also a serious problem of the TG exploitation at the unbalanced loading.

### REFERENCES

1. Izvekov V.I., Serihin N.A., Abramov A.I. *Proektirovanie turbogeneratorov* [Planning of turbogenerators]. Moscow, MEI Publ., 2005. 440 p. (Rus).
2. Kogan F.L. *Anormal'nye rezhimy moshchnykh turbogeneratorov* [Anormal modes of powerful turbogenerators]. Moscow, Energoatomizdat Publ., 1988. 188 p. (Rus).
3. Ter-Gazaryan G.N. *Nesimmetrichnye rezhimy sinkhronnykh mashin* [Asymmetrical modes of synchronous machines]. Moscow, Energiya Publ., 1969. 214 p. (Rus).
4. Shulzhenko N.G., Pantelyat M.G., Rudenko E.K., Zozulin Yu.V. Additional losses in a turbogenerator rotor under long-time unbalanced load. *Electrical engineering & electromechanics*.

ics, 2006, no.1, pp. 54-57. (Rus). doi: 10.20998/2074-272X.2006.1.11.

5. Yu.V. Zozulin, O.Ye. Antonov, V.M. Bychik, A.M. Borychevs'kyy, K.O. Kobzar, O.L. Livshyts', V.H. Rakohon, I.Kh. Rohovyy, L.L. Khaymovych, Cherednyk V.I. *Stvorennja novykh tytip ta modernizacija dijuchyh turbogeneratoriv dlja teplovykh elektrychnykh stancij* [Creation of new types and modernization of the existing turbogenerators for the thermal electric stations]. Kharkiv, PF Kolehium Publ., 2011. 228 p. (Ukr).

6. Bianchi Nicola. *Electrical Machine Analysis Using Finite Elements (Copyrighted Material)*. CRC Press, Taylor & Francis Group, University of West Florida, 2005. 276 p.

7. Milykh V.I., Polyakova N.V. Determination of electromagnetic parameters of electric machines based on numerical calculations of magnetic field. *Electrical engineering & electromechanics*, 2006, no.2, pp. 40-46. (Rus). doi: 10.20998/2074-272X.2006.2.09.

8. Milykh V.I., Polyakova N.V. Calculated and harmonic analysis of the magnetic fields in the active zone of the turbogenerator in the load mode. *Electrical engineering & electromechanics*, 2013, no.6, pp. 40-45. (Rus). doi: 10.20998/2074-272X.2013.6.07.

9. Tytko O.I., Melnyk A.M. Modelling and distribution of electromagnetic forces operated on the teeth and the cores of stator winding of the turbogenerator. *Tekhnichna elektrody-namika*, 2015, no.3, pp. 40-46. (Ukr).

10. Milykh V.I. Organization of the numerical-field calculations of electromagnetic processes in a turbogenerator at its asymmetrical loading. *Bulletin of NTU «KhPI». Series: «Electric ma-*

*chines and electromechanical energy conversion*», 2016, no.11(1183), pp. 3-10. (Rus).

11. Milykh V.I., Polyakova N.V. Organization of numerical calculation of turbogenerator magnetic field under load with specified output parameters control. *Electrical engineering & electromechanics*, 2012, no.1, pp. 36-41. (Rus). doi: 10.20998/2074-272X.2012.1.08.

12. Meeker D. *Finite Element Method Magnetics. FEMM 4.2 32 bit 11 Oct 2010 Self-Installing Executable*. Available at: [www.femm.info/wiki/OldVersions](http://www.femm.info/wiki/OldVersions) (accessed 10 March 2014).

13. Milykh V.I., Polyakova N.V. Automated calculations of the dynamics of turbogenerator electromagnetic processes in software environment FEMM. *Electrical engineering & electromechanics*, 2015, no.6, pp. 24-30. (Rus). doi: 10.20998/2074-272X.2015.6.04.

14. Milykh V.I., Polyakova N.V. Determination of electromagnetic parameters and phase relations in turbo-generators by the automated calculation of the magnetic field in the software environment FEMM. *Electrical engineering & electromechanics*, 2016, no.1, pp. 26-32. doi: 10.20998/2074-272X.2016.1.05.

Received 26.07.2016

V.I. Milykh, Doctor of Technical Science, Professor,  
National Technical University «Kharkiv Polytechnic Institute»,  
21, Kyrpychova Str., Kharkiv, 61002, Ukraine.  
phone +38 057 7076514, e-mail: mvikemkpi@gmail.com

#### How to cite this article:

Milykh V.I. The numerical-field analysis of the magnetic field and the electrical quantities in the turbogenerator stator under autonomous unbalanced loading. *Electrical engineering & electromechanics*, 2016, no.5, pp. 16-22. doi: 10.20998/2074-272X.2016.5.02.

M.A. Polyakov, T.Y. Larionova

## EFFICIENCY EVALUATION TECHNIQUE OF THE SEMICONDUCTOR DC-DC CONVERTER APPLICATION IN THE POWER-SUPPLY SYSTEM

*Purpose.* To specify efficiency evaluation of the DC-DC power semiconductor converter application in the power-supply system. *Methodology.* We have chosen application version of converter and then used the statistical modeling of DC-DC converter for its efficiency evaluation at varied input voltage according to proposed technique. We have compared the simulated result with the data presented in reference literature. *Results.* We have proposed the efficiency evaluation technique of converter application. *Proposed technique includes* detection of external factors influenced on the converter efficiency; development of efficiency evaluation models; selecting application version of converter; determination of the correlation coefficients between the values of external factors; definition of the converter efficiency; obtaining of the converter efficiency distribution. *Originality.* For the first time, we have developed the evaluation technique of converter efficiency corrected for application version of converter. *Practical value.* Presented in the study results could be useful for specialists in semiconductor equipment, electrical facilities and systems. References 10, figures 8.

*Key words:* semiconductor converter, efficiency of converter application, statistical modeling, evaluation of the effectiveness, converter efficiency.

*Разработана методика оценки эффективности использования полупроводникового преобразователя в системе электроснабжения. Методика включает выявление множества внешних факторов, влияющих на эффективность использования преобразователя; разработку модели оценки эффективности как функции внешних факторов; выбор варианта использования преобразователя; установление коэффициентов корреляции между значениями внешних факторов; определение значений КПД преобразователя; нахождение распределения КПД преобразователя. Применение предложенной методики проиллюстрировано на примере синхронного промежуточного вольтдобавочного преобразователя постоянного напряжения. Для этой цели выполнено статистическое моделирование преобразователя этого типа при стохастическом изменении входного напряжения. Библиография 10, рис. 8.*

*Ключевые слова:* полупроводниковый преобразователь, эффективность использования преобразователя, статистическое моделирование, оценка эффективности, КПД преобразователя.

**Introduction.** To meet the power requirements of different types and parameters, and to effectively manage its various distribution converting devices are needed. An important requirement which is presented to the converters is to provide high performance.

Semiconductor converters have a high efficiency, so are widely used in industrial equipment and electric transport [1].

To quantify the efficiency we use the ratio of output power (or energy) to the power consumed by the converter from the mains, at a certain input voltage and load, often nominal. For converters the value of efficiency contained in the documents and is one of the important indicators. Reduced efficiency in converters due to losses in the converter electronic components – power semiconductor devices (PSD), transformers, inductance, capacitance. Basic types of losses in converters are switching losses arising at the switching of power switches, conduction losses and [2]. Known studies [3-5] are aimed at finding the maximum efficiency of the converter which is achieved by selecting the topology optimization of the parameters of passive components, the use of PSD with a low resistance in the conducting state

and switching losses, choice of algorithm switching and PSD switching frequency. The quantity also depends on the efficiency of external factors such as input voltage, load resistance, and others. There are a number of applications of semiconductor converters which are characterized by a change in a wide range of input voltage and load current. It is for wind energy converters, power supply from the battery, electric motor and other. Researchers [6] revealed dependence  $E = f(V_{in}, I_o)$  which are the extremum in the middle ranges of values  $V_{in}$  and  $I_o$ . For example, the input voltage of the converter power supply system of own needs (SSON) of electric rolling stock (ERS) varies widely (on the susceptor of the electric rolling stock with a nominal voltage of 3000 V – from 2200 to 3850 V [7]). In this case, most of the time converter of the SSON works at non-optimal conditions, its efficiency is reduced [8].

**Problem definition.** In itself, the value of the efficiency does not provide complete information about the amount of energy loss in the converter in particular its application in the power supply system, as the use mode converter may differ from that in which the efficiency

was measured. In real terms the converter operates in a range of efficiency. Therefore, to the average evaluating the effectiveness of the use of the converter in the power supply system needs to take into account the nature of the change in time of the input voltage and load. Depending on the application, the converter, these changes can be both deterministic and stochastic.

**The goal of the work** is to update evaluation the effectiveness of the use of the DC voltage inverter in the power supply system.

For the efficiency density distribution and integral distribution function of the efficiency the applied method of statistical Monte-Carlo simulation is used.

### Results of investigations.

The proposed technique includes the following stages:

1. Identification of a number of external factors  $A_{ext}$  on which the efficiency of the converter depends. As a rule, they are voltage  $V_{in}$  and current  $I_o$ .

2. Development of a model for converter efficiency evaluation as a function of external factors  $\text{Efficiency} = f(A_{ext})$ . As is known, the converter efficiency is determined in the losses of its circuit elements. These losses depend on the ratings and the quality of its circuit elements, and the switching converter topologies key algorithms. At the stage of evaluation of the efficiency of the model are identified depending on the components of loss on external factors values.

3. To select the option of using the converter, which is described by some time interval  $[t_1, t_2]$ , duration  $\Delta t$ , in time changes the characteristics of the external factor values  $A_{ext} = f(t)$ ,  $t \in [t_1, t_2]$  including a range of possible values  $[A_{ext\_min}, A_{ext\_max}]$  and the duration of action to the converter of external factor with a value  $A_{ext}$ . At the stochastic nature of the change in time value of external factors  $A_{ext(i)}$  to determine the probability density function of values  $A_{ext(i)}$  on the converter model input.

4. To determine the correlation coefficients between the values of external factors on the inputs of the converter model. These factors are taken into account when setting the values of the dependent from each other external factors. For example, intelligent power supply control system can limit the load at lower voltage  $V_{in}$  to a critical value.

5. To calculate the converter efficiency by modeling his work with the given values of external factors for each subinterval  $\Delta t_i$  owned interval  $\Delta t$ . For stochastically changing external factors to conduct a series of experiments with the converter model and the values of the input factors, which are randomly selected, taking into account the probability of occurrence of a given value.

6. The resulting simulation efficiencies to divide into ranges of values and to determine the relative frequency

of efficiency values belonging to each interval. On the basis of these frequencies to determine the density distribution and the cumulative distribution function of the converter efficiency for the selected option of using it.

We illustrate the proposed methodology on the example of evaluating the effectiveness of the use of a synchronous buck-boost DC converter at random variation of the input voltage. Functional diagram of the considered converter is shown in Fig. 1 [9].

To evaluate the effectiveness of the converter we perform actions according to the proposed method.

1. As input factor we selected  $V_{in}$  which, as noted above, significantly influences the efficiency of the converter.

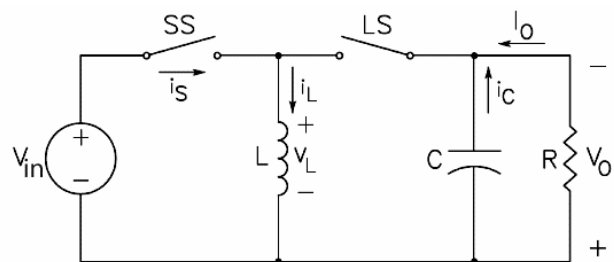


Fig. 1. Functional diagram of a synchronous buck-boost DC converter

2. To obtain the dependence of the efficiency of the converter voltage varying randomly we simulated a synchronous buck-boost DC converter. As the basis of the model a Simulink model of a synchronous DC buck-boost converter with a subsystem that performs the output power, the loss of power and efficiency of the converter calculation is taken [9].

Fig. 2 shows a model of a synchronous buck-boost DC converter and Fig. 3 demonstrates subsystems that perform calculation of output power, power losses and converter efficiency. The model takes into account the main factors affecting the efficiency of the converter: Key resistance in the open state; direct drain-source voltage; duty cycle; operating frequency; fall time and rise time when the key switch; static and dynamic losses in the inductor and the capacitor equivalent series resistance.

The presented in Fig. 3 model for calculation of efficiency determines the power losses in the converter as the sum of the power loss in the switch to the keys (SS Switch Loss and LS Switch Loss), the power loss in the keys in the conductive state (SS Conduction Loss and LS Conduction Loss), losses in «internal» key diode (LS Body Diode Loss), the losses due to «dead time» (Dead-Time Loss).

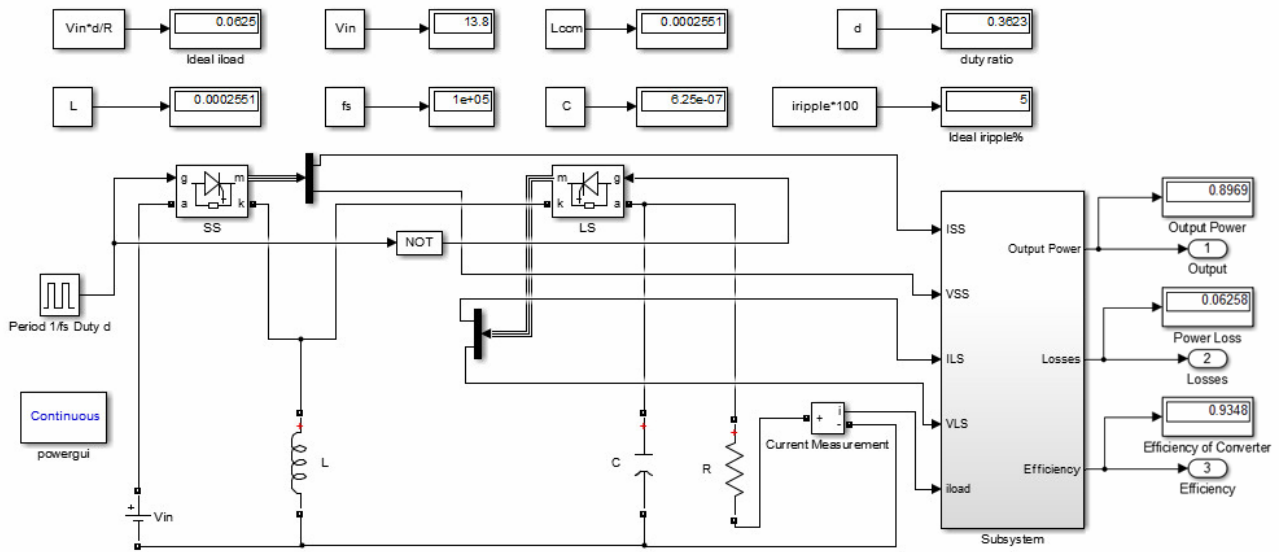


Fig. 2. A model of the synchronous buck-boost DC converter

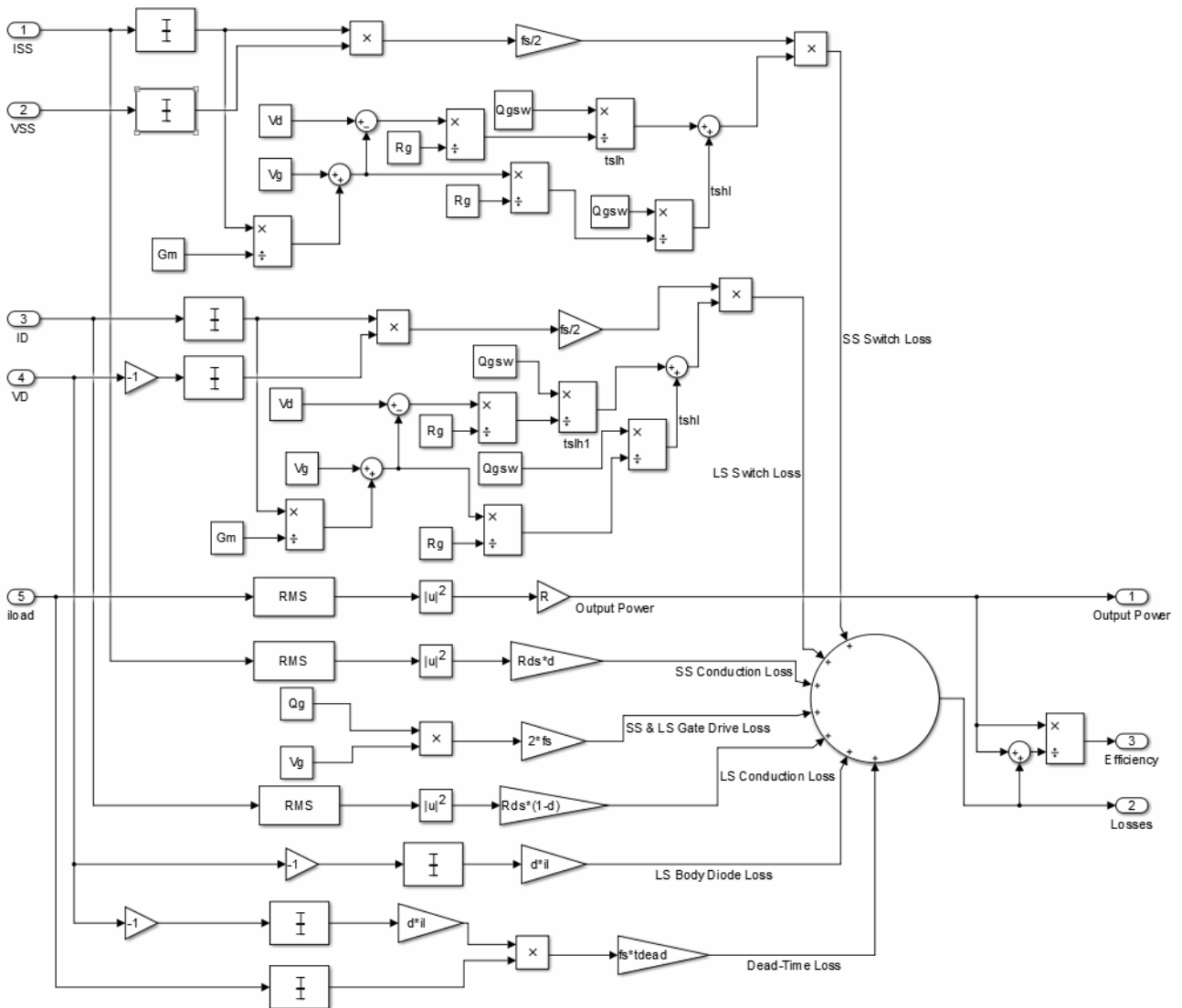


Fig. 3. A model of the subsystem calculating output power, power losses and efficiency

Parameters values of model's elements not specified in [9] are presented in the *m*-file listing (Fig. 4).

```

%Buck Evaluation Parameters
Vin=17.17; %Volt - Input Voltage, use highest value if source varies
Vout=5; %Volt - desired output voltage
fs=100e3; %1/Second - define switching frequency
vripple=0.05; %max acceptable voltage ripple
iripple=0.05; %max acceptable current ripple
R=80; %ohm - load resistance, purely resistive assumed (j0)
P=1/fs; %Second - switching period
d=Vout/Vin; %unitless ratio - duty ratio calculation
Qgs=20e-9; %MOSFET switching-point gate charge (Coulomb)
Qg=175e-9; %MOSFET gate charge (Coulomb)
il=0.15; %load current (Amp)
tdead=60e-9; %dead time (sec)
Rds=0.5; %RDS=PMOS forward conduction ON resistance (Ohm)
Gm=0.32e-3; %MOSFET transconductance
Vg=3; %MOSFET gate switching voltage
Rg=50; %MOSFET gate resistance
Vd=0.8; %voltage across diode
Lccm=((Vin-Vout)*R)/(2*fs*Vin); %Henry - minimum L value for CCM
Lambda=(2/iripple)*(Vout/R); %inductor scaling factor -
%intermediate calculation
L=Lccm; %Henry - inductor size at absolute minimum for CCM
%L=Lccm*Lambda %Henry - inductor size accounting for current ripple
C=(1-(Vout/Vin))/(8*L*vripple*fs^2); %Farad - capacitor calculation

```

Fig. 4. Listing of the *m*-file setting parameters of the converter's circuit elements

3. We simulate the conditions specific to the converter SSON ERS. The voltage at the input of the converter ( $V_{in}$ ) depends on the voltage of the traction substation, the ERS position relative to the points of the supply voltage to the contact wire, the presence of other loads at the site of the power station, weather conditions and other factors, wearing casual character. In accordance with the provisions of the central limit A.M. Lyapunov theorem if the random variable  $x$  is the sum of a very large number of mutually independent random variables, each of which impact on the entire amount is negligible, then  $x$  is distributed according to a law close to normal [10]. Therefore, we believe that the input voltage  $V_{in}$  converter has a normal distribution.

The density of the random variable  $V_{in}$  is given by [7]:

$$f(V_{in}; \mu, \sigma) = \frac{1}{\sigma\sqrt{2\pi}} e^{-\frac{(V_{in}-\mu)^2}{2\sigma^2}}, \quad (1)$$

where  $\mu$  is the average value (nominal input voltage of the converter);  $\sigma$  is the standard deviation.

For a DC converter SSON ERS [7, 10]  $\mu = 3000$  V and  $\sigma = 2.1$ . Modeling the circuit (Fig. 2) we assume  $\mu = 13.8$  V and  $\sigma = 2.1$ .

Random values of  $\mu$  are generated by functions NORM.INV and RAND of the Microsoft Excel Microsoft Office 2010.

Density plot of a probability distribution of the input voltage is shown in Fig. 5. The generated sample consists of 100 values. With this number of values of the maximum relative deviation of the generated density distribution of the density distribution determined by the

formula (1) does not exceed 12 % (Fig. 6), which is acceptable in engineering calculations.

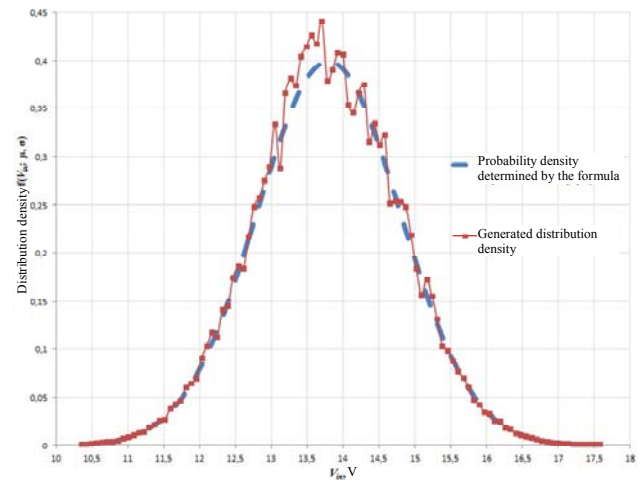


Fig. 5. Probability density generated and determined by formula (1) distribution density of the input voltage value  $V_{in}$

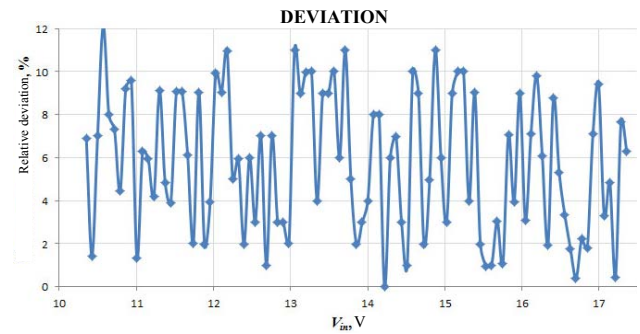


Fig. 6. Relative deviation of the generated distribution

4. As seen in the example of the effect of only one value (input voltage) of the converter efficiency, the correlations between the values of influencing factors are absent.

5. For generated random values  $V_{in}$  we simulated currents in the branches and the voltages in the circuit nodes, as well as the modeling of output power losses and converter efficiency. Simulation results with comparable input data agree to within 1 % of the data obtained in [10].

6. As a result of a series of experiments we obtained 100 values of the converter efficiency which are in the range of 0.9187 to 0.9584. Further, this range is divided into intervals (in this example – 0.005) and identified the relative and absolute frequency of the efficiency values within each interval. Based on these data, the density distribution plotted converter efficiency (Fig. 7) and the cumulative distribution function converter efficiency (Fig. 8).

The following distribution corresponds to Fig. 6:

$$f(E; \mu, \sigma) = \frac{1}{\sigma\sqrt{2\pi}} e^{-\frac{(E-\mu)^2}{2\sigma^2}},$$

where  $E$  is the converter efficiency;  $\mu$  is the average value;  $\sigma$  is the standard deviation.

In the correspondence with Fig. 7,  $\mu = 0.935$  and  $\sigma = 0.016$ .

In accordance with Fig. 8, the probability that the data in the efficiency of the converter at given conditions of use will be not less than 0.935, it is 0.65. Thus, account of risks of reducing the efficiency based on the proposed integrated assessment helps to clarify evaluate the effectiveness of the use of the converter in a particular application.

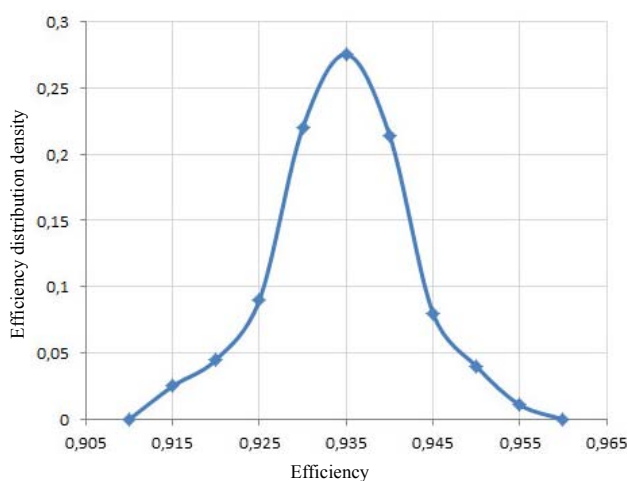


Fig. 7. Inverter efficiency distribution density built by results of stochastic modeling

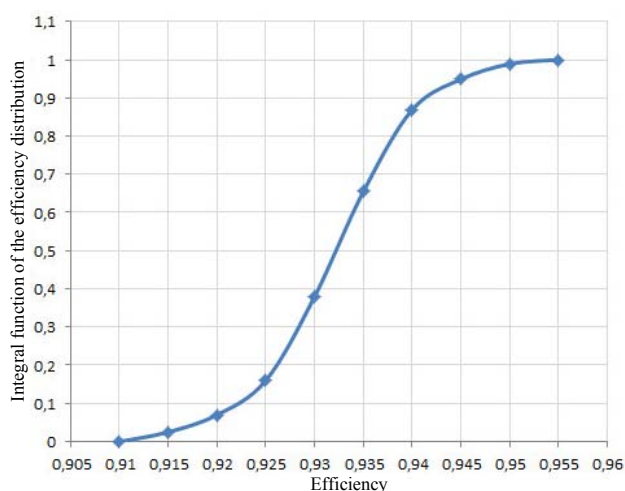


Fig. 8. Integral function of the converter efficiency distribution

## Conclusions.

1. A technique for evaluating the effectiveness of using of a semiconductor DC converter in the power supply system is proposed.

2. It is shown that the calculated by the proposed method the efficiency of the converter utilization is below the average efficiency values defined by the baseline method.

3. It is intended to use obtained results during converter design at the company «NII Preobrazovatel» (Zaporozhye, Ukraine).

## REFERENCES

1. Tittse U., Shenk K. *Poluprovodnikovaja shemotekhnika* [Semiconductor engineering]. Moscow, Mir Publ., 1983. 512 p. (Rus).
2. Lukutin B.V., Obuhov S.G. *Silovye preobrazovateli v elektrosnabzhenii* [Power converters in electricity supply]. Tomsk, TPU Publ., 2007. 144 p. (Rus).
3. Gildersleeve M., Forghani-zadeh H.P., Rincon-Mora G.A. A Comprehensive Power Analysis and a Highly Efficient, Mode-Hopping DC-DC Converter. *Proceedings. IEEE Asia-Pacific Conference on ASIC*, September 2002, pp. 153-156. doi: **10.1109/apasic.2002.1031555**.
4. Arvind Raj. *Application Report. Calculating Efficiency. PMP-DCDC Controllers: SLVA390* – February 2010. – Available at: <http://www.ti.com/lit/an/slva390/slva390.pdf> (accessed September 28, 2015).
5. Chen M., Afridi K.K., Chakraborty S., Perreault D.J. A high-power-density wide-input-voltage-range isolated dc-dc converter having a MultiTrack architecture. *2015 IEEE Energy Conversion Congress and Exposition (ECCE)*, Sep. 2015. doi: **10.1109/ecce.2015.7309945**.
6. Nowakowski R., Tang Ning. Efficiency of synchronous versus nonsynchronous buck converters. *Texas Instruments Analog Applications Journal*, 2009, no.4Q, pp. 15-18.
7. *GOST 6962-75. Transport elektrificirovannyj s pitaniem ot kontaktnoj seti. Rjad naprjazhenij* [State Standart 6962-75. Electrified transport with overhead system power supply. Voltage row]. Moscow, Izdatelstvo standartov Publ., 1975. 8 p. (Rus).
8. Larionova T.Y. Comparison of the auxiliary power supply systems of the electric railway rolling stock DC 3000 V according to the energy efficiency *Transactions of Kremenchuk Mykhailo Ostrohradskyi National University*, 2015, no.3(92), pp. 34-39. (Rus).
9. Katsikis V. *MATLAB – A Fundamental Tool for Scientific Computing and Engineering Applications – Volume 1*. InTech Publisher, 2012. 534 p. doi: **10.5772/2557**.
10. Sigorskij V.P. *Matematicheskij apparat inzhenera. Izd. 2-e. stereotip*. [Engineer's mathematical apparatus. 2nd ed. stereotype]. Kyiv, Tekhnika Publ., 1977. 786 p. (Rus).

Received 20.04.2016

*M.A. Polyakov*<sup>1</sup>, *Candidate of Technical Science, Associate Professor,*

*T.Y. Larionova*<sup>1</sup>, *Postgraduate Student,*

<sup>1</sup> Zaporozhye National Technical University,

64, Zhukovsky Str., Zaporozhye, 69063, Ukraine.

тел/phone +380 61 7698395,

e-mail: polyakov@zntu.edu.ua, electro-eng@yandex.ru

*How to cite this article:*

Polyakov M.A., Larionova T.Y. Efficiency evaluation technique of the semiconductor DC-DC converter application in the power-supply system. *Electrical engineering & electromechanics*, 2016, no.5, pp. 23-28. doi: 10.20998/2074-272X.2016.5.03.

M.I. Baranov, S.V. Rudakov

## AVERAGE GEOMETRICAL FEATURES OF THE ELECTRON WAVE PACKAGES DISTRIBUTION IN METALLIC CONDUCTORS WITH PULSED AXIAL CURRENT OF HIGH DENSITY

*Purpose. Calculation and experimental determination of average geometrical features of distributing of macroscopic electron wave packages (EWP) in round cylindrical metallic conductors with the pulsed axial current of high density. Methodology. Theoretical bases of the electrical engineering, bases of atomic and quantum physics, electrophysics bases of technique of high voltage and high pulsed currents. Results. The results of the conducted calculation and experimental researches are resulted on close determination of average geometrical features of distribution of longitudinal and radial EWP of macroscopic sizes in the indicated conductors. These descriptions are included by the average widths of «hot» and «cold» longitudinal and radial areas of conductor, and also average steps of division into the periods of similar areas. Results of the executed calculations and high temperature experiments for average geometrical features of longitudinal EWP in the zincked steel wire of diameter of 1.6 mm and length of 320 mm with the aperiodic impulse of current of temporal form 9 ns/160 ns and by amplitude 745 A coincide within the limits of 19 %. Originality. First with the use of methods of atomic and quantum physics the features of the stochastic distributing and mean values of basic geometrical sizes are analysed macroscopic longitudinal and radial EWP in round cylindrical metallic conductors with the pulsed axial current of high density. Practical value. Drawing on the got results in practice will allow more reliably to forecast geometrical sizes and places of localization of arising up in the probed metallic conductors with pulsed axial current of high density longitudinal and radial EWP. References 14, figures 2.*

*Key words:* metallic conductor, pulsed current of high density, electron wave package of conductor, «hot» and «cold» longitudinal and radial areas of conductor, quantization and averaging of geometrical features of electron wave packages of conductor.

*Приведены результаты приближенного выбора усредненного значения  $\bar{n}$  целого квантового числа  $n$  для мод квантованных волновых пси-функций  $n$ -го порядка и квантовомеханического расчета на основе найденного квантового числа  $\bar{n}$  усредненных геометрических характеристик квантованных периодических продольных и радиальных волновых электронных пакетов (ВЭП) в круглых сплошных металлических проводниках с большим импульсным аксиальным током. Данные характеристики включают усредненные ширины «горячих» и «холодных» продольных и радиальных участков указанных проводников, формируемых соответствующими ВЭП, и усредненные шаги периодизации в указанных структурах ВЭП. Выполненные эксперименты на мощном генераторе длительной аperiodической  $C$ -компоненты импульсного тока искусственной молнии с амплитудой его плотности до  $0,37 \text{ кА/мм}^2$  в оцинкованном стальном проводе радиусом  $0,8 \text{ мм}$  и длиной  $320 \text{ мм}$  подтвердили результаты выбора для него квантового числа  $\bar{n}$  и расчета усредненных ширин «горячих» и «холодных» участков продольных ВЭП, визуально наблюдаемых вдоль интенсивно нагреваемого этим током исследуемого провода за счет слабого рассеяния электронных полуоволн де Бройля на атомах кристаллической решетки его металла. Библ. 14, рис. 2.*

*Ключевые слова:* металлический проводник, импульсный ток большой плотности, волновой электронный пакет проводника, «горячие» и «холодные» продольные и радиальные участки проводника, квантование и усреднение геометрических характеристик волновых электронных пакетов проводника.

**Introduction.** In [1, 2] the results of theoretical and experimental studies of wave longitudinal and radial distribution of free electrons in a solid round metal conductor with a high density of pulsed axial current are presented. The results indicate the occurrence of stochastic character in the conductive structure of the conductor radius  $r_0$  and length  $l_0 \gg r_0$  containing the electronic quantum number  $n$  of half-waves of de Broglie, periodic quantized electron wave packets (EWP) [3]. A distinctive feature of the display data of macroscopic EWP is that they form a relatively «hot» and «cold» longitudinal and radial portions of the conductor, the geometric dimensions of which are defined set forth in [1, 2] laws in wave distributions drifting electrons and the quantized values of the longitudinal  $k_{nz} = \pi n / l_0$  and radial  $k_{nr} = \pi n / r_0$  wave numbers ( $n = 1, 2, 3, \dots, n_m$  – the integer

quantum number;  $n_m$  – the maximum value of the quantum numbers  $n$  defined by the principal quantum number  $n_k$  of the metal atoms of the conductor [3]). Moreover, the step of the periodic structure of EWP conductor is equal to the sum of the widths of its neighbors «hot» longitudinal  $\Delta z_{nh}$  (radial  $\Delta r_{nh}$ ) and «cold» longitudinal  $\Delta z_{nc}$  (radial  $\Delta r_{nc}$ ) sites. However, according to [2, 4] temperature levels Joule heating of «hot» and «cold» longitudinal and radial sections of EWP of the conductor may differ by 3.5 times. Data in [2] show that the quantum number  $n_m = 2n_k^2$  for copper, zinc and steel conductors ( $n_k = 4$  [3]) is 32, which indicates the possibility of having their internal conductive structure 32 modes of longitudinal  $\Psi_{nz}(z, t)$  and radial  $\Psi_{nr}(r, t)$  of the wave functions. This superposition (overlap) of the quantized wave psi-function of the

$n$ -th order and forms the conductor of its macroscopic quantized longitudinal and radial EWP. Each quantum number  $n$  will match their EWP placed along  $l_0$  length or  $r_0$  radius of the conductor. Mode indicator (number  $n$ ) for said quantized wave psi-function determined by the energy state of the electrons in a conductor-free time of the application to it of electrical voltage and started flowing through it conduction current [5]. The probabilistic nature of the occurrence in metallic conductors with electric current phenomenon quantized periodic macrolocalization free electrons when they drift [5] and, accordingly, the emergence in these conductive materials quantized longitudinal and radial EWP with  $n \leq 32$  greatly complicates the prediction of a picture of a periodic distribution in it of indicated EWP. Certain decisions of the electrophysical an issue of the quantum wave nature and importance electrotechnological value at the reference (pilot) evaluation of the results of local action high discharge pulse current to the current-carrying part of the wires (cables) power circuits of powerful high-voltage test of electrical installations [6], as well as shock pulse short circuit [4, 7], and a lightning [8] on the current-carrying parts of the power circuit of electric power facilities, will contribute to the knowledge of the average quantum number  $n$  values (the value  $\bar{n}$ ) and, accordingly, average geometric characteristics of the quantized periodic longitudinal and radial EWP in round metallic conductors with pulsed axial current  $i_0(t)$  of high density.

The goal of the paper is calculation and experimental determination of the average geometrical features of the distribution of macroscopic EWP in circular cylindrical metallic conductors with pulsed axial current of high density.

**1. Definition of the problem of the EWP distribution in the metal conductor with pulsed current.** We consider a cylindrical coordinate system fixedly positioned in the air straight solid non-magnetic metallic conductor of radius  $r_0$  and length  $l_0 \gg r_0$  (Fig. 1). Let air environment parameters correspond to normal atmospheric conditions (air pressure is  $1.013 \cdot 10^5$  and the temperature  $T_0$  equals to  $0^\circ \text{C}$  [3]). We consider that the opposite ends of the considered conductor with the conductivity  $\gamma_0$  of its material applied electrical potential difference, unipolar varying in time  $t$  by an arbitrary law. Let us assume that the investigated conductor of cross-section  $S_0 = \pi r_0^2$  along its longitudinal axis  $OZ$  takes pulsed unipolar conduction current  $i_0(t)$  characterized by the average density  $\delta_0(t)$ . We restrict ourselves to the case when the thickness of the skin layer of the current  $\Delta_i$  in the conductor material substantially greater than its radius  $r_0$ . For an approximate description of the behavior of electrons drifting free guide use the known single-electron Hartree-Fock approximation which despises their mutual influence on each other, as well as the influence of ions (nodes) of the conductor material of the crystal lattice in his itinerant electrons [2, 3]. Let the longitudinal and

radial distribution of the free electrons of the conductor will be determined on the assumption that their spatial distribution movement and accordingly to the coordinates  $r$  and  $z$  in the first approximation subject to a one-dimensional wave temporal Schrödinger equation [3]. Required quantum mechanical based approach in view of the approximate form obtained in [1, 2, 5] information about the longitudinal and radial distributions of wave drift of free electrons in a conductor under consideration to determine the spatial distribution of average characteristics in its electrically conductive material of uniform periodic quantized longitudinal and radial EWP.

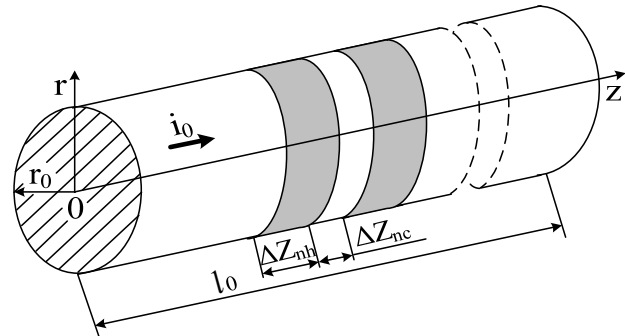


Fig. 1. A solid metal conductor of radius  $r_0$  and length  $l_0$  with pulsed axial current  $i_0(t)$  of high density containing quantized «hot» of width  $\Delta z_{nh}$  and «cold» of width  $\Delta z_{nc}$  longitudinal sections [2]

**2. Selection of the average values of the quantum number for the wave psi-functions of drifting electrons of the metal conductor with pulsed current.** For the quantized electron de Broglie half waves propagating along the length  $l_0$  and the radius  $r_0$  of the test conductor with a pulsed axial current  $i_0(t)$  are carried out following known analytical expressions [2]:

$$\lambda_{enz}/2 = l_0/n; \quad (1)$$

$$\lambda_{enr}/2 = r_0/n, \quad (2)$$

where  $\lambda_{enz} = h/(m_e v_{enz})$  is quantized wave length of the longitudinal drift of a free electron with the rest mass  $m_e = 9.109 \cdot 10^{-31}$  kg [3];  $v_{enz} = nh/(2m_e l_0)$  is the quantized longitudinal velocity of a free electron drift;  $\lambda_{enr} = h/(m_e v_{enr})$  is the quantized wave length of the longitudinal drift of free electron;  $v_{enr} = nh/(2m_e r_0)$  is the quantized radial velocity drift of free electron in the conductor material;  $h = 6.626 \cdot 10^{-34}$  J·s is the Planck constant [3].

Using (1) and knowing the limits of variation of the quantum number  $n = 1, 2, 3, \dots, n_m$ , we determine the beginning of the test the average length of the longitudinal conductor electron half-wave  $\lambda_{enz}^*/2$  as follows [9]:

$$\lambda_{enz}^*/2 = l_0 (n_m - 1)^{-1} \int_1^{n_m} n^{-1} dn = l_0 (n_m - 1)^{-1} \ln n_m. \quad (3)$$

From (2), similar to (3) for the average length of the radial half-wave electronic de Broglie  $\lambda_{enr}^*/2$  or step EWP

macroscopic radial structure in the electrically conductive material of the considered round conductor we find:

$$\lambda_{enr}^*/2 = r_0 (n_m - 1)^{-1} \ln n_m. \quad (4)$$

From (1)-(4) we see that for a quantum number  $n$  its average value  $\bar{n}$  satisfying the relations  $\lambda_{enz}^*/2 = l_0/\bar{n}$  and  $\lambda_{enr}^*/2 = r_0/\bar{n}$  can be written in the following analytical form [10]:

$$\bar{n} = (n_m - 1)/(\ln n_m). \quad (5)$$

From (5) for copper, zinc and steel wire ( $n_k=4$  [3];  $n_m=2n_k^2=32$ [2]) with pulsed current  $i_0(t)$  it follows that the average value for the quantum numbers  $n$  is determined by averaging the fashion wave psi-function in each periodic quantized longitudinal and radial EWP for such conductive materials, will be approximately equal  $\bar{n}=9$ . This number  $\bar{n}$  will correspond to the same average number of «hot» and «cold» longitudinal and radial portions, the amount of average widths which  $(\Delta z_{nh}^* + \Delta z_{nc}^*)$  and  $(\Delta r_{nh}^* + \Delta r_{nc}^*)$  formed in the material of the conductor averaged steps periodic structures longitudinal and radial EWP. Below, in section 5 will be given an experimental study on the proposed settlement choice (5) of the numerical value for the number in relation to the above conductive materials investigated current-carrying conductors.

**3. Average geometric features for periodic quantized longitudinal EWP in the metal conductor with pulsed current.** For the marginal zones of the test metal conductor adjacent to the places of its fastening in high-current circuit with a pulsed current  $i_0(t)$  and containing longitudinal EWP, taking into account (1) is satisfied the following relation [5]:

$$\lambda_{enz}^*/2 = \Delta z_{nh}^* + 2 \Delta z_{nce}^* = l_0/\bar{n}, \quad (6)$$

where  $\Delta z_{nh}^*$ ,  $\Delta z_{nce}^*$  are the respectively the average values of the quantized width «hot» and extreme «cold» longitudinal sections EWP conductor.

For internal conductor zones adjacent to the above its marginal zones or distant from their averaged geometric characteristics of the quantized longitudinal EWP will be described by the following analytical expression [5]:

$$\lambda_{enz}^*/2 = \Delta z_{nh}^* + \Delta z_{nci}^* = l_0/\bar{n}, \quad (7)$$

where  $\Delta z_{nci}^*$  is the average value of the quantized width internal «cold» longitudinal sections EWP conductor.

From (6) and (7) shows that the average quantized widths  $\Delta z_{nci}^* = \Delta z_{nc}^*$  of internal «cold» longitudinal sections of EWP twice the average quantized width  $\Delta z_{nce}^*$  of respective extremes of «cold» longitudinal sections conductor. To determine the estimated taking into account (6) and (7) of the averaged quantized values  $\Delta z_{nce}^*$  and  $\Delta z_{nci}^*$  it is necessary to find the average value of the quantized value of  $\Delta z_{nh}^*$ . To this end, in relation to the «hot» longitudinal section of EWP we use the fundamental principle of quantum electrodynamics (mechanics) - Heisenberg uncertainty as follows [3]:

$$\Delta z_{nh}^* \cdot \Delta p_{nz}^* \geq h/(4\pi), \quad (8)$$

where  $\Delta p_{nz}^* = m_e v_{enz}^* = \bar{n} h/(2l_0)$  is the averaged quantized longitudinal projection of the momentum of drifting in the microstructure of the conductor of free electrons;  $v_{enz}^* = \bar{n} h/(2m_e l_0)$  is the quantized average longitudinal velocity of electrons drifting free conductor.

Then from (8) for the smallest quantized value of the average width  $\Delta z_{nh}^*$  of «hot» EWP longitudinal portion of the conductor with pulsed axial current  $i_0(t)$  of high density we have:

$$\Delta z_{nh}^* = l_0/(2\pi\bar{n}) = l_0 \ln n_m / [2\pi(n_m - 1)]. \quad (9)$$

From (6), taking into account (9) for the averaged quantized widths  $\Delta z_{nce}^*$  of extreme «cold» longitudinal sections EWP of the test conductor in the approximate form we get the estimated relation of the form:

$$\Delta z_{nce}^* = l_0 \ln n_m (2\pi - 1) / [4\pi(n_m - 1)]. \quad (10)$$

From (7) and (9) for the average quantized widths  $\Delta z_{nci}^*$  of internal «cold» longitudinal sections EWP of the considered conductor we obtain the following approximate ratio for calculations:

$$\Delta z_{nci}^* = l_0 \ln n_m (2\pi - 1) / [2\pi(n_m - 1)]. \quad (11)$$

As a result, the average step for the longitudinal EWP of the test conductor of the periodic structure taking into account (9)-(11) can be determined from the following calculation expression:

$$\Delta z_{nh}^* + 2 \Delta z_{nce}^* = \Delta z_{nh}^* + \Delta z_{nci}^* = l_0 \ln n_m / [(n_m - 1)]. \quad (12)$$

**4. Average geometric characteristics for periodic quantized radial EWP in the metal conductor with pulsed current.** For the central and outer zones of the cylindrical conductor of radius  $r_0$  with current  $i_0(t)$  containing radial EWP using (2) we have:

$$\lambda_{enr}^*/2 = \Delta r_{nh}^* + 2 \Delta r_{nce}^* = r_0/\bar{n}, \quad (13)$$

where  $\Delta r_{nh}^*$ ,  $\Delta r_{nce}^*$  are the respectively the average values of the quantized width «hot» and extreme «cold» areas of radial conductor EWP.

For internal circular zones of the considered conductor radial averaged geometrical characteristics of EWP satisfy the following approximate calculated ratio [5]:

$$\lambda_{enr}^*/2 = \Delta r_{nh}^* + \Delta r_{nci}^* = r_0/\bar{n}, \quad (14)$$

where  $\Delta r_{nci}^*$  is the the average value of the quantized width internal «cold» curved sections EWP of the conductor.

We write further fundamental Heisenberg uncertainty for localized to the «hot» areas of EWP radial drift of free electrons in the form [3]:

$$\Delta r_{nh}^* \cdot \Delta p_{nr}^* \geq h/(4\pi), \quad (15)$$

where  $\Delta p_{nr}^* = m_e v_{enr}^* = \bar{n} h/(2r_0)$  is the quantized average radial projection pulse drifting in the microstructure of the test conductor free electrons;  $v_{enr}^* = \bar{n} h/(2m_e r_0)$  is the quantized average radial velocity drift of free electrons in a circular cylindrical conductor.

From (15) and (5) for the smallest quantized value of the average width  $\Delta r_{nh}^*$  of «hot» radial section of EWP test conductor with a pulsed current  $i_0(t)$  of high density we obtain:

$$\Delta r_{nh}^* = r_0 / (2\pi\bar{n}) = r_0 \ln n_m / [2\pi(n_m - 1)]. \quad (16)$$

As a result of (13) and (16) for the average quantized widths  $\Delta r_{nce}^*$  of extreme «cold» areas of the considered radial conductor EWP in the adopted approximation we find:

$$\Delta r_{nce}^* = r_0 \ln n_m (2\pi - 1) / [4\pi(n_m - 1)]. \quad (17)$$

From (14) with (16) to the averaged quantized widths  $\Delta r_{nci}^*$  of internal «cold» radial sections EWP of the test conductor write the following calculation ratio:

$$\Delta r_{nci}^* = r_0 \ln n_m (2\pi - 1) / [2\pi(n_m - 1)]. \quad (18)$$

Then, for the average pitch of the periodic localization of free electrons drifting in the «hot» areas of EWP along the outer radius  $r_0$  of the considered conductor (16)-(18) we have:

$$\Delta r_{nh}^* + 2 \Delta r_{nce}^* = \Delta r_{nh}^* + \Delta r_{nci}^* = r_0 \ln n_m / [(n_m - 1)]. \quad (19)$$

From (9)-(12) and (16)-(19) that have been found in this approximation averaged geometrical dimensions of the «hot» and «cold» areas of radial EWP in  $l_0/r_0$  times smaller than the corresponding average sizes for longitudinal EWP conductor pulse current  $i_0(t)$  of high density. This feature in the spatial distribution of longitudinal and radial EWP solid round conductor is important for a number of advanced electric technologies [11] using the flow of metal conductors for large pulsed currents with a view to their electrical explosion (EE). The most fully, it will be shown on receipt by EE gases in the thin metal wires of small «metal» of the plasma, and then, after separation of plasma nanoproducs and microdispersed conductive materials [12].

**5. The results of experimental verification of choice for the average features of quantized longitudinal EWP in the metal conductor with pulsed current.** To verify (the truth test) selection by (5) the average value of the quantum number  $n$  and the proposed settlement of the relations (9)-(12) with respect to the averaged quantized characteristics of longitudinal EWP in the test conductor use presented in [1, 2, 5], the results of experimental studies wave longitudinal distribution of free electrons and drifting respectively, «hot» and «cold» longitudinal sections in galvanized steel wire ( $r_0=0.8$  mm;  $l_0=320$  mm;  $S_0=2.01$  mm<sup>2</sup>;  $n_k=4$ ) with the thickness of the outer protective coating  $\Delta_0=5$  μm was tested in the discharge circuit of a powerful high voltage generator prolonged C- components of artificial lightning current [13] a direct impact aperiodic current pulse  $i_0(t)$  of temporary shape  $t_m/\tau_p=9$  ms/160 ms of large average density  $\delta_{0m} \approx I_{0m}/S_0 \approx 0.37$  kA/mm<sup>2</sup>. This corresponds to the maximum value of the amplitude  $\delta_{0m}$  unipolar current pulse  $I_{0m}=745$  A, the onset of which is equal to  $t_m=9$  ms. On  $0.5I_{0m}$  level measurements made in accordance with the help of an attorney in the metrology service coaxial

measuring shunt type IIIK-300, which has for the mode conversion factor of  $56.42 \cdot 10^2$  A/V [2, 13], the duration used in the experiments conducted by the pulse current was  $\tau_p=160$  ms, and the total duration of the flow through the wire of said current pulse in the partial destruction of its metal structure of intense Joule heating of non-magnetic material wire reached about 576 ms [1, 2]. Note that in the present case for the current round of the skin layer of the steel wire in a stationary mode, you kind of relation [2, 6]:  $\Delta_l/r_0 \approx 2r_0^{-1} [t_m/(\pi\mu_0\gamma_0)]^{1/2} \approx 42$ , where  $\mu_0=4\pi \cdot 10^{-7}$  H/m is the magnetic constant [3] and  $\gamma_0 \approx 8 \cdot 10^6$  S/m is the conductivity base wire used in experiments [3]). Running for  $\Delta_l/r_0$  of the specified quantitative value may be indicative of the appropriateness of the estimates for the amplitude of the average current density  $\delta_{0m}$ , for which the amplitude and temporal parameters (ATP) test aperiodic pulse type 9 ms/160 ms current steel wire taken from the corresponding experimental waveforms cited in [2].

Fig. 2 shows the results of electro-thermal effect to the selected contact steel wire aperiodic current pulse 9 ms/160 ms with indicated ATP ( $I_{0m} = 745$  A;  $t_m = 9$  ms;  $\tau_p = 160$  ms). It can be seen that in this case ( $\delta_{0m} \approx 0.37$  kA/mm<sup>2</sup>) along the longitudinal axis of galvanized steel wire are four sphere-like «hot» (quantized  $\Delta z_{nh} \approx 7$  mm width) and two cylindrical internal «cold» (mm quantized width  $\Delta z_{nci} \approx 27$ ) longitudinal sections of EWP. The other five «hot» and eight «cold» (of which the two extreme of width  $\Delta z_{nce} = \Delta z_{nci}/2$  experimentally confirmed in accordance with this ratio in [14]) longitudinal sections of EWP wire undergone a complete sublimation. The specified number of «hot» and «cold» sites of investigated EWP longitudinal wires can say that in this case the experimental stochastic quantum number  $n$ , the equality  $n = \bar{n} = 9$ . From the calculated ratio (9) at  $n_m = 2n_k^2 = 32$  and, accordingly,  $\bar{n} = 9$  that the value of the average width of the «hot» area of the longitudinal steel wire numerically EWP is about  $\Delta z_{nh}^* = 5.7$  mm (with the experimental value of this width  $\Delta z_{nh} \approx 7$  mm [1]). It is important to emphasize that found on (9) the average width  $\Delta z_{nh}^*$  of «hot» EWP longitudinal portion substantially corresponds to the numerical value of the quantized width  $\Delta z_{nh}$  of this site of EWP of indicated conductor, as defined in [1, 2, 5] on the following calculation relationship:

$$\Delta z_{nh} = e_0 n_{e0} h (m_e \delta_{0m})^{-1} [8 + (\pi - 2)^2]^{-1}, \quad (20)$$

where  $e_0 = 1.602 \cdot 10^{-19}$  K is the module of the electron electric charge;  $n_{e0}$  is the average density of free electrons in the metal conductor considered prior to flowing through it a current pulse  $i_0(t)$ .

From (20) obtained in [2, 5] based on the fundamental Heisenberg uncertainty relation [3] we have used for the steel wire at  $16.82 \cdot 10^{28}$  m<sup>-3</sup> [2, 3] and  $\delta_{0m} \approx 0.37 \cdot 10^9$  A/m<sup>2</sup> it follows that  $\Delta z_{nh} \approx \Delta z_{nh}^* \approx 5.7$  mm. These calculated width «hot» EWP longitudinal portions within 19% different from the previously experimentally obtained in [1] for the case of electro widths ( $\Delta z_{nh} \approx 7$  mm)

respective portions of said wire. It can be reasonably concluded that the quantized width  $\Delta z_{nh}$  of «hot» longitudinal portion EWP of the metal conductor according to (20) is also an averaged geometrical feature of the longitudinal EWP. Its numerical value at a constant value in the test conductor  $\delta_{0m}$  also remains unchanged, as evidenced by the results carried out at the Scientific-& Research Planning-& Design Institute «Molniya» of the NTU «KhPI» high-temperature experiments using such a steel wire ( $r_0=0.8$  mm;  $l_0=320$  mm;  $\Delta_0=5$   $\mu$ m;  $S_0=2.01$  mm<sup>2</sup>) [1, 2, 5]. The above computational and experimental data for the width of the EWP  $\Delta z_{nh}$  indicate the validity of the selection to (5), taking into account the relation  $n_m=2n_k^2$  of the average value  $\bar{n}$  for the whole of the integer  $n$ .



Fig. 2. External view of cooling in the air and asbestos cloth quantized sphere-like «hot» (width  $\Delta z_{nh} \approx 7$  mm) and cylindrical inner «cold» (width  $\Delta z_{nci} \approx 27$  mm) longitudinal sections (macroscopic areas of quantized longitudinal EWP) galvanized steel wire ( $r_0=0.8$  mm;  $l_0=320$  mm;  $\Delta_0=5$   $\mu$ m;  $S_0=2.01$  mm<sup>2</sup>) immediately after exposure to an aperiodic pulsed axial current  $i_0(t)$  of the temporary shape  $t_m/\tau_p=9$  ms/160 ms of high density ( $I_{om}=745$  A;  $t_m=9$  ms;  $\tau_p=160$  ms;  $\delta_{0m} \approx 0.37$  kA/mm<sup>2</sup>;  $n = \bar{n} = 9$ ) [1]

With regard to the average quantized width  $\Delta z_{nci}^*$  of internal «cold» longitudinal sections EWP of the steel wire, it is, according to (11) at  $n_m=32$  and  $\bar{n}=9$  and taking into account (5) numerically is about 29.9 mm (experimental value of this width  $\Delta z_{nci} \approx 27$  mm [1]). It is evident that the design for (11) the average value of width  $\Delta z_{nci}$  of internal «cold» EWP longitudinal section for the considered steel wire differs from the experimentally obtained it widths of longitudinal EWP  $\Delta z_{nci}$  corresponding portion within 10%.

To carry out even in rough form on a powerful high-voltage high-current electrical installation verification of the calculated relations (16)-(19) with respect to the averaged quantized geometric characteristics of radial EWP in the study of metallic conductors with an axial current pulse  $i_0(t)$  of high density now practically it is not possible due to lack of the necessary high-speed photorecording equipment. We hope for their experimental verification in future in the years to its own high current research or prospecting work of other scientists in the area of electrical physics.

## Conclusions.

1. In the framework of quantum-mechanical approach to the electric properties of high density periodic EWP of macroscopic dimensions arising from the pulsed axial current in circular metallic conductors certain scientific generalizations are carried out and calculation relations (3)-(5) are proposed for an approximate determination of the average value  $\bar{n}$  of integer quantum number  $n$  for propagating their electrically conductive material quantized modes of wave psi-functions of the  $n$ -th order and the quantized electron de Broglie half-waves and, based on the calculated ratio obtained by (9)-(12) and (16)-(19) for estimating the average geometric features of longitudinal and radial EWP periodically placed along the length  $l_0$  and radius  $r_0$  of investigated conductors.

2. Experimental verification on a powerful high-current high-voltage generator long-term aperiodic C- artificial lightning current component of the results of the proposed selection by (5) of the average value  $\bar{n}$  of integer quantum number  $n$  and approximate calculation according to (9)-(12) of averaged geometrical features of quantized longitudinal macroscopic EWP in continuous galvanized steel wire ( $r_0=0.8$  mm;  $l_0=320$  mm;  $\Delta_0=5$   $\mu$ m;  $S_0=2.01$  mm<sup>2</sup>) with aperiodic pulse temporal shape of the current 9 ms/160 ms of high density ( $I_{om} = 745$  A;  $t_m = 9$  ms;  $\tau_p = 160$  ms,  $\delta_{0m} \approx 0.37$  kA/mm<sup>2</sup>) confirmed their authenticity.

3. Verification of the calculation relations (16)-(19) for the average geometric features of the quantized radial EWP in electrically exploding metal conductors with high pulsed axial current requires to carry out in future complex and expensive experimental electrophysical studies in a high-voltage laboratory.

## REFERENCES

1. Baranov M.I. Features heating thin bimetallic conductor large pulse current. *Elektrichestvo*, 2014, no.4, pp. 34-42. (Rus).
2. Baranov M.I. The main characteristics of the wave distribution of free electrons in a thin metallic conductor with a pulse current of high density. *Elektrichestvo*, 2015, no.10, pp. 20-32. (Rus).
3. Kuz'michev V.E. *Zakony i formuly fiziki* [Laws and formulas of physics]. Kiev, Naukova Dumka Publ., 1989. 864 p. (Rus).
4. Baranov M.I. Local heating of electrical pathways of power electrical equipment under emergency conditions and overcurrents. *Russian Electrical Engineering*, 2014, vol.85, no.6, pp. 354-357. doi: 10.3103/s1068371214060030.
5. Baranov M.I. Quantum-wave nature of electric current in a metallic conductor and some of its electrophysical macro-phenomena. *Electrical engineering & electromechanics*, 2014, no.4, pp. 25-33. doi: 10.20998/2074-272X.2014.4.05.
6. Baranov M.I. *Izbrannye voprosy elektrofiziki. Tom 2, Kn. 2: Teoriia elektrofizicheskikh effektiv i zadach* [Selected topics of Electrophysics. Vol.2, Book 2. A theory of electrophysical effects and tasks]. Kharkiv, NTU «KhPI» Publ., 2010. 407 p. (Rus).
7. Orlov I.N. *Elektrotehnicheskij spravochnik. Proizvodstvo i raspredelenie elektricheskoy energii. Tom 3, Kn. 1* [Electrical engineering handbook. Production and distribution of electric energy. Vol. 3, Book 1. Ed. I.N. Orlov]. Moscow, Energoatomizdat Publ., 1988. 880 p. (Rus).

8. Baranov M.I., Kravchenko V.I. Electrothermal resistance wire and cable to the aircraft to the striking action pulsed current lightning. *Elektrichestv*, 2013, no.10, pp. 7-15. (Rus).
9. Dwight H.B. *Tablicy integralov i drugie matematicheskie formuly* [Tables of integrals and other mathematical data]. Moscow, Nauka Publ., 1973. 228 p. (Rus).
10. Baranov M.I., Rudakov S.V. Averaged characteristics of the wave drifting distribution of electrons in a metal conductor with a pulse current conduction of high density. *Bulletin of NTU «KhPI»*, 2013, no.60(1033), pp. 12-20. (Rus).
11. Guly G.A. *Nauchnye osnovy razrjadno-impul'snyh tehnologij* [Scientific basis of the discharge-pulse technology]. Kiev, Naukova dumka Publ., 1990. 208 p. (Rus).
12. Baranov M.I. Preparation of disperse materials with micron, submicron and nanostructured matter particles under electric explosion of thin metallic conductors. *Electrical engineering & electromechanics*, 2012, no.4, pp. 45-49. (Rus). doi: **10.20998/2074-272X.2012.4.09**.
13. Baranov M.I., Koliushko G.M., Kravchenko V.I., Nedzel'skii O.S., Dnyshchenko V.N. A Current Generator of the Artificial Lightning for Full-Scale Tests of Engineering Objects. *Instruments and Experimental Technique*, 2008, no.3, pp. 401-405. doi: **10.1134/s0020441208030123**.

How to cite this article:

Baranov M.I., Rudakov S.V. Average geometrical features of the electron wave packages distribution in metallic conductors with pulsed axial current of high density. *Electrical engineering & electromechanics*, 2016, no.5, pp. 29-34. doi: 10.20998/2074-272X.2016.5.04.

14. Baranov M.I. Theoretical and experimental results of research into explanation of de Broglie half-wave existence in the microstructure of an active metallic conductor. *Electrical engineering & electromechanics*, 2014, no.3, pp. 45-49. (Rus). doi: **10.20998/2074-272X.2014.3.09**.

Received 25.05.2016

M.I. Baranov<sup>1</sup>, Doctor of Technical Science, Chief Researcher,  
S.V. Rudakov<sup>2</sup>, Candidate of Technical Science, Associate  
Professor,

<sup>1</sup> Scientific-&-Research Planning-&-Design Institute «Molniya»,  
National Technical University «Kharkiv Polytechnic Institute»,  
47, Shevchenko Str., Kharkiv, 61013, Ukraine.

<sup>2</sup> National University of Civil Protection of Ukraine,  
94, Chernyshevska Str., Kharkiv, 61023, Ukraine.

phone +38 057 7076841,

e-mail: eft@kpi.kharkov.ua, serg\_73@i.ua

Yu.V. Batygin, E.A. Chaplygin, O.S. Sabokar

## MAGNETIC PULSED PROCESSING OF METALS FOR ADVANCED TECHNOLOGIES OF MODERNITY – A BRIEF REVIEW

*The aim of the article is dedicated to the brief review of the main achievements of the advanced technologies with usage of the energy of the pulsed magnetic fields. Originality. The new suggestions are represented. They are based on the results of development of the new scientific direction in area of the magnetic pulsed processing of thin-walled sheet metals when a penetration of the acting fields is quite significant. The known traditional approaches based on the skin-effect in electro-dynamics and were successfully implemented. Methodology of the analysis consist of careful theoretical and practical experiments review and its future development. Results of the research based on the existing experimental approbation were presented visually with the description followed The known approaches to solution actual production problems based on the skin-effect in electro-dynamics are described. Practical value. The first of practical propositions is related to stamping of the drawing the printed circuit boards on the cooper foil with thickness about ~50 mkm. This operation is realizing by the forces of magnetic pressure directly without any supplements introduction. The second consists in usage the magnetic pulsed attraction for external removing the dents in the car body. This operation does not demand disassembling of elemental base and allows preserving the paint of coverings. Both of these technologies could to minimize the working time, to decries the volume of the waste products and to make the manufacturing existed much cheaper. References 10, figures 3.*

*Key words: magnetic pulsed processing, metal forming, printed circuit boards stamping, external flattening.*

*Работа посвящена краткому обзору основных достижений передовых технологий с использованием энергии импульсных магнитных полей. Описаны известные традиционные подходы, основанные на скин-эффекта в электродинамике и были успешно реализованы. Представлены новые предложения, основанные на результатах развития нового научного направления в области магнитно-импульсной обработке тонкостенных листовых металлов, когда проникновение действующих полей весьма существенно. Первое из этих предложений связано с оттиском рисунка печатных плат на медной фольге толщиной около ~ 50 мкм. Эта операция реализуется силами магнитного давления непосредственно. Второе предложение заключается в использовании магнитного импульсного притяжения для внешнего удаления вмятин в кузове автомобиля. Эта операция не требует демонтажа элементной базы и позволяет сохранить краску покрытий. Библ. 10, рис. 3.*

*Ключевые слова: магнитно-импульсная обработка, обработка металлов, оттиск печатных плат, внешняя рихтовка.*

### Introduction and publications analysis.

The ecology, economy of resources and energy are the most sharp problems among the main problems of modernity. Discussion of what is the first one, what is the second one, and what is the third one has no sense. The different viewpoints may consider these problems, as they want. The main thing is in answers for questions: where energy and material resources can be taken, and how to preserve our environment for the next generations?

Solving these problems will define the future of the all Humanity.

The practical usage of energy of the pulsed electromagnetic fields (in the other terminology this is the «Electromagnetic Metal Forming» – «EMF») opens exclusive perspectives for creation of advanced technologies for processing of the materials of any physical nature. They have the doubtless advantages, among which there are ecological purity, low energy consumption, economic expenditure of the material resources, at last, high speed of the manufacture process.

A scientific technical information about the magnetic pulsed metal working (EMF) appeared beginning in the fifties year's end of the last century. First magnetic pulsed equipment for processing the tubular objects was demonstrated by «General Dynamics Corp» in Geneva at the Nuclear Energy Peaceful Usage Exhibition in 1958.

The intensive development of the magnetic pulsed technologies was continued till beginning of eighties approximately. The next fifteen - twenty years may be characterized by decreasing of the interest to the processing field methods. There were many different technical and

social obstacles. They are not interesting and should not be announced. But at the beginning of 2000th the magnetic pulsed processing technologies are again attracting attention of the industrial manufacture. The quantity of the science-practical publications essentially increases. They are devoted to elaboration and practical usage of the magnetic pulsed technologies in different branches of industrial manufacture in USA, Germany, France, Sweden etc. There are many reasons of the increasing interest to the magnetic pulsed methods. The new alloys appeared. They had some unique properties which may be displayed in the pulsed action only. For example, hyper-plasticity property was among them, when the relative deformations may reach ~200 %.

For the time being worsening of the natural conditions for the Humanity is one of reason of the high interest to the magnetic pulsed technologies. The world public is worried by exhausting of the natural resources, by pollution and poisoning of the Planet Earth. The Humanity owns by the known high productive technologies in the different areas of activity. But increasing of the work productivity becomes not a main problem of the Science Technical Progress. The ECOLOGY, RESOURCES and ENERGY SAVING are becoming by the main problems.

There are many European and American publications of the different authors devoted to the description of magnetic pulsed working metals, for example [1]. But the most of them are not acquainted with achievements of the former soviet schools (in the main question is about the Russian language scientific literature!) which was one of

© Yu.V. Batygin, E.A. Chaplygin, O.S. Sabokar

the first in this area of the SCIENTIFIC TECHNICAL PROGRESS [2]. That is why the main attention of this article will be concentrated on the publications of the scientists from former Soviet Union.

**Purpose of the article** is to make a brief review of the main achievements of the advanced technologies with usage of the energy of the pulsed magnetic fields.

**Main equipment for the magnetic pulsed metal processing.** The distinguishing particularity of the methods of the field action is an absence of any immediate contacts with processed object. The practical sense of this particularity becomes obvious, for example, in comparison the mechanical processing and electromagnetic stamping. The electromagnetic stamping is being realized without any puncheon (striking element!). The pressure forces are appearing during interaction of the field with metal of the conducting work-piece. Nevertheless, as it is in mechanics for the technological operation realization the two main components are necessary. These are a source of energy and the tool. The energy source is a system of the high voltage. In the special technical literature it was named «THE MAGNETIC PULSED INSTALLATION». The tool is a complex consisting of the generator of the field which is named «INDUCTOR» and a processed work-piece. In the whole, the present complex is the INDUCTOR SYSTEM.

Should mark if the energy source (the Magnetic Pulsed Installation!) is an universal element of equipment in different production operations, but the tool of the method has to be created for implementation of a particular manufacturing operation only. Thus, the MAGNETIC PULSED INSTALLATION plus the INDUCTOR SYSTEM are the necessary components of the technical equipment for the metal working with help of the energy of the pulsed magnetic fields [3](see Fig. 1).

**Some implemented and new advanced technologies.** First of all a brief information about the traditional implemented magnetic pulsed technologies should be given [1-3].

In the special literature there is some general adopted classification of the technological operations. It defines belonging to three of the possible scheme of their practical realization.

The first group unites the manufacturing processes, which are being fulfilled according to scheme what was named as «COMPRESSION». The magnetic pressure forces are directed to a system axis. They are working for compression.

The second group includes the production operations which were named «EXPANSION» according to the type of deformation of the work-pieces. In this case the INDUCTOR (tool!) was placed in inner cavity of the work-piece. The magnetic pressure forces are directed from the system axis. They are working for expansion.

The third group of operations is realized according to scheme what was named as «FLAT SHEET STAMPING». In this case the inductor and work-piece are the parallel flat objects divided by insulating inserts. The magnetic pressure forces are directed from inductor to work-piece. They are working for repelling. The last remark demands more precision. The last experiments showed that under decreasing of frequencies of the acting

magnetic fields the pressure forces are changing their direction. They are working for attraction the sheet work-piece to inductor. For the first time this phenomenon was displayed and described by scientists of the National Technical University «Kharkiv Polytechnic Institute» Professors Yu.V. Batygin, V.I. Lavinsky and L.T. Khimenko for a flat variant of the INDUCTOR SYSTEM. It may be suggested this phenomenon would appear and in a case of the known cylindrical constructions of the tools under some fixed conditions too. But should mark that it is hypothesis only. A final conclusion demands its experimental confirmation.

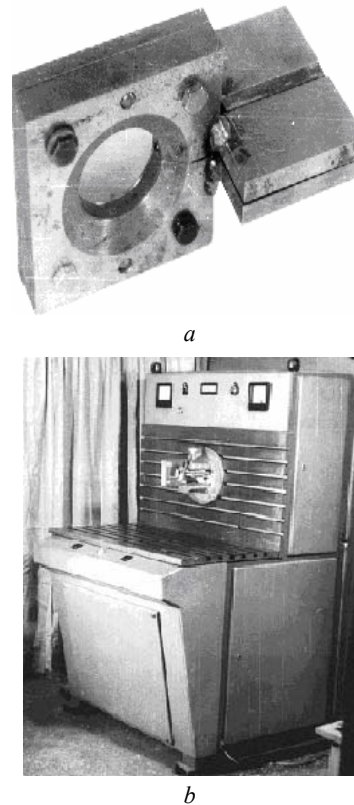


Fig. 1. The technical equipment created in the National Technical University «Kharkiv Polytechnic Institute» (Ukraine) for processing of the tubular work-pieces: a) it is the massive single turn INDUCTOR; b) it is the MAGNETIC PULSED INSTALLATION MIU-24 (the stored energy is ~ 24 kJ)

The given classification is general one. In its turn each of the distinguished schemes may be divided by sub-groups with more detailed any separate properties. All magnetic pulsed schemes which were pointed out above allow fulfilling not only different assemblage and separation in the production operations. The cold welding, all necessary and possible combinations of the schemes which were distinguished have to be mentioned too.

For example, the known compression of the cable tips is a clear illustration of the effective assemblage. A wire is being put into a cavity tip of the body. Then the body is being compressed by the magnetic pressure. Identically, not only cable tips for electrical engineering elements but also the tips onto flexible hoses, ropes etc. can be compressed by this way too. A quality of this connection is very high. Its strength till destruction, is not lower than analogical index for the material of the cable, rope, wire, as a rule.

The schemes of «compression» or «expansion» allow realizing the strength connections of the metal details with elements of glass, ceramics and other non-metal materials. Connection of metal with a non-metal by the magnetic pulsed action provides a high density and reliability of the connection, increasing the working exploitation characteristics in many cases.

All above enumerated the magnetic pulsed schemes of force action allow realizing the cold welding of not only the identical metals but also different ones (aluminum-cooper, aluminum-steel, cooper-steel etc.). For qualitative welded connection of the work-pieces their speeds of the movement in the opposite directions must have maximum values. In this case a mixed boundary layer of the metals is appearing during their clash at the expense of the inertial effects.

Some production operations for quite big areas on the flat metal sheets have to be distinguished particularly. Usually they are being fulfilled in accordance with scheme of the «flat sheet stamping». The most successful among them are forming of membranes, stamping of the automobile and airplane components, the pictures and inscriptions minting. These operations characterize possibilities of the magnetic pulsed action for processing of the quite large-scale articles of the ordered shape. In dependence on the energy-capacity of equipment a dimension of the processed area may be increased to  $\sim 0.2 \text{ m}^2$ .

Finishing description of the typical and successful magnetic pulsed technologies, should point out that all adduced examples had been implemented practically for the metals with high value of the specific electrical conductivity. The processing is being fulfilled under condition of the skin-effect regime when the field penetration processes through the work-piece are not essential and they do not decrease the magnetic pressure forces.

The scheme of the traditional magnetic pulsed processing demands some supplements to design of the tool when the question is about deformation of the bad conductors or enough thin metal objects.

The most effective supplement in the inductor systems turned out usage of the «sputniks» together with elastic transmitting inserts. This solution suggests placement (for any scheme of the magnetic pulsed action!) by layers: the inductor - the good conductor (it is the «sputnik»!) - the elastic insert which is transmitting the force action on the object of processing. The magnetic pressure is acting on the well conducting «sputnik». This pressure is being transmitted on the work-piece through elastic insert. Usually, the «sputnik» is made from a cooper. Some special sorts of rubber are being used as transmitting inserts. As well, some liquids may be used for this goal.

The usage of «sputniks» at the radio manufacture allows successful to fulfill some production operations for stamping small flat details and to print quite complicated picture on the cooper foil for fixing of different components of radio apparatus.

In spite of successful usage «sputniks» for solving many production problems this technical solution essentially decreases effectiveness of the process deforming and excludes the non-contact force action on the work-

piece what is the main advantage of the magnetic pulsed metal processing.

Unlike the known methods of processing massive conductors in the skin-effect regime the qualitatively new direction in the magnetic pulsed working of metals provides the intensive non-contact force action on thin-walled metal objects (practically, the «transparent» for magnetic fields!) was founded and was formulated in the works of scientists of the National Technical University «Kharkiv Polytechnic Institute» at beginning of the last century. Its physical essence consists in creation of the demanded spatio-temporal distribution of the acting magnetic field in the metal work-piece [3, 4].

The investigations of processes of the force interaction between the pulse magnetic fields and thin-walled («transparent» for acting fields!) conductors led to the patented technical solutions for designs of the inductor system which permit the practical realizing the most important production operations in the modern industrial manufacture.

The new progressive technology of the magnetic pulsed stamping the printed circuit boards for the electrical engineering devices was suggested for the first time. This operation for stamping of the conducting drawing in the charging-rectifying device of the micro-calculators «Electronics» was tested experimentally. The positive results were got. The experimental specimens are represented on Fig. 2.

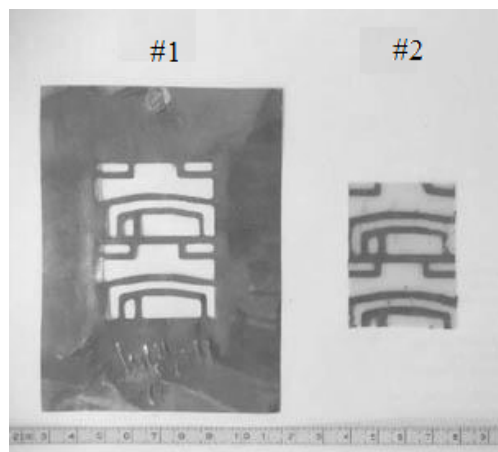


Fig. 2. The experimental specimens of the printed circuit boards conducting elements which were stamped in the cooper foil with thickness  $\sim 50 \text{ mkm}$  by the magnetic pulsed pressure:

- #1 – it is the drawing in the cooper foil;
- #2 – it is the ready-made printed circuit board

The principle action of the inductor system was based on the phenomenon in the electrodynamics. Its essence consists in what the packet of the flat electromagnetic waves does not penetrate practically through thin-walled conductive screens into the free space. Technically, this phenomenon is being realized with help of the inductor system where a drawing in a foil sheet has to be stamped with help of a dielectric die.

Should mark what the practical usage of the suggested inductor systems is not limited by stamping of printed circuit boards from the cooper foil only. The accepted principle action permits realizing the effective magnetic pressure on the thin-walled objects from the

wide class of metals with different electrophysical and mechanical characteristics.

Continuing discussion of processing the thin-walled metals should particularly distinguish a clear example of new usage of the electromagnetic energy under low frequencies of the acting fields. A question is about a practical realization of the magnetic pulsed attraction of the sheet work-pieces under excitation of the electrodynamic forces.

For the first time at 2004 the scientists from the National Technical University «Kharkiv Polytechnic Institute» (Professors Yu.V. Batygin, V.I. Lavinsky, L.T. Khimenko) had watched an interesting phenomenon. The question is about the force action of the pulsed magnetic fields with enough low working frequencies on the steel specimens. As it followed from experiments, decreasing of the frequency till a definite limit was leading to the work-piece attraction in direction to the working surface of the single turn inductor-tool. The question is about the deforming and pulling out of a part of the sheet metal [5].

A practical application of the displayed effect may be an operation for the dent removing on the body car without any mechanical contacts with it and without possible damages of their outer painted coats. Should mark the more deep sense of this direction of the magnetic pulsed working metals. It consists in essential widening of possibilities of the force action with help of the energy of the electromagnetic fields. A combination of the magnetic pulsed repelling and the magnetic pulsed attracting can give absolutely new solutions for creating absolutely new flexible progressive technologies of the future.

Let us stop on the attraction for the dent removing. For the time being some positive results have a place here already. Some experimental results could be illuminated more in detail [6, 7].

Many technical solutions for the outer magnetic pulsed flattening of the airplane are known long ago. The most practical and interesting suggestions in this area are belonged to the American engineers from the «Boeing», «ElectroImpact» and «Fluxtronic». As it follows from their publications the attraction could be realized with help of a single turn inductor with two pulsed currents of the different frequencies [8, 9].

Should mark the suggestion of the magnetic pulsed attraction with help of superposition of «slow» and «quick» magnetic fields had been discussed in the works of the former soviet scientists too [3].

The physical essence of these both suggestions is identical. Eventually they are based on superposition of the magnetic fields with low and high frequencies which are excited in the inductor system.

The technical level of these ideas for practical realization is approximately identical too. According to these suggestions the real devices for the magnetic pulsed attraction of the sheet metals must have two synchronized power sources, the high-voltage and high-current electronics for the complicated controlling systems, etc. All these factors are the reasons of a high cost and of low reliability what decreases essentially a practical significance of these elaborations.

The practical usage of the displayed effect of the steel sheets attraction by the forces of the low-frequency

magnetic fields opens new possibilities for creating enough simple, reliable and relatively cheap devices for the magnetic pulsed flattening the sheet metals.

These devices must have the evident advantages.

Among them the following positions may be distinguished particularly.

- Any mechanical contacts with a processed surface are absent, the magnetic pulsed forces are acting.
- The list of the processed metals (steel and its different alloys which are being used in the auto branch of the manufacture) is quite wide.
- Flattening is being realized from the outer side of the body car without any disassembling what is sure necessary in the traditional technologies.
- The possible preserving of the outer coating (without any damages!) on the surface being worked.
- There is possibility of the damaged element restoration till the initial state with preserving the existing coating.

The experimental model of the inductor system allowing to excite the magnetic pulsed attracting forces was elaborated, made and tested in the real conditions for different specimens of the sheet steels.

The single turn inductor was connected to output of the magnetic pulsed installation (power source) with energy stored ~4.5 kJ.

Creating and removing the dents in the different parts of the metal sheet were fulfilled. One of them will be removed but other dent will stay for comparison.

The first operation was dedicated to creating the dents with help of the attraction forces. Two dents with half-sphere shape with diameter about ~ 0.03 m and depth about ~ 0.002 m were pulled from the steel sheets after eight repetitions of the force action.

The next experiment was dedicated to removing of one of the before created dents on the sheet surface with help of the attraction forces too. This specimen was placed on the flat insulated surface of the inductor so that the interior of existing dent turned out opposite the inner hole of the inductor. Removing the dent was produced by the same way as it was created by the magnetic pulsed attraction.

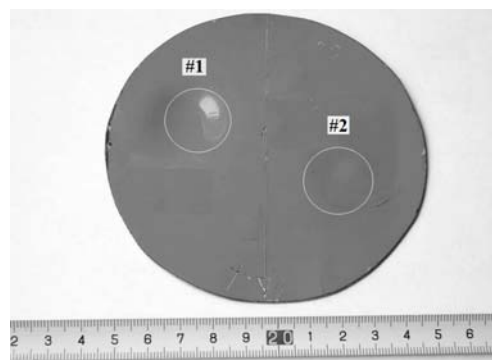


Fig. 3. The experimental specimen from the sheet steel of the body car «Mitsubishi» with the painted covering: #1 – is the dent got by the magnetic pulsed attraction from the assigned part of the experimental sheet specimen, #2 – is the part of the experimental sheet specimen with removed dent

After five repetitions the dent had been practically removed. The surface of the sheet, where it was, had

become quite smooth. The subsequent magnetic pulsed attraction would lead to appearance of a new dent with opposite curvature in relation to the initial.

The experimental specimen with initial and removed dents is shown on Fig. 3.

The main results of the conducted experiments are the following.

- The energy of the force action what is necessary for the dent removing is essentially smaller what is necessary for the dents creating on the smooth surface.
- In fulfilling production operations of the magnetic pulsed attraction the repetition stability of the got results was marked. This fact testifies about reliability of the tested method for the practical application. For example, it could be external flattening of a damaged body car.

Ending a description of the conducted experiments should mark that the magnetic pulsed attraction with help of the presented equipment may be realized for the ferromagnetic steels only.

Besides should point out that the practical achievement not only for steels but and suggestions for non-magnetic metals are represented on Web Site of Laboratory of the Electromagnetic Technologies (Kharkiv National Automobile & Highway University, Ukraine) [10].

#### Conclusions.

The conducted review is briefly illuminating the main achievements of the advanced technologies with usage of the energy of the pulsed magnetic fields.

1. The known approaches to solution actual production problems based on the skin-effect in electrodynamics are described. They were demonstrated their effectiveness in many cases of the practical approbation and were implemented in different branches of the industrial manufacture.

2. The new suggestions of the magnetic pulsed force action are represented.

They are based on the results of development of the new scientific direction in area of the magnetic pulsed processing thin-walled sheet metals when a penetration of the acting fields is quite significant. The first of these suggestions is related to stamping of the drawing the printed circuit boards on the cooper foil with thickness about 50mkm. The second suggestion consists in usage the magnetic pulsed attraction for external removing the dents in the car body. The operation does not demand disassembling of elemental base. As well the paint of coverings may be preserved.

#### How to cite this article:

Batygin Yu.V., Chaplygin E.A., Sabokar O.S. Magnetic pulsed processing of metals for advanced technologies of modernity – a brief review. *Electrical engineering & electromechanics*, 2016, no.5, pp. 35-39. doi: 10.20998/2074-272X.2016.5.05.

#### REFERENCES

1. Psyk V., Risch D., Kinsey B.L., Tekkaya A.E., Kleiner M. Electromagnetic forming – A review. *Journal of Materials Processing Technology*, 2011, vol.211, no.5, pp.787-829. doi: **10.1016/j.jmatprotec.2010.12.012**.
2. Belyj I.V., Fertik S.M., Himenko L.T. *Spravochnik po magnitno-impulsoj obrabotke metallov* [Directory of magnetic-pulse treatment of metals]. Kharkiv, Vishcha shkola Publ., 1977, 189 p. (Rus).
3. Batygin Yu.V., Lavinskiy V.I., Khimenko L.T. *Impul'snyye magnitnyye polya dlya progressivnykh tekhnologiy. Tom 1. Izdaniye vtoroye, pererabotannoye i dopolnennoye*. [Pulsed magnetic fields for advanced technologies. Vol.1. 2nd edition, revised and enlarged.] Kharkov, MOST-Tornado Publ., 2003. 284 p. (Rus).
4. Batygin Yu.V., Lavinsky V.I. Electromagnetic processes in an inductor system for stamping printed circuit boards. *Electrical Technology Russia*, 2001, no.4, pp. 129-136.
5. Batygin Yu.V., Lavinsky V.I., Khimenko L.T. Direction Change of the Force Action upon Conductor under Frequency Variation of the Acting magnetic Field. *Proceedings of the 1<sup>st</sup> International Conference on High Speed Metal Forming*. March 31/April 1, 2004. Dortmund, Germany, pp. 157-160.
6. Yuriy V. Batygin, Sergey F. Golovashchenko, Andrey V. Gnatov. Pulsed electromagnetic attraction of sheet metals – fundamentals and perspective applications. *Journal of Materials Processing Technology*, 2013, vol.213, no.3, pp. 444-452. doi: **10.1016/j.jmatprotec.2012.10.003**.
7. Batygin Yu.V., Golovashchenko S.F., Gnatov A.V., Chaplygin E.A. Pulsed Electromagnetic Attraction Processes for Sheet Metal Components. *Proceedings of the 6<sup>th</sup> International Conference High Speed Forming 2014*, May 26-29, 2014, Daejeon, Korea, pp. 253-260.
8. *Electromagnetic Dent Removal*. Available at: <http://www.electroimpact.com/EMAGDR/overview.asp> (accessed 25 May 2014).
9. *Need an electromagnetic dent remover on hand. Fluxtronic offers the best: the Portable Flux 3 dent remover*. Available at: <http://www.fluxtronic.com/product.php> (accessed 07 August 2014).
10. *Laboratoriia elektromagnitnykh tekhnologii* (Laboratory of Electromagnetic Technology) Available at: <http://electromagnetic.comoj.com> (accessed 10 July 2014).

Received 13.06.2016

Yu.V. Batygin<sup>1</sup>, Doctor of Technical Science, Professor,  
E.A. Chaplygin<sup>1</sup>, Candidate of Technical Science, Associate Professor,

O.S. Sabokar<sup>1</sup>, postgraduate student,  
<sup>1</sup>Kharkiv National Automobile and Highway University,  
25, Petrovskogo Str., Kharkiv, 61002, Ukraine.  
phone +38 057 7073727, e-mail: batygin48@mail.ru,  
chaplygin.e.a@gmail.com, o.s.sabokar@gmail.com

V.K. Beliaev, H.N. Panenko

## DETERMINATION OF INSULATION PARAMETERS OF CURRENT TRANSFORMERS AT MULTIPLE MEASUREMENTS IN MONITORING SYSTEMS UNDER WORKING VOLTAGE

*Features of the data processing procedures of multiple measurements of the dielectric loss tangent of the high-voltage insulation, which are based on the comparison method, were considered. Three procedures were compared: the one procedure uses an assignment of a particular standard object for comparison, and two procedures don't use assignments of the special standard objects. Expressions of methodical errors of studied procedures were obtained. Analysis and calculations, which use the obtained expressions were made. Evaluations showed that an influence of a change of the tangent of dielectric loss of one from the monitoring objects on results of estimation of the tangents of other monitoring objects is the distinctive feature of the procedures without assignment of the standard object. Errors of these procedures more than errors of the traditional procedure, with assignment of the standard object. The study demonstrated that procedures without assignment of standard objects lead to difficultly predictable methodological errors, which hinder to estimate the actual value of the loss tangent and to estimate outcomes of the monitoring, by means comparing with allowable values. Moreover, the decrease of estimations of loss tangents of all objects, as a result of occurrence of at least one the object with strongly bad parameters, hides occurrence of other unsuccessful objects with smaller deviations and makes difficult recognition of such deviations at early stages. Improvements in processing techniques which reduce earlier specified errors and reduce the amount of measurements are proposed. The study results are useful in monitoring and diagnostic of basic insulation of current transformers or high-voltage bushings. References 8, tables 1, figures 5.*

*Key words:* high voltage insulation, diagnostics, data processing procedure, processing procedure error, dielectric loss tangent, current transformer.

*Рассмотрены особенности методик обработки результатов множественных измерений тангенса угла диэлектрических потерь высоковольтной изоляции, основанных на методе сравнения. Проанализированы известные методики определения тангенса потерь с выделением отдельного эталонного объекта и без выделения такого эталона. Получены выражения для определения методических погрешностей. Проведено сравнение и показано, что применение методик обработки без выделения отдельного эталонного объекта может приводить к существенным сложностям в оценке результатов контроля изоляции. Предложены усовершенствования методик обработки, уменьшающие указанные погрешности методик и трудоемкость измерений. Библи. 8, табл. 1, рис. 5.*

*Ключевые слова:* высоковольтная изоляция, диагностика, методика обработки, погрешность, тангенс угла диэлектрических потерь, трансформатор тока.

**Introduction.** The power companies of Ukraine introduced technologies of condition monitoring of high-voltage insulation of measuring current transformers without decommissioning (under operating voltage) [1-5]. At present, as the main method of such control for oil-filled current transformers (insulation of capacitor type) should be considered differential control in which among all tested current transformers (hereinafter referred to as objects of control – OC) of one phase they select «reference» having the best condition of the insulation, and others' state is evaluated by the change of dielectric loss tangent with respect to the selected reference [3, 6]. We can select the technologies of periodic and continuous monitoring which differ, in fact, by the frequency of measurement of the insulation of objects of control (OC) which is a consequence of the degree of automation of the measurement process [3, 5]. Similar tools can be used in both technologies (bridge, vector meters) and measuring methods.

To increase the efficiency of control technology it is proposed [2, 5] to use multiple measurements during which it is assumed that each OC is alternately used as a

reference for all other controlled OC (without determination of separate reference object). Indicated approach eliminates the need for special control and awkward shifts of reference objects. These methods of measurements results treatment differ from the processing technique at selection of a reference by using various kinds of averages over all the results that will naturally lead to reduction of influence of random variations caused by, for example, short-term noises. At the same time, in [7] it is indicated on the possibility of occurrence at such treatment of additional errors not arise at traditional measurements processing with special release of the reference object.

**The goal of the work** is definition of error of techniques of results treatment of multiple measurements of the loss tangent of the insulation without selection of the reference object, the development of methods to reduce the error.

**Fundamentals of methods of processing the results of measurements of loss tangent of insulation.** A basis of differential control is a bridge method of

comparison with a reference (standard) [3, 6]. Using AC bridge (recently high-precision measuring vector meters, for example [1] are used), they measure by tangent ( $tg\delta_{meg}$ ) of the difference of dielectric loss angles of OC ( $\delta_{ok}$ ) connected to the input «X» and angle of reference loss ( $\delta_e$ ) connected to the input «0», so that (because of the smallness of the actual loss angles the tangent of the difference from the difference of tangents can be ignored):

$$tg\delta_{ok} = tg\delta_{meg} + tg\delta_e. \quad (1)$$

The problem is that the actual value of the loss tangent of the reference object used as the base for counting, during the measurement (control) is unknown, and instead of it we use the approximate values that is a source of systematic errors – the calculated tangent differs from the actual OC loss tangent.

In the case of measuring a plurality of objects under operating voltage for one phase OC at any time  $k$ , we write the formula (1) as follows (for simplicity hereinafter instead  $tg\delta$  we write  $\delta$ ):

$$\delta_{j(k)} = \partial\delta_{ij(k)} + \delta_{i(0)}, \text{ or } \partial\delta_{ij(k)} = \delta_{j(k)} - \delta_{i(0)}, \quad (2)$$

where  $\delta_{j(k)}$  is the loss angle tangent of the  $j$ -th OC;  $\partial\delta_{ij(k)}$  is the tangent of the differential angle at the measurement for the  $j$ -th OC at the  $i$ -th standard (the first index is for standard, the second one is for the tested OC). Here, according to [3], the measured tangent of OC loss of the angle difference and the standard is called as tangent of the differential angle.

At the differential control is determined not the tangent of the OC differential angle is determined but its increment ( $\Delta\delta_{ij}$ ) relative to baseline values – at the beginning of the control [3, 6]. So, at the measurement at time  $k$  for the  $j$ -th OC at the  $i$ -th reference (one pair measurement), the increment of tangent of the differential angle:

$$\Delta\delta_{ij(k)} = \partial\delta_{ij(k)} - \partial\delta_{ij(0)} = -\Delta\delta_{ji(k)}, \quad (3)$$

where  $\partial\delta_{ij(0)}$  is the initial value of the tangent of the differential angle measured at the taking of objects in the control.

According to the procedure 1 described in Standard COY-H MIE [3], the measurements are carried out with the selected reference OC ( $i$  is the reference index). Using the obtained according to (3) increment, they determine the current estimated value of the tangent of the checked OC [3, 6]:

$$\delta_{j(k)} = \Delta\delta_{ij(k)} + \delta_{j(0)}, \quad (4)$$

where  $\delta_{j(0)}$  is the initial value of the tangent for the  $j$ -th OC determined at the taking of objects in the control.

For the reference OC:

$$\delta_{i(k)} = -\Delta\delta_{ij(k)} + \delta_{i(0)}. \quad (5)$$

The obtained values are compared with the permissible values of loss angle tangent (0.005 ... 0.008) normalized in [3] (rejection criteria).

Substituting the definition (3) in the formula (4), after transformations we obtain the following expression for determining the calculated value of tangent:

$$\delta_{j(k)} = \partial\delta_{ij(k)} + \delta_{i(0)}. \quad (6)$$

Comparing (6) with the exact expression (2) for the actual value of OC tangent we see that in the procedure 1 at determining the calculated tangent it is proposed instead of unknown during measurement value of the reference OC tangent  $\delta_{i(0)}$  to use the value of objects in the control determined at the taking of objects in the control  $\delta_{i(0)}$ . The resulting calculated value of the tangent of the loss angle  $\delta_{j(k)}$  (which is compared with the permissible norm) will differ from the actual  $\delta_{j(k)}$  to the value of increment of the tangent of the reference object tangent for the time from the start of control.

At mass monitoring of OC insulation on the outdoor switchgear, there are certain inconveniences with the choice and the control of the state of the reference OK, and when selection one standard for all OC phases (the most convenient option), formula (5) to assess the standard OC becomes unacceptable [5]. Indeed, for each checked OC without changing the reference we obtain individual different result from the others for  $\Delta\delta_{ij(k)}$  and as a consequence – different values of calculated tangent  $\delta_{i(k)}$  for the same  $i$ -th reference.

To be able to control the reference OC, in the Dniprovsk Power Grid [5] it was proposed instead of one particular measured value  $\Delta\delta_{ij(k)}$  to use in (5) the average increment for all  $N$  received values for the controlled objects on the phase:

$$\delta_{i(k)} = -\frac{1}{N-1} \sum_{j \neq i}^N (\Delta\delta_{ij(k)}) + \delta_{i(0)}, \quad (7)$$

where  $i$  is the reference index.

**Processing techniques without selection of the individual reference.** In cases of an automated continuous or periodic monitoring of current transformers, several methods (algorithms) for determining the calculated tangent based on conducting plurality of measurements without selection of individual OC reference are proposed [2, 7]. In these measurements each OC alternately serves as a reference for the other checked OC of the same phases. As each OC passes measurements in pair with another one, the total number of measurements increases considerably – as the square of OC number.

Method 2 used AT nine substations OF THE Donbass power system [5] At the control of  $N$  objects on the phase it is proposed in determining the current value of each OC calculated tangent instead of formulas (4) and (5) using the following expressions constructed by analogy with formula (7):

$$\delta_{i(k)} = -\Delta\delta_{iav(k)} + \delta_{i(0)}, \Delta\delta_{iav(k)} = \frac{1}{N-1} \sum_{j \neq i}^N \Delta\delta_{ij(k)}, \quad (8)$$

where the index  $iav$  indicated the value average for all OC (excluding the  $i$ -th one).

We merge (8) in one expression and substitute the definition (3):

$$\begin{aligned} \delta p_{i(k)} &= -\frac{1}{N-1} \sum_{j \neq i}^N \Delta \delta_{ij(k)} + \delta_{i(0)} = \\ &= \frac{1}{N-1} \sum_{j \neq i}^N \left( -\partial \delta_{ij(k)} + \delta_{j(0)} \right) = -\partial \delta_{iav(k)} + \delta_{iav(0)}. \end{aligned} \quad (9)$$

The obtained expression shows (cf. (6)) that, according to this method, the calculated value of the loss tangent is the average of all paired results (each OC with everyone, except as with itself) carried out according to the method 1.

Procedure 3 proposed in [2] for use in the continuous control system at 330 kV substation of the Dnepr power system. According to [2], at the control of  $N$  objects eponymous phase is first determined by the intermediate values of tangent ( $\delta 1_{ij(k)}$ ) for each  $i$ -th OC at paired measurements with different standards  $j$  by the formula similar to (6), where instead of the tangent of the reference in the beginning of the control, use the calculated value of the tangent of the  $i$ -th OC obtained in previous measurements. To determine the final estimated value for the  $i$ -th OC taken the average of all intermediate values for this OC at different references  $j$ . The described in the formula expression can be written as follows:

$$\delta 1_{ji(k)} = \delta p_{j(k-1)} - \partial \delta_{ij(k)}, \quad \delta p_{i(k)} = \frac{1}{N-1} \sum_{j \neq i}^N \delta 1_{ji(k)}. \quad (10)$$

We write last formulae as follow:

$$\begin{aligned} \delta p_{i(k)} &= \frac{1}{N-1} \sum_{j \neq i}^N \left( -\partial \delta_{ij(k)} + \delta p_{j(k-1)} \right) = \\ &= -\partial \delta_{iav(k)} + \delta p_{iav(k-1)}. \end{aligned} \quad (11)$$

Comparing the expressions (11) and (9) we see that the results of the processing algorithms to determine the estimated value of the tangent of the last two methods, without isolation of the individual reference, differ only in the values taken for the baseline from which the increments are counted. In the second method of the base taken the average of all values of the tangents at the OC to take control in the third uses an average of all the values calculated in the previous measurement. Both techniques are used an average of the measured values of the tangent of the differential angle.

**Comparison of methods' of errors.** Of interest is the analysis of systematic errors arising as a result of the loss tangent calculation formulas given above, instead of the exact formula (2). Under the methodological error of the specific techniques mean difference between the calculated values of OC tangent, obtained by treatment of the appropriate expression of its real value:

$$D_{j(k)} = \delta p_{j(k)} - \delta_{j(k)}.$$

Presenting each technique as a separate model to determine the output value (the estimated tangent), this error can be seen as error adequacy model showing the lowest possible error when using the model-technique [8]. The resulting expression for determining  $b_{i(k)}$  of all the considered methods are given in the Table 1. For the methods of quality characteristics it is advisable to carry out sensitivity analysis, identifying the corresponding coefficients of sensitivity (influence) that bind each change of the input variable with the resulting change in the output. The table gives the expressions for the coefficients  $b_{i(k)}$  characterizing the sensitivity of the resulting changes in the estimated value of tangent  $j$  OC at  $k$  time  $\varepsilon \delta p_{j(k)}$  to change in the actual value of the tangent of each  $i$  OC  $\varepsilon \delta_{i(k)}$ :

$$\varepsilon \delta p_{j(k)} = \sum_{k=1}^k \left( \sum_i b_{i(k)} \varepsilon \delta_{i(k)} \right) + \sum_i b_{i(0)} \varepsilon \delta_{i(0)}, \quad i, j = 1 \dots N. \quad (12)$$

Here the general expression of connection is presented. Obviously, the components associated with the timing of 1 to  $k-1$  appear only when using the method 3. Assuming little change input values, sensitivity coefficients were determined based on derived respective functional connections of the output variable with input [8]. The coefficients of the last part of the above expression ( $k=0$ ) is characterized by sensitivity to errors taking of objects in the control.

The presented in Table 1 expressions show that the greatest impact on the estimated result for any checked OC values have the latest measurements on the same OC ( $b_{j(k)}=1$ ). Values of other OC tangents no effect on the inspected result in the case of OK method 1, but can significantly affect the use of other techniques. This effect is inversely proportional to the number of OC.

Negative signs of influence factors  $b_{i \neq j(k)}$  indicate that any increase in the value of the tangent at any OC would reduce the calculated values on other OC tangents.

For example, we suppose that the change occurred at one («damaged») OC. Let up to the  $k$ -th point in time no changes have occurred. The  $k$ -th time at the  $m$ -th OC abruptly changed by the amount of loss tangent  $\varepsilon \delta_{m(k)} = \delta_{m(k)} - \delta_{m(k-1)} = d$ , the remaining OC changes were not tangent ( $\varepsilon \delta_{j \neq m(k)} = 0$ ) and at subsequent times tangent values at all OC is not changed ( $\delta_{i(k+n)} = \delta_{i(k+1)} = \delta_{i(k)}$ ) for all  $i, n$ . In accordance with the values of the coefficients of influence by (12) we change tangent calculation and by the expressions in Table 1.

We define  $D_{j(k)}$  errors:

- By method 1: for «damaged» OC  $\varepsilon \delta p_{m(k)} = d, D_{j(k)} = 0$ ; for other OC  $\varepsilon \delta p_{j \neq m(k)} = 0, D_{j \neq m(k)} = 0$ .
- By method 2: for «damaged» OC  $\varepsilon \delta p_{m(k)} = d, D_{j(k)} = 0$ ; for other OC  $\varepsilon \delta p_{j \neq m(k)} = -d/(N-1), D_{j \neq m(k)} = -d/(N-1)$ .
- By method 3: for «damaged» OC at time  $k$ :  $\varepsilon \delta p_{m(k)} = d, D_{j(k)} = 0$ ; at the next time  $\varepsilon \delta p_{j \neq m(k+1)} = -d/(N-1), D_{j \neq m(k+1)} = -d/(N-1)$ ; for other OC at time  $k$ :  $\varepsilon \delta p_{j \neq m(k)} = -d/(N-1), D_{j \neq m(k)} = -d/(N-1)$ ; at the next time  $\varepsilon \delta p_{j \neq m(k+1)} = -d/(N-1)^2, D_{j \neq m(k+1)} = -d(N-2)/(N-1)^2$ .

As we can see, using methods 2 and 3, the calculated values differ from the actual tangent of its values ( $\varepsilon\delta_{j(k)} \neq \varepsilon\delta_{j(k)}$ ,  $D_{j(k)} \neq 0$ ) to appear for «healthy» OC. When using 3 methods calculated tangents differ from the actual not

only in «healthy», but also in «damaged» OC – not at the moment of change, but starting from the next measurement.

Table 1

Expressions for the considered methods' errors and sensitivity (influence) coefficients

Method No., Calculation formula	Error $D_{j(k)}$ :	Sensitivity coefficient
1, (4), $i$ – reference	$-(\delta_{i(k)} - \delta_{i(0)})$	$b_{j(k)} = 1, b_{i(k)} = -1, b_{i(0)} = 1$
2, (9)	$-\frac{1}{N-1} \sum_{i \neq j}^N (\delta_{i(k)} - \delta_{i(0)})$	$b_{j(k)} = 1, b_{i \neq j(k)} = -1/(N-1), b_{i \neq j(0)} = 1/(N-1)$
3, (11)	$-\frac{1}{N-1} \sum_{i \neq j}^N (\delta_{i(k)} - \delta_{i(k-1)})$	$b_{j(k)} = 1, b_{i \neq j(k)} = -1/(N-1), b_{j(k-1)} = -1/(N-1),$ $b_{i \neq j(k-1)} = 1/(N-1)^2, \dots, b_{j(0)} \rightarrow 0$
4, (13)	$-\frac{1}{Nm-1} \sum_{i \neq j}^{Nm} (\delta_{i(k)} - \delta_{i(0)})$	$b_{j(k)} = 1, b_{i \neq j(k)} = -1/(Nm-1), b_{i \neq j(0)} = 1/(Nm-1)$ .

In actual control of a plurality of current transformers may be situations where the aging of the insulation at the same time gradually increasing tangents at several objects at different speeds. Upon reaching the critical normalized values of tangents at one of OK decision on further testing or withdrawal from service. [3] In such cases, the effect of varying tangents of one OK on other using methods 2 or 3 difficult to assess the condition of the insulation.

For example, we consider a model situation of control of several OC ( $N=6$ , in [5] it is recommended to use no more than 6 OC due to the laborious measurements). Fig. 1 shows an idealized picture of the actual values change tangents insulation of OC (initial values from 0.0015 to 0.001) during the operation at a constant rate – from measurement to measurement ( $k$  is time, measuring index). For OC No. 2 strong change leads to achievement on the 20th step of monitoring a large critical value (0.005), in the OC No. 3, 4 growth weaker, for OC No. 1 poorly discernible rise (20 times less than that for No. 2), for two of the remaining changes are absent.

Fig. 2-4 show graphs of the calculated tangents, respectively defined by the formulas (4), (9) and (11) corresponding to the methods 1, 2 and 3. When using the method 1 (Fig. 2) as the reference OK No. 1 is adopted with a slight, but not with the smallest change that occurs in practice.

Accordingly, the calculated values of the tangents at the monitored objects smaller than actual (Fig. 1) to the value of growth of the reference OC tangent. For OC with the same with the real tangents will fix them a slight decrease (for the same value). Status of the reference OK by this method is not evaluated.

Fig. 2 also shows the calculated reference OK No. 1 tangents defined by the formula (7) (graph as 1a is

indicated), which show that the evaluation of the situation in the considered yields a significant underestimation of the tangent, is the same as using the method 2 (see Fig. 3 below).

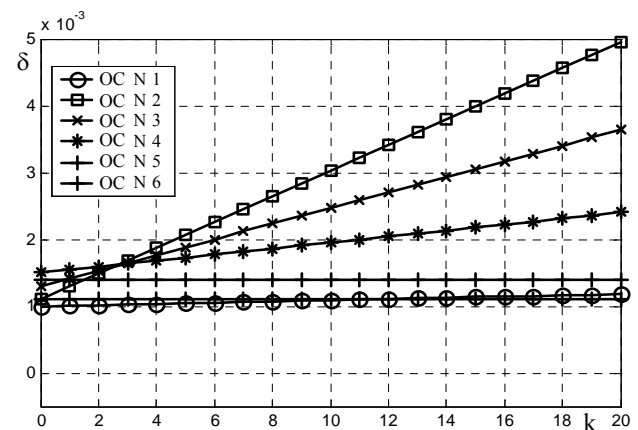


Fig. 1. Changes of real values of OC insulation loss tangents

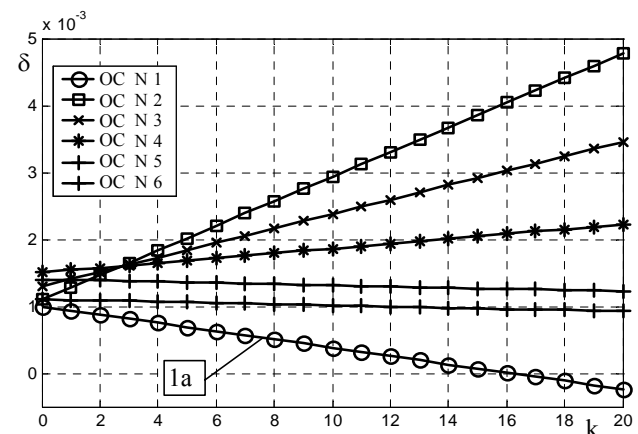


Fig. 2. Changes of calculated values of OC insulation loss tangents determined by method 1

The graphs in Fig. 3 and 4 clearly show a strong change OK tangent tan calculated values but significantly different from the actual values. It is also readily determined by the relative state of isolation of objects of control, but to determine how big the actual values of tangents (which is necessary to identify the values exceeds the regulation) and how fast they are growing, it is difficult. To recognize errors in such an object with a small increase of the tangent (the initial stages of development defects) is a hardly feasible task.

It should be noted that when using the method of 3 difference between the calculated values of the tangents from the actual more than method 2. Method 1 is easier to have the predicted error (determined by the state of the reference OC). Given that the selected object as a reference in the best condition, an error procedure is one less than the methods 2 and 3.

The difficulty of assessing the real value of tangents and their trends according to methods 2 and 3 caused by  $D_{j(k)}$  error dependence ( $k$ ) not only on the number of controllable OC, but the total gain change reality tangents (see expression in Table 1) which is unknown value in advance. The real situation is complicated by the uneven growth of losses, the temperature dependence of the measured insulation value (different even for the same type of real-OC) the inability to completely weed out the external random and non-random influence.

Obtained expressions for  $D_{j(k)}$  make it possible to estimate the error (low value of real systematic error) after receiving the results of an increase in the calculated tangents at OC  $\delta p_{j(k)}$ , assuming that the increase in real tangents corresponds to an increase of calculated ( $\delta_{j(k)} - \delta_{j(0)} = \delta p_{j(k)} - \delta_{j(0)}$ ). Also expressions allow to assess the expected error in the determination of tangents calculated in the control system, making the assumption that the increase in real tangents at a few OC.

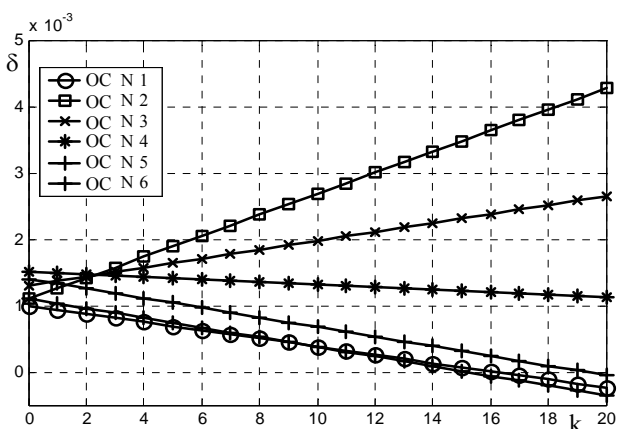


Fig. 3. Changes of calculated values of OC insulation loss tangents determined by method 2

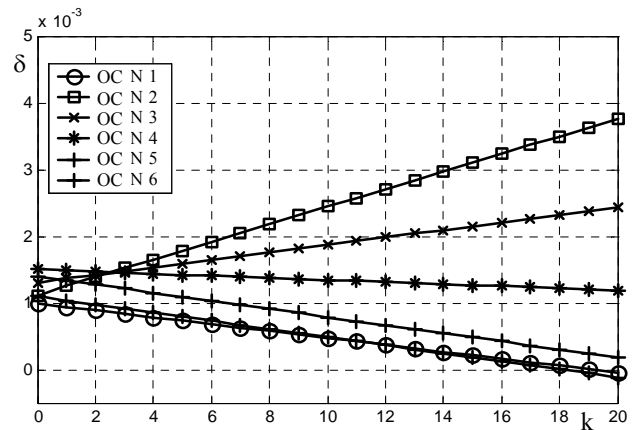


Fig. 4. Changes of calculated values of OC insulation loss tangents determined by method 3

As a result, it can be stated that the processing technique without isolating individual standard (methods 2 and 3) do not provide the advantages of precision in determining results but require substantially more measurements ( $N^2$  against  $N$  in method 1).

**Methods improvement.** Reducing methods' errors without isolation of the individual standard can be achieved by changing the order of calculation as follows. Averaging the results of measurements conducted in (7), (9) or (11) for determining the calculated tangent should be not OC in all, and on the selected smaller group of objects of volume  $Nm$ . The composition of this «support» group defined in the previous ( $k-1$ ) time measurement step, by choosing OC with the smallest increase calculated relative to the tangent of the initial values: ( $\delta p_{j(k-1)} - \delta_{j(0)}$ ). With this selection of averaging excluded objects bearing potential danger of a large distortion of the calculated results, which reduces the expected error (total gain of tangents «support» of the group is less than the total increase). Thus, for example, the formula (7), (9) at the modified procedure will be written:

$$\begin{aligned} \delta p_{i(k)} &= -\frac{1}{Nm-1} \sum_{j \neq i}^{Nm} \Delta \delta_{ij(k)} + \delta_{i(0)} = \\ &= \frac{1}{Nm-1} \sum_{j \neq i}^{Nm} (-\delta \delta_{ij(k)} + \delta_{j(0)}) \end{aligned} \quad (13)$$

if the  $i$ -th OC is included in the selected group, if not – to in (13) instead  $Nm-1$  we should write  $Nm$ .

Taking into account the low probability of simultaneous significant deterioration in many OC, «support» group may contain only a few objects smaller than the total number of OC. The greater part of the OC group, the less can change its composition.

To substantially reduce the number of measurements at each time step (from  $\approx N^2$  to  $\approx N$ ), one can determine the differential angle tangent of two OC in (7) and (9), (11), (13) by not a direct measurement but by calculation using measurements of the tangent with selection of an individual reference object:

$$\partial\delta_{ij(k)} = \partial\delta_{ij(k)} - \partial\delta_{li(k)},$$

where  $l$  is the index of the selected reference object.

With this definition  $\partial\delta_{ij(k)}$  we lose the opportunity to further test the results by comparing the results of the «direct» and «reverse» measurements ( $\partial\delta_{ij(k)} \approx -\partial\delta_{ji(k)}$ ), proposed in [2, 7]. Note that the specified test when necessary, without losing efficiency deviation of unsuccessful results it is possible to replace by the control deviations at the statistical processing of the results of repeated measurements with the selected reference.

Fig. 5 shows the variation of the calculated tangent defined by the formula (13), an improved method for modeling the situation described previously. When calculating the chosen «reference» group of 4 OC (66% of total OC) having the lowest increase at the current time step, thus it was possible distorting effect of 2 and 3 OC on the results of the evaluation (changes to OC 1 and 4 continue to influence, causing error). It can be seen that the calculated tangents better reproduce the values and trends of the real tangents than in methods 2 and 3. In contrast to the method 1 are controlled by all OC including standard.

Errors of methods without selection of the standard less at more controlled and OK with a smaller total change of tangents (a smaller increase in the values of real tangents, fewer OC to deterioration).

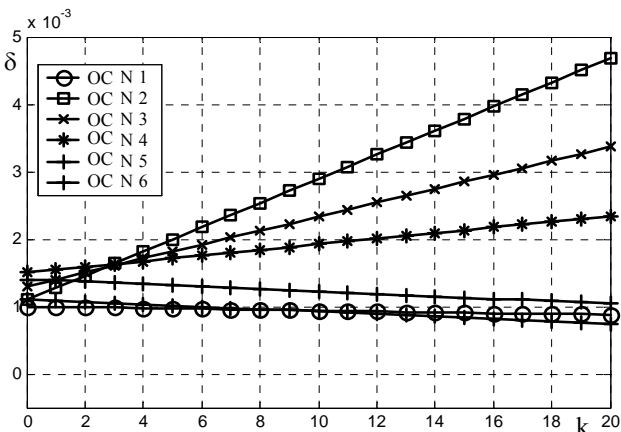


Fig. 5. Changes of calculated values of OC insulation loss tangents determined by improved method

**Conclusions.** A distinctive feature of methods without selection of reference is the impact of changes in loss tangent of one OC on the results of the assessment of other OC tangents leading to difficult to forecast the methodological errors that make it difficult to estimate the actual value of tangent and can cause errors in the assessment of controlled objects.

Appearances of at least one OK with severely deteriorating real parameters leads to a decrease in the estimated loss tangents of all OC that disguises the

appearance of other disadvantaged OC with smaller deviations, and makes it difficult to identify such deviations for determining the developing insulation defect in the early stages.

The proposed improvement of methods for determining the estimated values of tangent with averaging over a dedicated «support» OC group allows reduce the negative impact of objects with deteriorating performance on the assessment of other OC tangents and reduce errors, while maintaining the ability to simultaneously control of all OC.

Utilization of the calculation method for determining the differential angle tangents of two OC on the results of measurements by the results of measurements using selected standard permits to significantly reduce the number of required measurements (till the value required in the traditional method with the selection of the standard).

In conclusion, conclusions are valid for both basic current transformers insulation control as well as for insulation monitoring of high-voltage bushings.

#### REFERENCES

1. Beliaev V.K., Borshchev P.I., Obodovskii V.D., Kanivetskii Iu.V., Bekhtev G.V., Bogdanov S.G., Masenko D.A., Dvoinykh V.P. Instrumentation and experience of monitoring of capacitor type insulation under operating voltage. *Electrical networks and systems*, 2012, no.4, pp. 68-72. (Rus).
2. Sakhno A.A. Measurement algorithm of the dielectric loss tangent of basic insulation of current transformers and bushings 330-750 kV under monitoring under a working voltage. *Electrical engineering & electromechanics*, 2010, no.2, pp. 54-56. (Rus.) doi: 10.20998/2074-272X.2010.2.14.
3. SOU-H MPE 40.1.46.301:2006. *Perevirka izoliatsii transformatoriv strumu 330-750 kV pid napruhoiu. Metodichni vkazivky* [Standard of organization H MPE 40.1.46.301:2006. Check of insulation of current transformer 330-750 kV under voltage. Methodical instructions]. Kyiv, Minpalyvenerho Publ., 2006. (Ukr).
4. Stognii B.S., Pilipenko Iu.V., Sopol' M.F., Tutik V.L. Hardware-software monitoring complex of insulation of current transformers and high-voltage bushings of power transformers. *Works of the Institute of Electrodynamics of the National Academy of Sciences of Ukraine*, 2010, is.26, pp. 38-45. (Rus).
5. Shinkarenko G.V., Onishchenko V.A., Ornatskii O.A. Technologies of measurement of insulation parameters of oil-filled transformers 330-750 kV under operating voltage. *Electrical networks and systems*, 2012, no.3, pp. 67-71. (Rus.)
6. Svi P.M. *Metody i sredstva diagnostiki oborudovaniia vysokogo napriazheniia* [Methods and diagnostic tools of the equipment of a high voltage]. Moscow, Energoatomizdat Publ., 1992. 240 p. (Rus).
7. Beliaev V.K., Panenko H.N. Features of definition methods of insulation parameters in the monitoring systems of current transformers under working voltage. *Bulletin of Kharkiv Petro Vasylenko National Technical University of Agriculture. Series: Technical science*, 2014, no.153, pp. 122-124 (Rus).

8. Beliaev V.K., Obodovskii V.D., Panenko H.N. The analysis of sensitivity of diagnostic models for the monitoring of a transformer windings condition under load. *Tekhnichna elektrodynamika*, 2013, no.4, pp. 81-87. (Rus).

*Received 11.06.2016*

*V.K. Beliaev<sup>1</sup>, Candidate of Technical Science, Associate Professor,*

*H.N. Panenko<sup>2</sup>, Postgraduate Student,*

<sup>1</sup> Scientific Industrial Enterprise «OST»,

33-D, Bulvarno-Kudryavskaya Str., Kyiv, 01054, Ukraine.

e-mail: bel\_vk@ua.fm

<sup>2</sup> National Technical University of Ukraine «Kyiv Polytechnic Institute»,

37, Prospect Peremohy, Kyiv-56, 03056, Ukraine.

*How to cite this article:*

Beliaev V.K., Panenko H.N. Determination of insulation parameters of current transformers at multiple measurements in monitoring systems under working voltage. *Electrical engineering & electromechanics*, 2016, no.5, pp. 40-46. doi: 10.20998/2074-272X.2016.5.06.

O.V. Golik

## STATISTICAL PROCEDURES FOR TWO-SIDED LIMIT OF A CONTROLLED PARAMETER IN THE PROCESS OF PRODUCTION OF CABLE AND WIRE PRODUCTS

*Purpose.* To consider issues of statistical control in the process of mass production of cable and wire products on the example of enameled wire. To analyze the results of direct control of the diameter of the wire in two-layer polyimide insulation in a continuous technological cycle. To submit to the control map of maximum probability of the exit diameter outside a specific range. To analyze the conditions under which maximum sensitivity of process control. *Methodology.* Study of the sensitivity of the control map of maximum probability of the exit option for regulatory of limit in the field deviations of the centered parameter close to zero. The existence of stable trends in the change of a controlled parameter can reduce the sensitivity of punishment to instability of the process. *Results.* To achieve maximum sensitivity of control of the technological frontier should be selected on the basis of the achieved level of the average value of the parameter and its statistical scattering. Process boundaries must be changed in accordance with the achieved level of the average value of the parameter and its statistical scattering. Such a change may serve as a quantitative indicator of trends in the increase or decrease in the reliability of the technological system. *Originality.* In particular the tasks of current control using engineering tolerances for controlled parameter are impractical. Control on  $P_{\max}$  should be directed to the exception of manufacturing, the parameters of which extend beyond the technical tolerances. *Practical value.* The exception is the manufacture of bulk cable products, the parameters of which extend beyond the technical tolerances. References 5, figures 1.

*Key words:* enameled wire, double polyimide insulation, control card, maximum probability of the parameter exit for the regulatory limit.

*Рассмотрены вопросы статистического контроля в процессе производства массовой кабельно-проводниковой продукции на примере эмальпроводов. Получены результаты непосредственного контроля диаметра эмальпровода с полиимидной двухслойной изоляцией в непрерывном технологическом цикле. Представлена контрольная карта максимальной вероятности выхода диаметра за пределы определенного диапазона. Библ. 5, рис. 1.*

*Ключевые слова:* эмальпровод, двойная полиимидная изоляция, контрольная карта, максимальная вероятность выхода параметра за нормативный предел.

**Introduction.** In the process of quality control of insulation of enameled wires it is convenient to use the so-called control card. Control card is a special form in which the statistical indicators for measured indicator in the chronological sequence of manufacturing [1] are included. On the form control frontiers which limit the range of permissible values of statistical indicators are presented. If during the inspection results are outside the regulatory frontier, it is perceived as information on the rejection of the process from normal. Using control cards the main is a method used to determine the control limits.

In the production the following types of cards are used most often: a card of arithmetic, a card of the standard deviation, a card of number of defects per unit of product. The most effective is the use of these control cards in the complex, from the input control stage to the output control. Here, it is necessary to select such a card type and parameters of the card that are informative in all stages of control. For example, this is the application for card building of the mathematical apparatus of interval statistical models.

**Analysis of publications.** In [2] tasks of the theoretical basis of application of methods of interval statistical models to the lower values of the mean interval are solved, in fact, in one phrase: «to take everything with

a minus.» For solving applied mathematical problems of process control that is not enough, since at the bilateral frontiers upper and lower deviations of values of the controlled parameter may appear in any order.

For all bounded signs  $f$  belonging to the class  $\mathfrak{F}_{00} : \mathfrak{F}_{00} = \{f : \sup|f(x)| < \infty\}$  interval averages  $\underline{M}f; \overline{M}f$  exist. Axioms of interval models of averages adopted [2] as main uniquely associate lower and upper averages by changes of sign of the controlled parameter. For all upper bounded signs:

$$\mathfrak{F}_0 = \{f : \sup f(x) < \infty\}; \overline{M}f < \infty.$$

According to the axiom of the change of sign [2] for all upper bounded:  $\underline{M}(-f) = -\overline{M}f$ , from here  $\underline{M}(-f)$  is determined on  $-\mathfrak{F}_0$ .

That is the change of sign of the parameters of the class  $\mathfrak{F}_0$  results in the class where there are lower averages  $\underline{M}f$  and at their intersection there are those and other that are the interval averages.

Such unambiguous linking the upper and lower averages by change of sign can, in principle, contrary to the physical meaning of some parameters in real control

problems. However, it may be convenient for the mathematical description and simultaneously be physically adequate if in a particular problem to use *centered* feature set.

**The goal of the paper** is investigation of maximum sensitivity of control at bilateral limitation of the controlled parameter in the production of power cables and wires.

**Results of investigations.** Using of centered parameters set becomes fundamental for the real control problem in which the measured value is only positive, and technological limitation bilateral.

The function  $g(x)$  majorizing the set of primary characteristics  $f(x)$  belongs to a semilinear shell with non-negative coefficients  $c^+_i$  and an arbitrary free term  $c$ :  $g(x) = c + \sum c^+_i g_i(x)$ ;  $g_i(x) \geq f_i(x)$ . Centering of the majorizing function  $g(x)$  allows to find the best approximation of the primary function  $f(x)$  [2]:

$$\begin{aligned} g^{\circ}_i(x) &= g_i(x) - \overline{M} g_i; \quad \overline{M} g^{\circ}_i = 0; \\ \overline{M} &= \inf \left\{ c + \sum c^+_i g_i(x) : c + \sum c^+_i g_i(x) \geq f(x) - \sum c^+_i g_i(x) \right\} = (1) \\ &= \inf \sup \left[ f(x) - \sum c^+_i g_i(x) \right]. \end{aligned}$$

In addition, centering of the majorizing function  $g(x)$  permits to use in real control the deviation of the measured parameter from its primary average, i.e. instead of  $x$  to use the  $\Delta x$  that allows to remove this contradiction between the considered positive random value of the measured characteristic at the control with two-way restriction, with one side, and the of the change of sign [2] for all low limited parameters, from the other side:  $\underline{M}(-f) = -\overline{M}(f)$ , from here  $\underline{M}(-f)$  is defined only on  $-\overline{\mathfrak{F}}_0$ .

For example, for controlling the primary indication of the dielectric loss tangent in [3] as a controlled parameter they use the deflection of the measured characteristic  $Y$  from its primary average  $M^*[Y]$  and use the majorizing function as a parabola with three parameters:

$$g(Y - M[Y]) = C + C_{2(+)} ((Y - M[Y]) - C_1)^2, \quad (2)$$

which majorizes the indicator sign (the relative number of the primary characteristic values that have fallen into the set interval)  $\alpha_1 \dots \alpha_2$ , and if the upper limit  $\alpha_2$  has no technical meaning as in the problem of control of the dielectric loss tangent), then:

$$\begin{aligned} A\{\alpha_1 \leq (Y - M[Y]) \leq \alpha_2\} &\leq C + C_{2(+)} \\ (\alpha_1 - C_1)^2 &\geq 1. \end{aligned} \quad (3)$$

That  $M(Y - M^*[Y]) = 0$ , for the minimal majorizing function  $\inf \left\{ C + C^{(+)} (\alpha_1 - C_1)^2 \right\} = 1$  determines the parabola's parameters:

$$\begin{aligned} C &= 0, C_1 = -M_{\max} ((Y - M[Y]) / \alpha_1), \\ C_{2(+)} &= (\alpha_1 - C_1)^{-2}. \end{aligned} \quad (4)$$

Relations (3), (4) allowed the use of an assessment of the relative maximum number of primary attribute values that exceed the upper permissible limit  $\alpha_1$  to organize control at the top technological limitation [3]:

$$A_{\max} \{ \Delta Y \geq \alpha_1 \} = (1 + \alpha_1^2 / M_{\max} [(\Delta Y)^2])^{-1}, \quad (5)$$

where the indicator sign  $A_{\max}$  is the relative maximum average number of the primary characteristic values that exceed  $\alpha_1$ , i.e. the maximum probability of controlled parameter  $\Delta Y$  exit for the upper limit  $\alpha_1$ :  $P_{\max} \{ \Delta Y \geq \alpha_1 \}$ .

For bilateral limitation in accordance with the axiom of the change of sign [2] of interval models medium, lower and upper averaged are connected by controlled characteristic's sign change. For example, at the control of the enamel wire diameter  $D$  the maximum probability  $P_{\max}$  of the controlled parameter  $\Delta D$  exit outside the range frontiers  $\overline{E} \dots \underline{E}$  is defined as the sum of the corresponding probabilities of the parameter exit outside of one-sided limits. Here, the probability of the controlled parameter  $\Delta D$  exit outside the lower bound is taken with minus:

$$P_{\max i} = \overline{P_{\max i}} - \underline{P_{\max i}}; \quad (6)$$

$$\overline{P_{\max i}} = \frac{[\sup(\Delta D_{i,2} \Delta D_{i,2-1})]^2}{[\sup(\Delta D_{i,2} \Delta D_{i,2-1})]^2 + (\overline{E} - \frac{1}{2} \sum_{i,2-1}^{i,2} D)^2}; \quad (7)$$

$$\underline{P_{\max i}} = \frac{[\inf(\Delta D_{i,2} \Delta D_{i,2-1})]^2}{[\inf(\Delta D_{i,2} \Delta D_{i,2-1})]^2 + (\underline{E} - \frac{1}{2} \sum_{i,2-1}^{i,2} D)^2}. \quad (8)$$

where  $D$  is the wire's diameter;  $\overline{E}$  is the upper technological frontier of the diameter;  $\underline{E}$  is the lower technological frontier of the diameter;  $\Delta D_{i,2}$  is the difference between the current diameter of the sample No.  $i$  and average diameter value determined during the process cycle:  $\Delta D_{i2} = D_{i2} - \frac{1}{i * 2} \sum_1^{i2} D$ .

Fig. 1 shows results of the direct control of enamel wire diameter with polyimide insulation in continuous process cycle and presents the control card of the maximum probability of the diameter exit outside the range frontiers determined in accordance with (6) – (8).

A comparison of Fig. 1,a and Fig. 1,b shows the information content of the technological control of the maximum probability  $P_{\max}$  of the parameter exit outside the predetermined bilateral range:

1) the control card represents the processing stability period during which  $P_{\max}$  does not exceed by the absolute value the level of 0.25 (dotted line) which analytically from (9) reflects increase in sensitivity of control with increasing deviation from the average;

2) the control card reflects a stable tendency to reduce the control parameter values that will prevent  $P_{\max}$  exit outside the level of 0.25 which made it possible to determine the cause of the trend of the decreasing in the  $D$  – increase the conductor drawing during the technological cycle.

Here we have used an analytical study of the derivatives of (4) to assess the control frontiers in the  $P_{\max}$  control card with unilateral constraint [3]. Control by  $P_{\max}$  at the bilateral limitation posed the question about the need to study the sensitivity of the  $P_{\max}$  control card in the centered parameter deviations area close to zero. In this area, the presence of the stable trend in the change of the controlled parameter may reduce the sensitivity of the card to the instability of the technological process.

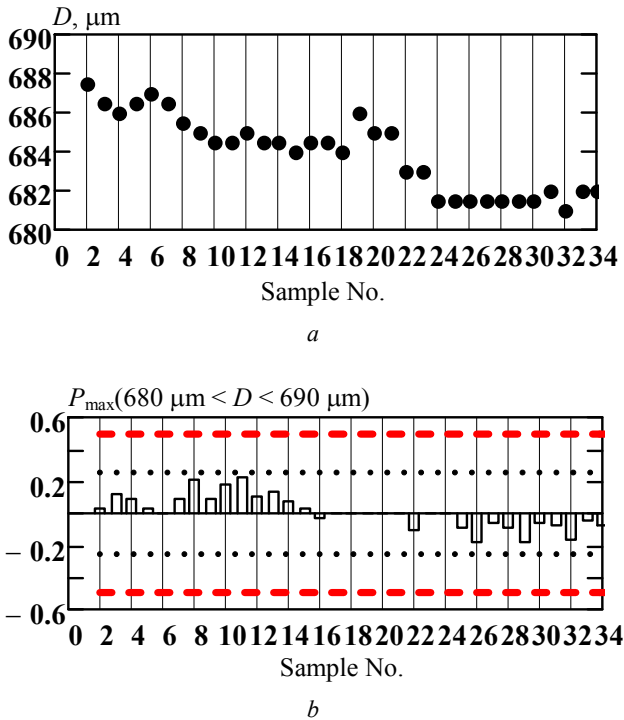


Fig. 1. Control of diameter  $D$  of enameled wires in the continuous technological process cycle by the maximum probability  $P_{\max}$  of the parameter exit outside the predetermined frontiers of the given bilateral range:  $a$  – results of measurements of  $D$ ;  $b$  – control card of the probability of the parameter exit outside of the range's frontiers (680 ... 690)  $\mu\text{m}$

Because the value  $[(\Delta D_{i,2} \Delta D_{i,2-1})]^2$  is the square of the largest current change of the diameter, this value generally is the maximum estimate of the variance of the controlled parameter in the current sample  $\underline{S}^2$ . Accordingly, the change of sign for reversing for the probability of exit outside the lower limit, value

$\inf[(\Delta D_{i,2} \Delta D_{i,2-1})]$  is a square of the largest current change of diameter towards the lower limit of the specified range. That is, this value is the maximum variance estimation of the controlled parameter in the current sample at its changing toward the lower limit  $\underline{S}^2$ . We denote the current deviations of the average value of the parameter in the sample from the upper to lower bounds as  $\underline{\alpha} \dots \bar{\alpha}$ .

Then we can represent (2) as a function of four variables:

$$\bar{\alpha} = \bar{E} - \frac{1}{2} \sum_{i=2-1}^{i-2} D; \underline{\alpha} = \underline{E} - \sum_{i=2-1}^{i-2} D, \quad (9)$$

$$P_{\max} = \frac{\bar{S}^2}{\bar{S}^2 + \bar{\alpha}^2} - \frac{\underline{S}^2}{\underline{S}^2 + \underline{\alpha}^2}. \quad (10)$$

$P_{\max}$  sensitivity to change in the controlled parameter values is a total differential (10). In the case of mutual independence of variables, the following expression permits to analyze theoretically  $P_{\max}$  sensitivity to bilateral limitation:

$$\begin{aligned} dPM &= \frac{\partial P_{\max}}{\partial \bar{S}} + \frac{\partial P_{\max}}{\partial \bar{\alpha}} - \frac{\partial P_{\max}}{\partial \underline{S}} - \frac{\partial P_{\max}}{\partial \underline{\alpha}} = \\ &= \frac{2 \cdot \bar{S} \cdot \bar{\alpha}^2 d\bar{S}}{(\bar{S}^2 + \bar{\alpha}^2)^2} - \frac{2 \cdot \bar{S} \cdot \bar{\alpha} d\bar{\alpha}}{(\bar{S}^2 + \bar{\alpha}^2)^2} - \frac{2 \cdot \underline{S} \cdot \underline{\alpha}^2 d\underline{S}}{(\underline{S}^2 + \underline{\alpha}^2)^2} + \\ &+ \frac{2 \cdot \underline{S} \cdot \underline{\alpha} d\underline{\alpha}}{(\underline{S}^2 + \underline{\alpha}^2)^2}. \end{aligned} \quad (11)$$

Separately for upper and lower limitations:

$$\frac{\partial \bar{P}}{\partial \bar{S}} + \frac{\partial \bar{P}}{\partial \bar{\alpha}} = \frac{2 \cdot \bar{S} \cdot \bar{\alpha}^2 d\bar{S}}{(\bar{S}^2 + \bar{\alpha}^2)^2} - \frac{2 \cdot \bar{S} \cdot \bar{\alpha} d\bar{\alpha}}{(\bar{S}^2 + \bar{\alpha}^2)^2}, \quad (12)$$

$$\frac{\partial \underline{P}}{\partial \underline{S}} + \frac{\partial \underline{P}}{\partial \underline{\alpha}} = \frac{2 \cdot \underline{S} \cdot \underline{\alpha}^2 d\underline{S}}{(\underline{S}^2 + \underline{\alpha}^2)^2} + \frac{2 \cdot \underline{S} \cdot \underline{\alpha} d\underline{\alpha}}{(\underline{S}^2 + \underline{\alpha}^2)^2}. \quad (13)$$

### Conclusions.

Maximum sensitivity of the control card  $P_{\max}$  occurs at well-defined ratios of variables within the established boundaries. Outside these limits control by  $P_{\max}$  is not effective. Therefore, in the specific problems of monitoring of cable and wire products utilization of technical tolerances for the controlled parameter is inappropriate. Control by  $P_{\max}$  should be directed to the exclusion of the manufacture of products (such as enameled wire) the parameters of which are beyond the technical tolerances.

Therefore, to achieve the maximum sensitivity of control technological boundaries, first, must be chosen based on the achieved level of average value of the parameter and its statistical scattering.

Second, technological boundaries need to be changed in accordance with the achieved level of the average value of the parameter and its statistical

dispersion. Such a change can be a quantitative indicator of the trend of the increase or decrease the reliability of the technological system.

#### REFERENCES

1. Shchebeniuk L.A., Golik O.V. *Matematychni osnovy nadiynosti izolyatsiyi elektroobladnannya* [Mathematical foundations of the reliability of electrical insulation]. Kharkiv, NTU «KhPI» Publ., 2003. 102 p. (Ukr).
2. Kuznetsov V.P. *Interval'nye statisticheskie modeli* [Interval statistical models]. Moscow, Radio i sviaz' Publ., 1991. 352 p. (Rus).
3. Karpushenko V.P., Shchebeniuk L.A., Antonets Y.O., Naumenko O.A. Control card – instrument of quality of cable products. *Power cables of low and medium voltage. Design, technology, quality*. Kharkiv, Region-Inform Publ., 2000. pp. 270-289. (Ukr).
4. Shchebeniuk L.A., Golik O.V. A method of constructing control charts the probability of an exit sign beyond the regulatory limit. *Bulletin of Kharkiv State Polytechnic University*, 2000, no.127, pp. 35-38. (Rus).
5. Golik O.V. *Metod operativnogo kontroliia parametrov dvukhsloinoi poliimidnoi izoliatsii emal'provoda v protsesse proizvodstva*. Diss. cand. techn. nauk [Method of controlling parameters of a two-layer polyimide insulation enameled wire in the production process. Cand. tech. sci. diss.]. Kharkov, 2009, 168 p. (Rus).

Received 29.04.2016

*O.V. Golik, Candidate of Technical Science, Associate Professor,*  
National Technical University «Kharkiv Polytechnic Institute»,  
21, Kyrpychova Str., Kharkiv, 61002, Ukraine.  
phone +380 57 7076010, e-mail: unona928@gmail.com

#### How to cite this article:

Golik O.V. Statistical procedures for two-sided limit of a controlled parameter in the process of production of cable and wire products. *Electrical engineering & electromechanics*, 2016, no.5, pp. 47-50. doi: 10.20998/2074-272X.2016.5.07.

V.V. Rudakov, A.A. Korobko

## A HIGH SENSITIVE MICROWAVE MEASURING DEVICE OF THE MOISTURE CONTENT IN THE NON-POLAR DIELECTRIC LIQUIDS BASED ON AN INHOMOGENEOUS STEP COAXIAL RESONATOR

*Purpose. Objective is to create a moisture meter for non-polar liquid dielectrics with low volumetric moisture content of more than  $10^{-3}$  %. Methodology. Moisture measuring is based on dielectric method. It is implemented as a resonant method of determining a capacitance measuring transducer. Measuring transducer capacitive type has a working and parasitic capacitance. It was suggested the definition of moisture on four of resonance frequencies: when the measuring transducer is turned off, one by one filled with air, «dry» and investigated liquid, to determine the parasitic capacitance of the measuring generator, and the parasitic capacitance of the measuring transducer and humidity. Measurement frequency was increased up to microwave range to increase the sensitivity. Measuring transducer with distributed parameters representing a step heterogeneous coaxial resonator is used by. This measuring transducer has a zero stray capacitance, because the potential electrode has a galvanic connection with an external coaxial electrode. Inductive ties loop is used to neglect parasitic capacitance of the measuring generator, and to increase the quality factor of the system. Measuring moisture is reduced to measuring the two frequencies of resonance frequency and «dry» and investigated liquid. Resonant characteristics transducer in a step inhomogeneous coaxial resonator have been investigated to determine the quality factor of filled with air and transformer oil, and experiments to measure the moisture content in transformer oil have been conducted. Results. Measuring transducer of distributed type is developed and researched – it is step inhomogeneous coaxial resonator. It has a smaller geometric length and larger scatter of the first and second resonant frequencies. Expression is obtained for determination of moisture on the basis of two resonant frequencies. The formula of the two frequencies to determine the moisture is correct. Resonant characteristics are obtained for measuring transducer. Its quality factor has been determined – it does not depend on what it is filled with air or oil. The moisture content in transformer oil for the amount of water to  $10^{-3}$  % with an error of no more than 6.7 % has been determined. Originality. It has been proposed to use of an inhomogeneous step coaxial resonator as a measuring transducer. Original high sensitive moisture meter for the fluid at rest and flowing fluid with low values of parasitic capacitances has been developed and researched. An original method of determining the moisture by measuring the two frequencies of resonance has been proposed and implemented. Practical value. This meter may be used to determine moisture in any of the non-polar liquid with high speed and accuracy. Moisture meter can be used in electrical engineering, aeronautical engineering, in the chemical and food industries. References 6, tables 1, figures 8. Key words: moisture meter, non-polar liquid dielectrics, measuring transducer, step inhomogeneous coaxial resonator, measuring generator, resonance characteristics, volumetric water content, transformer oil, water.*

*Рассматривается высокочувствительный измеритель влагосодержания в неполярных жидких диэлектриках. Аргументированы пути повышения чувствительности классического диэлектрического метода. Приводится описание разработанной конструкции измерителя влажности на основе ступенчатого неоднородного коаксиального резонатора. Рассмотрены результаты анализа резонансных характеристик измерительного преобразователя, а также определены величины объемного влагосодержания смесей трансформаторное масло – вода в диапазоне влагосодержания ( $10^{-3} - 10^{-4}$ ) см<sup>3</sup>/м<sup>3</sup>. Библ. 6, табл. 1, рис. 8.*

*Ключевые слова: измеритель влагосодержания, жидкие неполярные диэлектрики, измерительный преобразователь ступенчатый коаксиальный неоднородный резонатор, измерительный генератор, резонансные характеристики, объемное влагосодержание, трансформаторное масло, вода.*

**Introduction.** Measuring the moisture content of the nonpolar liquid dielectrics is important for many practical applications, such as: electrical engineering, chemical industry, food industry, in the military and aviation equipment. So, for the electrical equipment is important to determine the moisture content of transformer oil, chemical and food industry – determination of moisture content in a variety of mineral oils, for the military and aviation equipment – determination of moisture content in diesel, aviation fuel. In most of the areas studied fluid (transformer and sunflower oils, diesel and jet fuel, etc.) are nonpolar liquid dielectrics.

It should be noted that the lower limit of the moisture content measurements in all of these applications is very low: the minimum value of the measured volumetric water content is not more than  $10^{-3}$  % which creates difficulties for conventional measurements of these known methods. Traditional methods such as Karl-Fischer method and liquid-

chromatographic method requires special equipment rather expensive consumables and quite a long time.

**The goal of the work** is development of a meter moisture content in non-polar liquid dielectrics with a lower limit of volumetric water content not more than  $10^{-3}$  % allowing to quickly perform measurements with a minimum of material and time costs.

**Substantiation of ways to solve the defined problem.** To solve this problem dielectric method of measuring the moisture content was chosen based on the moisture content depending on the dielectric constant study watered nonpolar liquid dielectrics [1]. The measured dielectric constant which is proportional to moisture content, characterizes the water content value itself.

To the improvement of this method in [2] a simplified model of the emulsion «water – non-polar dielectric» is proposed that allowed simply to determine

the amount of volumetric water content in the mixture  $W$  as a function of dielectric permittivity  $\varepsilon_2$  mixture and dehydrated nonpolar liquid  $\varepsilon_1$  in the following form:

$$W = \frac{\varepsilon_2 - \varepsilon_1}{3 \cdot \varepsilon_1} \quad (1)$$

In [3] it is proposed the use of the resonance method for determining dielectric permittivities  $\varepsilon_1$  и  $\varepsilon_2$  implemented for the measuring transducer (MT) of the capacitive type, to be filled successively and dehydrated liquid test mixture (emulsion). Thus MT connected to the capacitive measuring generator (MG) contains the amplification circuit and the feedback coil [3]. Unknown values  $\varepsilon_1$  and  $\varepsilon_2$  are expressed in four frequency values MG generation (frequency of MG with disconnected MT, frequency of MG with MT filled with air, frequency of the MG with MT filled with dehydrated test liquid, and frequency of the MG with MT filled with test mixture), and the values of design parameters of MT. This approach allowed in the MG frequency range from 100 kHz to 2 MHz practically solve the problem of determining the moisture content of the non-polar dielectrics in the range of  $0.1\% \leq W \leq 10\%$ . However, using at this approach of MG and MT systems in the form of lumped elements (a coil for the IG and a measuring capacitor for MT) which had the parasitic parameters are not allowed to fully realize the potential of the resonance dielcometry to measure extremely low levels of moisture content [3].

The analysis shows that the main directions of improving the sensitivity of the proposed in [3] dielcometry resonance method are as follows: increase in operating frequency of measurement, minimizing the parasitic capacitance of the inductive element of the MG and MT, increased frequency stability of MG generation in all four modes, the maximum reduction in the number of measured frequencies.

For the implementation of indicated directions by the authors MT with distributed parameters has been proposed as a step inhomogeneous coaxial resonator (SICR) [4]. Here, SICR resonance spectra were investigated in the frequency range up to 1.8 GHz. As a result of investigations carried out in [4] significant advantages of MT performed as SICR have revealed as compared to a MT with lumped parameter and compared with known MT of microwave range as quarter-wave homogeneous resonators.

Further development of the theory of SICR application in resonant dielcometry of nonpolar liquid media was developed in [5] which held as a mathematical analysis of electromagnetic processes in SICR and their simulation in Micro Cap environment. The result of these studies was to optimize for SICR for dielcometric goals and the definition of its metrological characteristics. Based on the above, the following methodology for the design of the meter was adopted:

1. The moisture content of the mixture is determined by the difference of the dielectric permittivities of the dehydrated liquid and mixture.

2. To determine the dielectric permittivities IT as SICR is connected to and alternately filled by dehydrated liquid and mixture.

3. The operating frequency of MG is selected as maximal possible taking into account the frequency dispersion of the dielectric permittivity of water.

4. SICR and MG have minimum values of parasitic parameters, which reduces the number of frequency measurements from four to two and reduce the experimental time by 2 times.

5. In order to improve the stability of the frequency generated by the MG, the MT is designed as a system with distributed parameters: SICR which has a substantially higher  $Q$  than the lumped system «MT – MG».

**Description of the meter.** A flowchart of the meter is shown in Fig. 1. Used MT converter, in the form of SICR, is connected to the MG. The MG frequency generation is measured by a frequency meter F, and the temperature of the MT – by an electronic thermometer T.

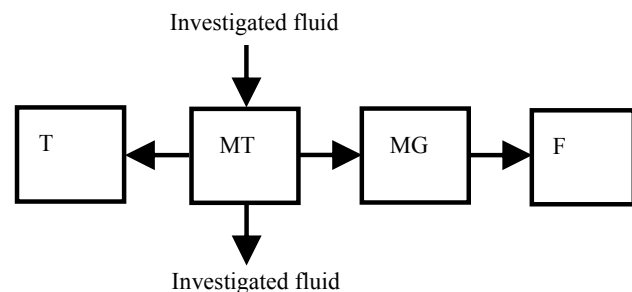


Fig. 1. Flowchart of the meter

Schematic diagram of the meter (MT together with MG) is shown in Fig. 2. Its MT transducer as SICR formed as two coaxial lines  $Z_1$  and  $Z_2$  of equal length with different wave impedances  $Z_1 = 77.61 \Omega$ ,  $Z_2 = 4.09 \Omega$ . Using inductive loop of communication  $A$  transmitter is connected to the MG on the transistors Q1, Q2 which are collected by the scheme «common base» (at the MG output) – «common collector» (at the MG input).

This circuit solution of MG is selected to minimize the effect of parasitic MG parameters on the parameters of MT (cascade with «common base» has a maximum output impedance and cascade with «common collector» has maximum input impedance). The signal from the emitter follower transistor Q2 is input (emitter) of the amplifying stage transistor Q1 on, the output of which is connected to the MT communication via an inductive loop  $A$ . The output of the MG through «isolation» amplifier transistor Q3 is input to a digital frequency divider U3, which is included under the scheme divider into 80. The output of the frequency divider through a «decoupling» emitter follower transistor Q4 signal is fed to a frequency. For maximum stability, it MG frequency generating stages (Q1 – Q3) and digital stages (U3, Q4) are fed from different linear regulators U1 (9) and U2 (5 V) voltage, respectively.

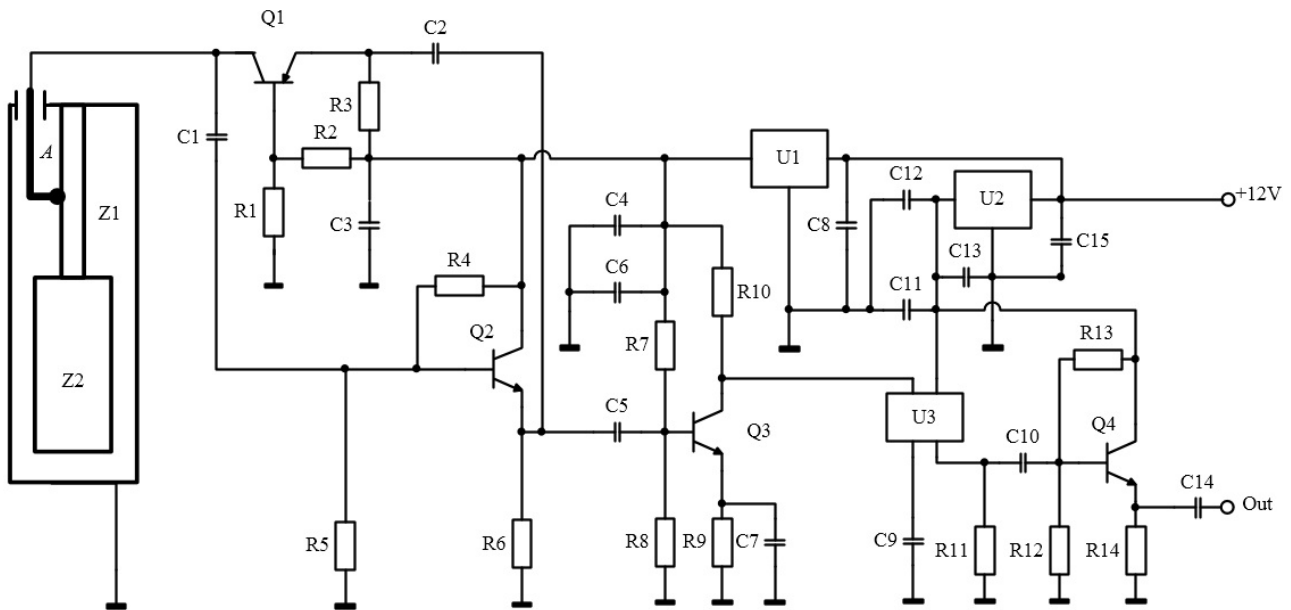


Fig. 2. Schematic diagram of the meter (MT together with MG)

Structurally, MT together with MG is a collapsible system, the bottom of which is MT and at the top – MG. In the lower part of the MT test liquid is supplied which after filling its entire volume goes to the drain. General view and the view with the cover removed measuring moisture content is shown in Fig. 3. In this constructive execution of MT and MG the MT operation is possible both in stationary mode and a test liquid flow mode. Furthermore, this design provides the IG minimize the effects of parasitic resonance frequency parameters to MT (which is determined by the geometrical dimensions of the lines Z1 and Z2 and the magnitude of test liquid dielectric constant) due to the following factors:

1. The values of the coupling coefficient of the equivalent oscillating circuit formed by lines Z1 (inductive element) and Z2 (capacitive element) with MT does not exceed 0.08. Therefore, the parasitic parameters of the IG, the MG which «are introduced» in the loop, do not exceed in magnitude  $(0,08)^2 = 0.0064$ . In combination with high input impedance values (for Q2) and output (for Q1) is part of an IG ensures high quality of the oscillatory system and a small influence on the frequency of the MG meter generation.

2. Place of the connection of inductive loops A, as close as possible to the point of the oscillating system, which has zero potential. This fact provides a minimum distortion of the longitudinal electric field in SICR.

3. Mechanical fixation of the central electrode line Z1, the value of parasitic capacitance provides MT is almost zero, which also helps improve the accuracy of the proposed measuring moisture content.

The described meter has the following main characteristics:

1. The frequency generation of MG with MT filled with air, about 158 MHz.
2. The frequency generation of MG with MT filled with transformer oil, about 104 MHz.
3. The sensitivity of the meter – no worse than  $1 \text{ cm}^3/\text{m}^3$ .

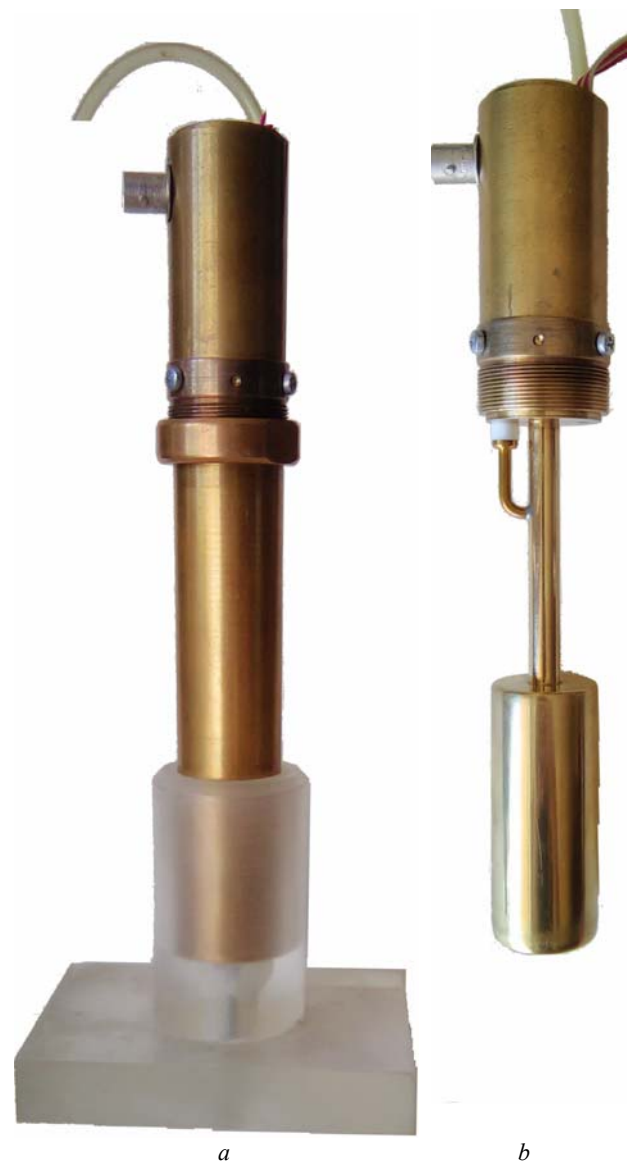


Fig. 3. General view of the assembled meter of the moisture content (a) and view with removed coaxial outer electrode (b)

**Results of experimental investigations.** To confirm the correctness of the chosen design and technical solutions of the MG and MT pilot studies were carried out in two stages.

In the first stage using the meter amplitude-frequency characteristics (AFC) of the type X1 – 42 studied the resonance characteristics of IT filled with air, and IT filled with dehydrated transformer oil.

The block diagram on which the moisture meter investigated to determine the AFC is shown in Fig. 4.

Fig. 4 shows: 1 – 42 meter AFC X1 (at the top – measuring part; at the bottom – generating part); 2 – IT; 3 – Inductive loop; 4 – the medium under study; 5 – high-resistance (external) input X1 – 42; 6 – output X1 – 42 (50 Ω).

Here, for removing reaction the meter X1 – 42 in the AFC output X1 SP – 42 was agreed by 50 Ω resistor, and to increase the input impedance a series with the input the 100 kΩ – 0.5 pF chain was included.

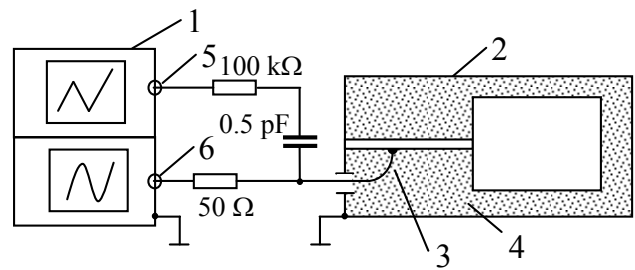


Fig. 4. Block diagram for MT AFC measurements

Results of IT investigations as MT AFC are shown in Fig. 5-8. The resulting AFC have been deciphered for the purpose of determining the value of the loaded  $Q$  of the measuring transducer. Loaded  $Q$  (MT is loaded on 50 Ω) is determined using  $2\Delta F$  value (AFC width at 3dB) and  $F$  (central resonance frequency).

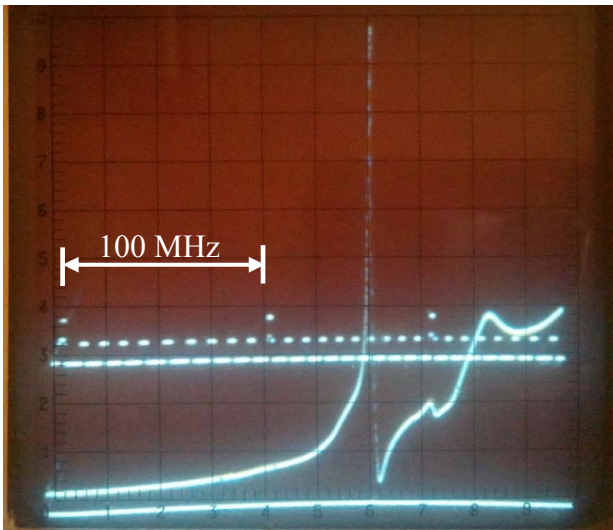


Fig. 5. Amplitude-frequency characteristics of MT filled by air

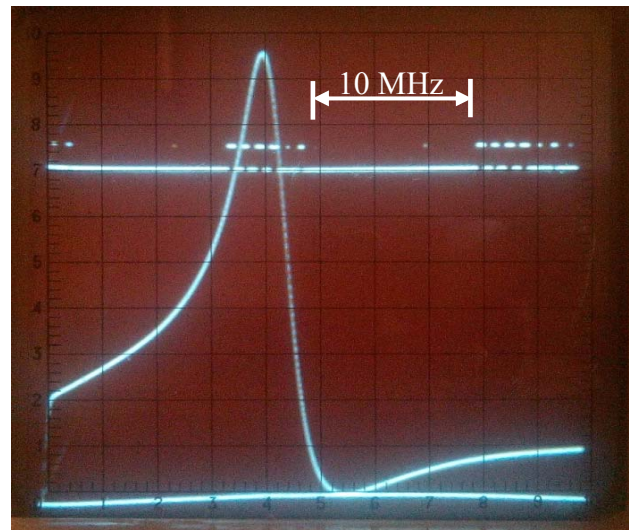


Fig. 6. Amplitude-frequency characteristics of MT filled by air

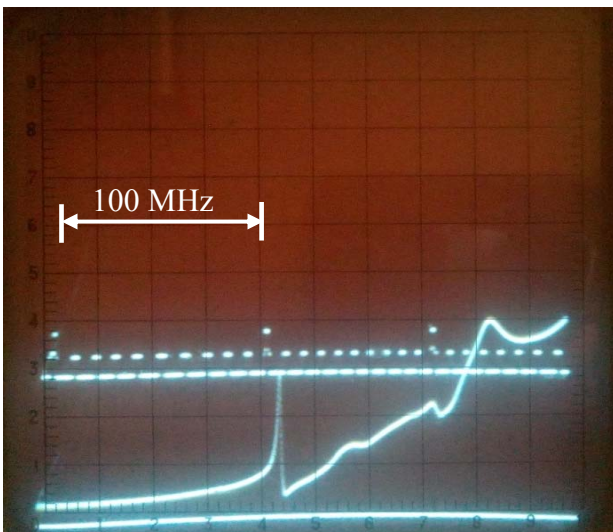


Fig. 7. Amplitude-frequency characteristics of MT filled by oil

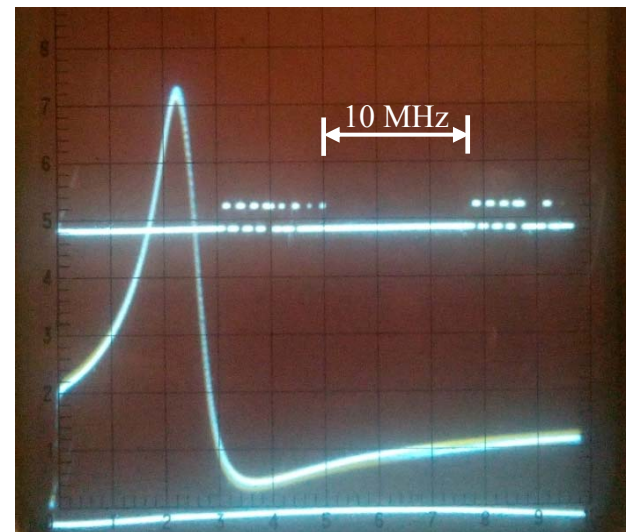


Fig. 8. Amplitude-frequency characteristics of MT filled by oil

As the results of processing with accuracy up to 5% loaded  $Q$  value of MT with air ( $Q_1, F_1$ ) and with transformer oil ( $Q_2, F_2$ ) are practically the same indicating a weak influence of oil on  $Q$  of MT:

$$Q_1 = \frac{F_1}{2\Delta F_1} = \frac{160 \cdot 10^6}{2 \cdot 10^6} = 80;$$

$$Q_2 = \frac{F_2}{2\Delta F_2} = \frac{108 \cdot 10^6}{1,3 \cdot 10^6} = 83;$$

$$Q_1 \cong Q_2.$$

In the second stage of the experimental studies were identified value of volumetric moisture content of the prepared mixtures «transformer oil – water» in the moisture content range  $(10 - 10^4) \text{ cm}^3/\text{m}^3$ . In the course of experiments with micro-stamps «Hamilton» in pre-dehydrated oil of volume  $(500 \pm 0.6) \text{ cm}^3$  was injected the required amount of water. Thereafter, the homogeneous emulsion was prepared with the desired moisture content.

Then, to remove gas from the non-moistured transformer oil and emulsions prepared with these vessels were placed in a vacuum chamber. After that, through the transmitter shed investigated liquid at controlling the temperature MT and the MG frequency generation is flowed. In the process of research and MT and MG temperature is kept constant with an accuracy of  $\pm 0.03 \text{ }^\circ\text{C}$ . Thus, 12 measurements are carried out by the frequency generation MG are divided into 80 for dehydrated oils ( $F_3$ ) and the test mixture ( $F_4$ ) and are processed by standard methods for direct measurement of [6].

To determine the functional dependence of the water content  $W$  on the frequency we use the formula for determining the moisture content of the moisture meter as described in [3]:

$$W = \frac{1}{3} \cdot \frac{\frac{1}{F_4^2} - \frac{1}{F_3^2}}{\frac{1}{F_3^2} - \frac{1}{F_1^2}}, \quad (2)$$

where  $F_1$  is the resonance frequency at switched off MT;  $F_3$  is the resonance frequency for MT filled with dehydrated oil;  $F_4$  is the resonance frequency at MT filled with considered mixture.

The design of the proposed moisture meter based on SICR is such that it does not contain a structural dielectric material supporting the inner electrode potential. Structurally, the inner electrode potential tightly connected to the outer electrode and the test liquid is in the space between the electrodes. In this case, the transducer structure may be represented as a short-circuited quarter-wave line. Then moisture meter based on SICR has frequency  $F_1 = \infty$ , and  $1/F_1 = 0$  and the expression (2) is converted to the form:

$$W = \frac{1}{3} \cdot \frac{\frac{1}{F_4^2} - \frac{1}{F_3^2}}{\frac{1}{F_3^2}} = \frac{1}{3} \cdot \frac{F_3^2 - F_4^2}{F_4^2}. \quad (3)$$

For small values of the moisture  $W$  content when the inequality holds is correct:

$$\frac{F_3^2 - F_4^2}{F_4^2} < 0,1, \quad (4)$$

formula (3) for the moisture content is simplified:

$$W \approx \frac{2}{3} \cdot \frac{F_3 - F_4}{F_4}. \quad (5)$$

The results of the moisture content of treated experimental values  $W$ ,  $W_0$  and frequencies  $F_3$ ,  $F_4$  are shown in Table 1.

Table 1

Treated results of measurements				
$W_0, \text{ cm}^3/\text{m}^3$	Frequency, Hz		$W, \text{ cm}^3/\text{m}^3$	Relative error, %
	$F_3$	$F_4$		
10±1	1335497.4±0.6	1335478.3±0.8	9.51±0.5	5.2
50±1	1335558.1±0.6	1335459.8±0.6	49±0.4	1.9
100±5.1	1304712.0±0.7	1304519.7±0.8	98.3±0.6	1.8
499±5.6	1335558.1±0.6	1334602.2±1.3	477.7±0.7	4.6
999±11.2	1304658.8±0.7	1302569.9±1.2	1069.9±0.7	6.7
9901±111.8	1304658.8±0.7	1286722.6±34.4	9357.7±18.4	5.8

Thus, when the concentration of moisture in the prepared emulsion  $W_0 = 10 \text{ cm}^3/\text{m}^3$  the measured value of the moisture content is  $W = 9.51 \text{ cm}^3/\text{m}^3$  and the value of  $\Delta W = \pm 0.5 \text{ cm}^3/\text{m}^3$  that enables measurement of moisture content in the range  $10^{-3} \% < W < 0.1 \%$  with a relative error (defined as the difference in moisture content of the emulsion prepared and measured divided by the moisture content of the cooked) is not more than 5.2%.

Analysis of the experimental results shows that the created meter is characterized at determining the moisture content by a relative error less than 6.7% in the range  $10 \text{ cm}^3/\text{m}^3 \leq W \leq 10^5 \text{ cm}^3/\text{m}^3$ .

### Conclusions.

1. For the development of the dielectric method for determining the moisture content in nonpolar liquid dielectrics a microwave meter the moisture content with a measuring transmitter as a step inhomogeneous coaxial resonator operating in resonant mode is developed.

2. The correctness of the proposed for implementation of the meter the moisture content the simplified physical model of emulsion «water in oil» type is experimentally confirmed.

3. A moisture meter on the basis of an inhomogeneous step coaxial resonator which has higher frequency stability, lower parasitic parameters and higher operating frequency greater compared with a measuring instrument on the basis of a capacitive transducer and a measuring lumped generator is developed.

4. The proposed meter design allows to determine the moisture content of the test fluid at rest, and in the stream.

5. The designed meter of moisture content allows at minimum of material and time costs quickly determine the moisture content in the range of  $10^{-3} \% < W < 0.1 \%$  by using measurement of two resonant frequencies of the measuring transmitter (with MT filled with dehydrated oil and with MT filled with the test emulsion) and calculation of moisture content by formula [5].

### REFERENCES

1. Melkumyan V.E. *Izmerenie i kontrol vlazhnosti materialov.* [Measurement and control of humidity of materials.]. Moscow,

Komitet standartov mer i izmeritelnyih priborov pri Sovete Ministrov SSSR Publ., 1970. 138 p. (Rus).

2. Rudakov V.V., Korobko A.I., Korobko A.A. Electrophysical model of behavior emulsion mineral oil – water engineering type. *Bulletin of NTU «KhPI»*, 2009, no.39, pp. 158-161. (Rus).

3. Rudakov V.V. Korobko A.A. Increasing the sensitivity of the moisture content measurements in transformer oil dielectric method in resonant mode. *Bulletin of NTU «KhPI»*, 2014, no.50(1092), pp. 143-149. (Rus).

4. Rudakov V.V., Korobko A.A. The resonance spectra of inhomogeneous coaxial resonators to determine the dielectric constant of liquid media in the microwave band. *Bulletin of NTU «KhPI»*, 2015, no.20(1129), pp. 129-137. (Rus).

5. Rudakov V.V., Korobko A.A. Research of metrological characteristics of transmitters in the form of a step coaxial resonator for dielectric inhomogeneous liquid media in the

microwave range. *Bulletin of NTU «KhPI»*, 2015, no.51(1160), pp. 91-95. (Rus).

6. Dvoryashin B.V. *Osnovyi metrologii i radioizmereniya* [Fundamentals of metrology and radio measurements]. Moscow, Radio i svyaz Publ., 1993. 320 p. (Rus).

Received 19.09.2016

V.V. Rudakov<sup>1</sup>, Doctor of Technical Science, Professor,  
A.A. Korobko<sup>1</sup>, Postgraduate Student,

<sup>1</sup> National Technical University «Kharkiv Polytechnic Institute»,  
21, Kyrpychova Str., Kharkiv, 61002, Ukraine.

phone +380 93 6508088, e-mail: andarleks@gmail.com

How to cite this article:

Rudakov V.V., Korobko A.A. A high sensitive microwave measuring device of the moisture content in the non-polar dielectric liquids based on an inhomogeneous step coaxial resonator. *Electrical engineering & electromechanics*, 2016, no.5, pp. 51-56. doi: 10.20998/2074-272X.2016.5.08.

S.P. Shalamov

## AN INDUCTION SENSOR FOR MEASURING CURRENTS OF NANOSECOND RANGE

**Purpose.** A current meter based on the principle of electromagnetic induction is designed to register the current flowing in the rod lightning. The aim of the article is to describe the way of increasing the sensitivity of the converter by means of their serial communication. **Methodology.** The recorded current is in the nanosecond range. If compared with other methods, meters based on the principle of electromagnetic induction have several advantages, such as simplicity of construction, reliability, low cost, no need in a power source, relatively high sensitivity. Creation of such a meter is necessary, because in some cases there is no possibility to use a shunt. Transient properties of a meter are determined by the number of turns and the constant of integration. Sensitivity is determined by measuring the number of turns, the coil sectional area, the core material and the integration constant. For measuring the magnetic field pulses with a rise time of 5 ns to 50 ns a meter has turns from 5 to 15. The sensitivity of such a meter is low. When the number of turns is increased, the output signal and the front increase. Earlier described dependencies were used to select the main parameters of the converter. It was based on generally accepted and widely known equivalent circuit. The experience of created earlier pulse magnetic field meters was considered both for measuring the magnetic fields, and large pulse current. **Originality.** Series connection of converters has the property of a long line. The level of the transient response of the meter is calculated. The influence of parasitic parameters on the type of meter transient response is examined. The shown construction was not previously described. **Practical value.** The results of meter implementation are given. The design peculiarities of the given measuring instruments are shown. References 6, figures 9.

**Key words:** magnetic field strength, corona current, surge characteristic, electromagnetic induction, bi-exponential pulse, induction transformer's calibration, distributed parameter line.

*Представлены результаты реализации высокочувствительного датчика токов наносекундного диапазона индукционного типа для измерения импульсов тока, протекающих на стержневом молниеприемнике. Проведен анализ современных достижений в области измерений слабых импульсных токов. Представлены результаты расчета датчика, показано влияние паразитных параметров на вид переходной характеристики датчика. Описаны основные особенности конструкции. Приведены параметры созданного датчика и результаты калибровки.* Библ. 6, рис. 9.

**Ключевые слова:** напряженность магнитного поля, ток короны, переходная характеристика, электромагнитная индукция, биэкспоненциальный импульс, калибровки индукционного преобразователя, линия с распределенными параметрами.

**Introduction.** Knowledge of the gas discharge area are used in various fields of modern science. Corona discharge occurs in strongly inhomogeneous electric fields characteristic for electrode systems «needle-plane». The effect occurs at applying potential of certain value required for the implementation of self-discharge form. There is a voltage range in which the discharge current is a stable pulse sequence. Increasing the voltage across the discharge gap, while not changing external conditions, is leading to the increase in the pulse repetition frequency. Today at the Scientific-&Research Planning-&Design Institute «Lightning» of the NTU «KhPI» they are working on the study of corona discharge from lightning receivers in the ominous atmosphere. The results will create a warning system of thunderstorm danger. To register the discharge current flowing in the needle electrode an inductive transducer is used. As on the stationary rod electrodes it is impossible to install a shunt, the inductive transducer in this case is an indispensable tool which does not need electrical contact with the lightning receiver.

**The goal of the paper** is the creation of measurement system which will be the basis for a thunderstorm hazard warning system.

**Problem definition.** Modeling of process of the corona of rod lightning receivers is carried at a high-voltage test bench BBC-1.2 of the Scientific-&Research Planning-&Design Institute «Lightning» of the NTU «KhPI». Lightning receiver is placed between two parallel

metal planes. Dimensions of planes: lower –  $4.02 \times 6.56$  m, upper –  $3.63 \times 5.22$  m. The lower plane is grounded, the upper plane is potential. The rod was placed on the bottom plane and has a connection with grounded plane through a shunt resistance of  $75 \Omega$ . An induction converter allowed to galvanically separate the measuring system from installation components under a high potential.

Typical waveforms of the measured current are shown in Fig. 1.

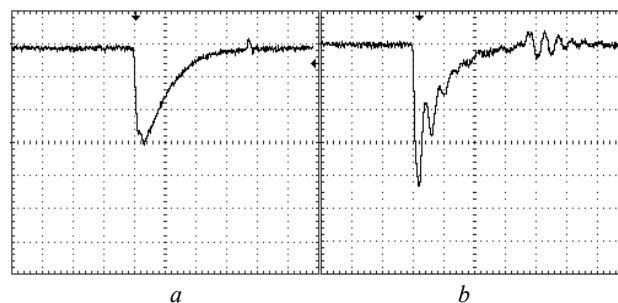


Fig. 1. Typical waveforms of current of the unit streamer (vertical scale – 100 mV/cell; horizontal scale – 100 ns/cell)

For different values of the electric field strength in the space and, depending on the geometry of the structure, changes of the amplitude-temporal parameters of the

current of the streamer are possible but they are within a certain range: the current pulse rise time of 14.8 ns to 20.5 ns, amplitude – from 4 mA to 20.5 mA.

Formulae for calculating the rise time of the transient response, the meter constant of integration at using  $RL$ -integrator and transducer sensitivity are of the form [2, 3]:

$$T_{riseTime} = 3,35\sqrt{L_d C_d} ; \quad (1)$$

$$T = \frac{L_d}{R_I} ; \quad (2)$$

$$K_n = \frac{\mu_0 \mu_r S w \cdot \cos \varphi}{T} , \quad (3)$$

where  $T_{riseTime}$  is the rise time of the transient response;  $L_d$  is the inductance of the inductive transducer;  $C_d$  is the total parasitic capacitance;  $T$  is the constant of integration of the itself integrating inductive transducer;  $R_I$  is the sum of own and integrating resistance;  $K_n$  is the conversion factor;  $\mu_0$  is the magnetic permeability constant;  $\mu_r$  is the magnetic permeability of the core material;  $S$  is the turns area;  $w$  is the turns number;  $\varphi$  is the angle between the magnetic field strength vector and the normal to the frame.

To ensure reliable registration of streamer current, measuring sensitivity is taken not less than 2.5 mV per 1 mA.

**1. Analysis of the latest achievements in the field of measuring the pulsed currents.** In [2] the meter of high pulsed currents for measuring in circuits with high operating voltage and the absence of the possibility of using a shunt is described. A schematic diagram of the meter is shown in Fig. 2. The design is illustrated in Fig. 3.

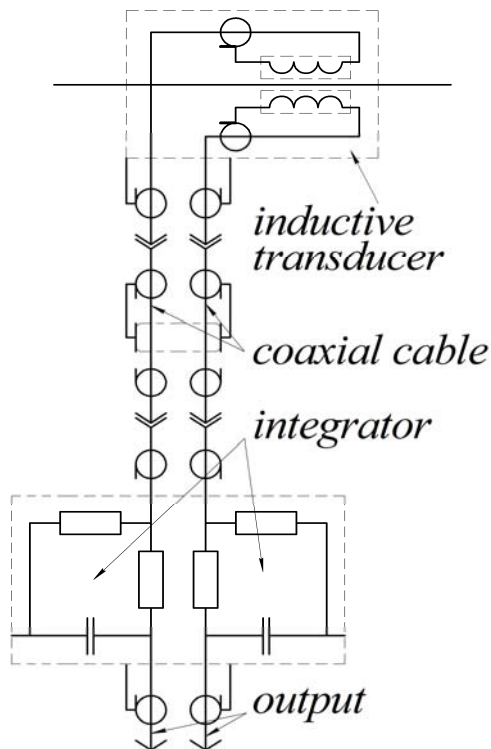


Fig. 2. A schematic diagram of the meter

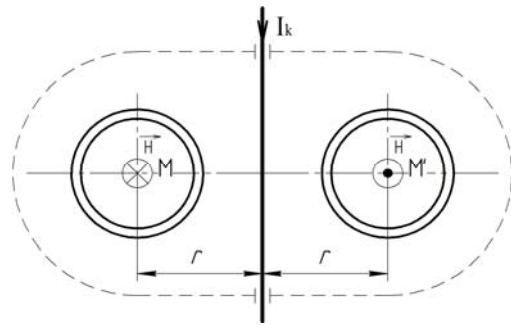


Fig. 3. Design of the meter

The signal is integrated on the  $RC$ -integrator. Measured current  $I_k$  is passed along a straight conductor. Around the conductor the magnetic field is generated that coincides in shape with the current pulse. In symmetric with respect to the conductor points  $M$  and  $M'$  coplanar and in opposite phase two inductive measuring transducers are installed.

The entire construction is enclosed in an electromagnetic shield of cylindrical shape. At the electromagnetic field action in both converters equal in magnitude but opposite in phase EMF occur that in subsequent devices are integrated and then subtracted in the differential amplifier of the oscilloscope. Developed design can effectively get rid of the noise.

In [4] the results of the development of tools for measuring pulsed magnetic fields of electric discharge facilities used to test hardware on the lighting resistance are presented. The theory of operation of pulsed magnetic fields meters of induction type is described. The requirements for meter's parameters for reliable measurement of bi-exponential fields are presented. The meter's parameters shall be as follows:

$$T_{inc} \geq (3 \div 5) T_{riseTime} ; \quad (4)$$

$$T_{dec} \geq (10 \div 50) T_{fallTime} , \quad (5)$$

where  $T_{fallTime}$  is the fall time of the transient response;  $T_{inc,dec}$  is the front time and fall time of the measured magnetic field pulses.

To measure the broadband pulsed magnetic fields a measuring circuit consisting of two independent channels: wave front measurement and a channel of the pulse width measurement is described. A schematic diagram is shown in Fig. 4.

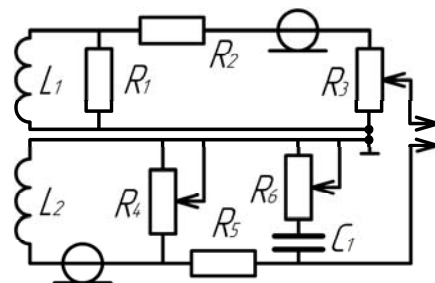


Fig. 4. Circuit of the broadband magnetic field strength meter

The wave front measurement channel reliably measures the shape of the pulse in the time range from nanoseconds to 10  $\mu$ s, and the fall measurement channel – in the time range from 10  $\mu$ s to several tens of

milliseconds. To integrate the signal they use  $RL$  (elements  $L_1, R_1$ ) and  $RC$  (elements  $R_3, C_1$ ) integrators. Elements  $L_1$  and  $L_2$  are the inductance of the front and fall measurement channels. For proper operation of the meter it is necessary to achieve matching shapes of signals on the fall of the pulse front measuring channel and the pulse front of the measuring channel of the fall. This is achieved by adjusting  $R_d$ . Regulation of signal amplitude from the front channel measurement is performed by resistor  $R_3$ . At the signals summation there is a signal failure at the joint of signals which eliminates by the adjustable of  $R_6$ . Resistor  $R_2$  allows to align the cable. In [5] a broadband meter of the magnetic field strength is implemented.

In [6] the principle of operation, productivity, limitations and development of current measurement technology using the Rogowski coil are considered and measures to improve the design of the integrator which allows for bandwidth up to 10 MHz are presented. The analysis of the behavior of the Rogowski coil at high frequency currents measurements is carried out. A simplified equivalent circuit of the Rogowski coil is shown in Fig. 5.

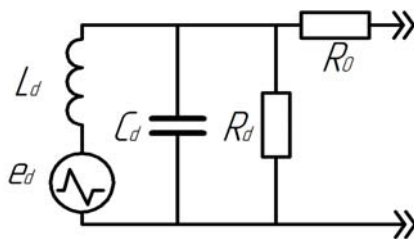


Fig. 5. An electrical equivalent circuit of the coil with loading resistance  $R_d$  and series resistor  $R_0$  ( $R_0 \gg R_d$ )

Elements  $L_d$  and  $C_d$  are the inductance and capacitance of the coil,  $R_0$  is the integrating resistance. To provide the necessary attenuation the selection of  $R_d$  is carried out in accordance with the expression:

$$R_d = \frac{\pi}{2} \sqrt{\frac{L_d}{C_d}}. \quad (6)$$

$R_d$  value is higher than the characteristic impedance of the coil  $\rho = (L/C)^{0.5}$  although there is reason to assume that the coil should be loaded on  $\rho$ . But it was found that (6) gives the best transient response. Moreover, the measuring cable capacitance will increase the equivalent capacitance of the coil and thus significantly reduce throughput. To avoid this effect, the series resistance  $R_0$  is set at the end of the coil as shown in Fig. 5. This resistor forms part of a  $RC$  integrator [6].

**2. Description of the sensor's design.** The meter consists of series-connected inductive transducers, as shown in Fig. 6. The output signal increases in proportion to the number of connected meters if the system has the property of a long line. This occurs when the measuring field wavelength is comparable to the electrical length of the coil's conductor. Selection of resistance  $R_d$  can be performed in accordance with (6) but the sensor operates in an oscillating mode. Fig. 7 shows the results of calculation of the transient response at the value  $\rho$  of the coil equal to 160  $\Omega$ .

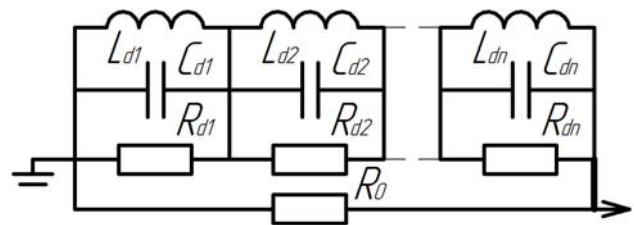


Fig. 6. A schematic diagram of the meter ( $R_d$  – damping resistor)

To achieve the minimum rise time of the transient response  $T_{riseTime}$  it is necessary to choose  $R_d$  equal to  $(\pi/2)\rho$ . If it is necessary to obtain an aperiodic transient response, it is recommended to take  $R_d \leq \rho$ .

The created meter is a coil wound around a ferromagnetic core of rectangular cross section. The meter's parameters are as follows: coil resistance 2  $\Omega$ , parasitic capacitance 100 pF, inductance 5  $\mu\text{H}$ .

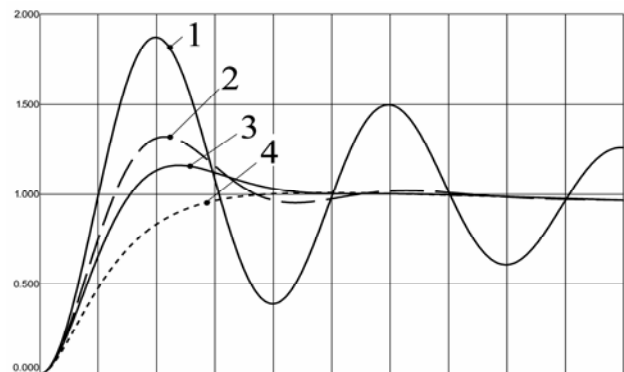


Fig. 7. Results of calculation of the transient response of the meter (1 –  $R_d$  is absent; 2 –  $R_d = (\pi/2)\rho$ ; 3 –  $R_d = \rho$ ; 4 –  $R_d = \rho/2$ ; the vertical scale – relative units; the horizontal scale – 5 ns/cell)

Fig. 8 shows the signal from the meter (2) obtained at measuring the current of rectangular shape (1) with the front of 5 ns. The load resistance  $R_d$  is taken equal to  $(\pi/2)\rho$ .

Fig. 9 shows the waveforms of signals of the sensor and shunt with resistance of 75  $\Omega$  installed on the rod lightning receiver. The current of crown is measured.

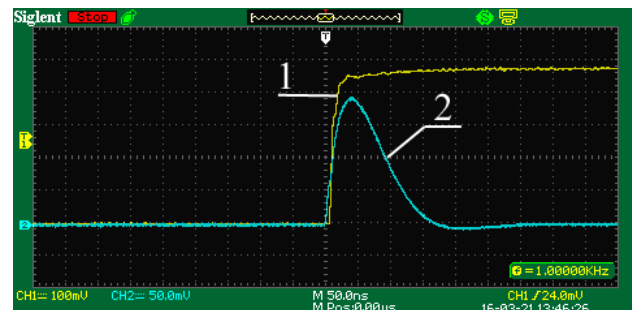


Fig. 8. Waveforms of the output voltage from the meter (1 – signal from the generator; 2 – output signal from the meter)

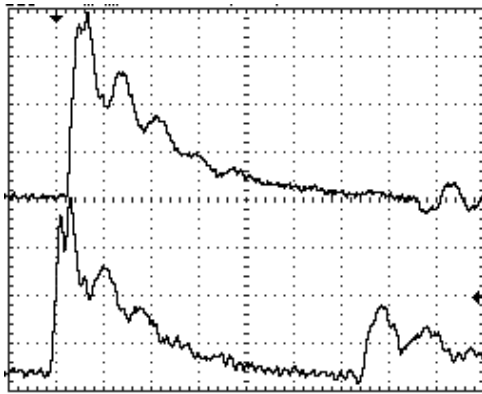


Fig. 9. Waveforms of output voltage signals from the shunt and the meter (channel 1: the vertical scale – 100 mV/cell; the horizontal scale – 50 ns/cell; channel 2: the vertical scale – 20 mV/cell; horizontal scale – 50 ns/cell)

From Fig. 8: measuring sensitivity – 8 mV/mA, front duration of the output signal – 25 ns.

**3. Peculiarities of the sensor's design.** Two identical converters connected opposite can be used to increase the sensitivity and noise immunity of the meter. If inductive transducer is loaded to a small resistance, in fact, a short-circuit mode, there is the opposite field close to the largest value of the measured field and displaces the measured magnetic field from volume of the inductive transducer. If one uses two transducers and during the measurements to set them close one to each other, the output signal from the transducers will be substantially less than if they were located relative to each other at a long distance. To solve this problem, there are several ways: the use of small cross-section wires to increase own resistance and, as a result, reduce the current in the coil, or separation of the transducers and removing them from each other until mutual inductance of meters will negligible.

The author thanks Yu.S. Nemchenko for help in the research. The work was carried out in the frame of the project 0115U000611 funded by the Ministry of Education and Science of Ukraine.

How to cite this article:

Shalamov S.P. An induction sensor for measuring currents of nanosecond range. *Electrical engineering & electromechanics*, 2016, no.5, pp. 57-60. doi: 10.20998/2074-272X.2016.5.09.

**Conclusions.**

1. A measuring complex is developed for thunderstorm danger warning system which includes an induction transmitter. To increase the sensitivity of the induction-type sensors a circuit of their serial connection is used. Such a connection of sensors has the property of a long line in the case that the measured field wavelength is comparable to the electrical length of the coil conductor.

2. Calculations of transient response for different values of the electrical parameters of the created sensor elements are carried out.

3. A sample of the induction-type sensor for measuring currents in the nanosecond range is manufactured. Duration of its transient response increase is 25 ns and sensitivity – 8 mV/mA.

REFERENCES

1. Chernuhin A. Yu., Kniaziev V.V. The streamer corona from the rod lightning arresters. *East European Scientific Journal*, 2016, no.6, iss.2, pp. 39-46. (Rus).
2. Nemchenko Yu.S., Lesnoy I.P., Lantushko B.N, Knyazev V.V. Metrological maintenance operation of high-voltage pulse electric discharge equipment. *Bulletin of NTU «KhPI»*, 2004, no.35, pp. 29-54. (Rus).
3. Shalamov S.P. Measurement of pulsed magnetic fields. *Bulletin of NTU «KhPI»*, 2014, no.50, pp. 161-168. (Rus).
4. Nemchenko Yu.S. Wideband means of measuring pulse magnetic fields. *Bulletin of NTU «KhPI»*, 2007, no.20, pp. 132-146. (Rus).
5. Nemchenko Yu.S., Shalamov S.P. Induction converter pulsed magnetic field of lightning. *Bulletin of NTU «KhPI»*, 2015, no.20, pp. 99-108. (Rus).
6. Power Electronic Measurements Ltd (PEM). Available at: <http://www.pemuk.com/publications.aspx> (Accessed 08 April 2013).

Received 10.09.2016

S.P. Shalamov, Postgraduate Student,  
National Technical University «Kharkiv Polytechnic Institute»,  
21, Kyrpychova Str., Kharkiv, 61002, Ukraine.  
phone +38 057 7076010, e-mail: shalamov.stas@i.ua

A.V. Voloshko, Ya.S. Bederak

## A METHOD OF AUTOMATIC DETERMINATION OF THE NUMBER OF THE ELECTRICAL MOTORS SIMULTANEOUSLY WORKING IN GROUP

*Purpose. Propose a method of automatic determination of the number of operating high voltage electric motors in the group of the same type based on the determination and analysis of the account data of power consumption, obtained from of electric power meters installed at the connection of motors. Results. The algorithm of the automatic determination program for the number of working in the same group of electric motors, which is based on the determination of the motor power minimum value at which it is considered on, was developed. Originality. For the first time a method of automatic determination of the number of working of the same type high-voltage motors group was proposed. Practical value. Obtained results may be used for the introduction of an automated accounting run of each motor, calculating the parameters of the equivalent induction motor or a synchronous motor. References 7, figures 2.*

*Key words: induction and synchronous motors, group of the same type of electric motors, running.*

*Целью исследований является разработка метода автоматического определения количества работающих электродвигателей высокого напряжения в группе однотипных на основе определения и анализа учетных данных электропотребления, полученных с приборов учета электроэнергии, установленных на присоединениях электродвигателей. Разработан алгоритм программы автоматического определения количества работающих электродвигателей в группе однотипных. Полученные результаты могут быть использованы для внедрения автоматизированного ведения учета пробега каждого электродвигателя, расчета параметров эквивалентного асинхронного (АД) или синхронного двигателя (СД), которые в свою очередь в дальнейшем могут применяться для оценки эффективности работы группы одинаковых электродвигателей, проведение расчетов статической и динамической устойчивости системы электроснабжения промышленного предприятия, содержащей АД или СД. Библ. 7, рис. 2.*

*Ключевые слова: асинхронный и синхронный электродвигатели, группа однотипных электродвигателей, пробег.*

**Introduction.** In practice it is impossible to determine the number of network-connected induction (IM) or synchronous (SM) electric motors in a group of one kind without visual control.

Often in electrical equipment to tires 6-10 kV multiple IM are connected, in general, of different type and capacity. In assessing the resulting impact of motors on the short-circuit current at the site of injury it is advisable to replace all the motors or some of their groups by one equivalent IM. For the equivalentation of IM the following parameters are input: the nominal value of the rated power  $P_{nom}$ ; the relative value of starting current  $I_n$ ; multiplicity of starting  $m_n$  and maximum  $m_{max}$  torques. In the formulas for calculating the equivalent IM they use their number of similar IM  $n$  in the group [1]. For example, nominal active power of equivalent IM  $P_{nom.ekv}$  of the group consisting of  $n$  motors of rated power of each  $P_{nom}$  is determined by the formula [1]:

$$P_{nom.ekv} = \sum_{j=1}^n P_{nom}$$

Therefore, to obtain accurate value of equivalent IM parameters we must determine accurately their number. A similar problem is and for groups of SM, too.

**The goal of the work** is to develop a method for automatically determining the number of working electrical motors of voltage of 6 kV in a group of similar ones based on the definition and analysis of power consumption credential obtained from electricity meters installed on electric connections of motors. The feature of electric motors operation is that the load on their shaft to vary widely. So, when operating multiple IM or SM simultaneously, simple definition of electric power

consumption by the group of motors makes it impossible to determine the number of working motors

**Analysis of recent investigations and publications.** Parameters of equivalent IM or SM (power factor, load factor, maximum and starting torques, parameters of equivalent circuit, etc.) are used to assess the effectiveness of the group of the same IM or SM, calculation of static and dynamic stability of electricity supply systems of industrial enterprises which includes IM or SM, periodic component of the inrush current, to determine residual voltage on tires of power supply during self of IM or SM and other problems. [1]. The theoretical basis of operation modes of IM and SM are developed by Syromiatnikov I.A. in [2]. Problems of stability of a single IM or SM as well as their groups are considered in works by Gurevich I.E. [1]. The tasks of increasing the stability of IM and SM at a temporary loss of power are considered in works by Fishman V.S [3], Tidzhev M.O. [4], Mikhalev S.V. [5].

### Material and results of investigations.

IM or SM can operate in a wide range of power capacity from non-working power to nominal one. Therefore, it is necessary to select a minimum value as a percentage of the nominal power which would be indicative of the on state of each motor. According to [2] the current non-working course of IM  $I_{is}$  is calculated as follows:

$$I_{is} = I_{nom} \cdot \left( \sin \varphi_{nom} - \frac{\cos \varphi_{nom}}{b_{nom} + \sqrt{b_{nom}^2 - 1}} \right),$$

where  $I_{nom}$  is the rated current of the electrical motor;  $\cos \varphi_{nom}$  is the rated power factor;  $b_{nom}$  is the ratio of

maximum torque to nominal one on the IM shaft Calculations carried out by IM catalogue data ( $\cos\varphi_{nom} = 0.8...0.92$ ;  $b_{nom} = 2...2.7$ ) suggest that the minimal value  $I_{is}$  is in the range of 25 % to 40 % of the rated current of the motor. The minimum load on the SM shaft ranges from 35% to 50% of the rated current of the motor [2]. These ratios are used to determine the working state of IM or SM.

To determine the number of IM or SM in is proposed to set in relay compartment on each connecting of high-voltage electric motors (Fig. 1) electronic multifunction electricity meters that measure in real-time current, voltage, power, frequency and other parameters of the power consumption mode, and ensure the collection, processing and data transfer in the automated system of control and accounting of electrical energy (ASCAE) in real time.

To the tires of 6 kV of the substation (Fig. 1) three identical high voltages IM are connected. On each IM connection an electronic energy meter is installed. All meters are connected to ASCAE of the enterprise. The values of active power of the electric motor are collected in real time.

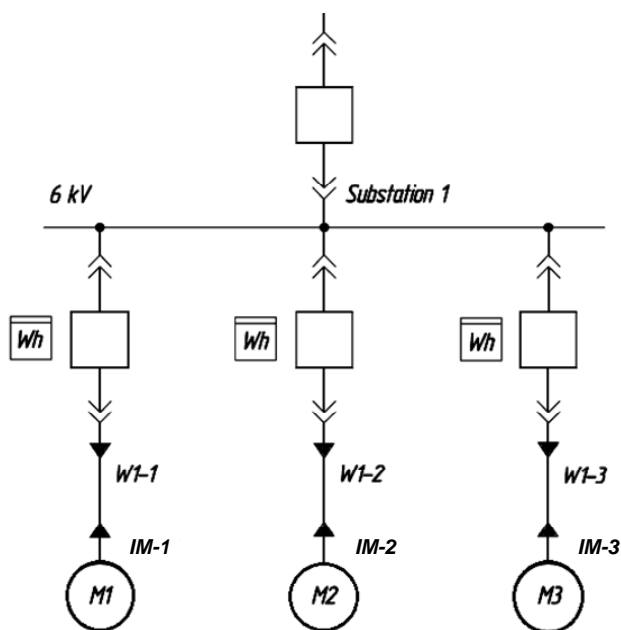


Fig. 1

The measured values after checking for faults are used in specially developed software controlling the IM or SM on state. When the load on each IM or SM more than 25 % of the rated power  $P_{nom}$  of the electric motor, it is deemed to be on.

An algorithm of the software that monitors switched IM or SM is shown in Fig. 2.

The software operates as follows.

The initial data are the number of mounted  $m$  and operating  $n$  electric motors measured by the meter value of power of the  $i$ -th motor and its rated power. The counter of the software starts counting from 0. When the load on the first electric motor exceeds  $0.25P_{nom}$  of the motor, it is deemed to be on. The same procedure is followed with each next motor. When and  $i = m$ , then the

procedure completes its operation and as output the calculated number of operating electric motors in the group of the same type is obtained.

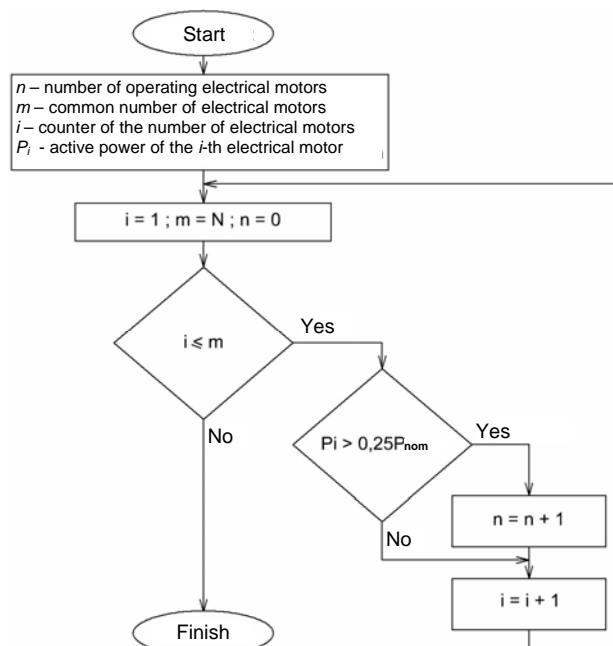


Fig. 2. Algorithm of software controlling the on state of the IM or SM

The analysis showed that knowledge of the number of operated IM and SM be used and for another task of maintenance and repair of electric motors (calculation of each electric motor run, calculate of its overhaul period).

Journal of IM and SM run allows to obtain the exact duration of its operation which guarantees the overhaul period. For timely repair of main electrical equipment it is necessary to fill in an electrical motors run journal at the enterprise. In [6] it is proposed to fill in the run journal electronically but not defined ways of the solution to this problem. Calculation of the number of on motors in real-time makes it possible to solve this problem with minimal cost of labor staff.

To calculate the run of each electric motor it is necessary to know if it operates at the current moment of time or not. So, when in real-time there is information about on state of each IM or SM it is possible to determine the number of hours they operated for any length of time (month, year). By these data turnaround time is calculated. Called turnaround time is interval of equipment operation between next running repair which is measured by the number of hours operated [7].

### Conclusions.

1. A method for determining the number of operated IM or SM in a group of similar electric motors by controlling the load on each motor connection by electricity meters which allows for a wide range of varying load on the motor shaft is developed.

2. The resulting value of the number of operating IM or SM may be used for automated accounting of each motor run, determine the parameters of the equivalent IM or SM which are used for the calculation of static or dynamic stability of electricity supply systems in the industry, evaluating the effectiveness of the group of identical

motors, periodic component of inrush current, determine the residual voltages on the tires of the power source at self, etc.

#### REFERENCES

1. Gurevich I.E., Libova L.E., Khachatryan E.A. *Ustoichivost' nagruzki elektricheskikh system* [Resistance load of electrical systems]. Moscow, Energoizdat Publ., 1981. 208 p. (Rus).
2. Syromiatnikov I.A. *Rezhimy raboty asinkhronnykh i sinkhronnykh dvigatelei* [Modes of operation of asynchronous and synchronous motors]. Moscow, Energoatomizdat Publ., 1984. 240 p. (Rus).
3. Fishman V.S. Voltage dips in the grids of industrial enterprises. Minimizing the consequences. *Electrical Engineering News*, 2004, no.6. Available at: <http://www.news.elteh.ru/arh/2004/30/05.php>. (accessed 18.05.2016). (Rus).
4. Tidzhiev M.O. Improving of the sustainability of continuous production processes during short power failure. *Tez. dokl. Vserossiisk. nauk.-tekhn. konf. «Elektropotreblenie, energosberezhenie, elektrooborudovanie»* [Abstracts of All-Russia Sci.- Techn. Conf. «Power consumption, energy saving, electrical equipment»]. Russia, Orenburg, 2003. pp. 28-29. (Rus).
5. Poliakhov N.D., Mikhalev S.V. Enhancing of the stability of synchronous motors with a short-term power loss. *Proceedings of ETU «LETI»*, 2012. no.10, pp. 62-68. (Rus).
6. Voloshko A.V., Bederak Ya.S. The monitoring system of mode power consumption of the industrial enterprise. *Energy: economics, technology, ecology*, 2014, no.4, pp. 50-59. (Rus).

#### How to cite this article:

Voloshko A.V., Bederak Ya.S. A method of automatic determination of the number of the electrical motors simultaneously working in group. *Electrical engineering & electromechanics*, 2016, no.5, pp. 61-63. doi: 10.20998/2074-272X.2016.5.10.

7. *Sistema tekhnicheskogo obsluzhivaniia i remonta tekhnologicheskogo i teploenergeticheskogo oborudovaniia khimicheskikh predpriiatii Ministerstva promyshlennoi politiki Ukrainy. Utverzhdena Pervym zamestitelem Ministra promyshlennosti Ukrainy A. G. Golubovym 25 apreliia 1996 g.* [System of maintenance and repair of heat and power technology equipment on chemical enterprises in the Ministry of Industrial Policy of Ukraine. Approved by the First Deputy of Minister of Industry of Ukraine A.G. Golubov on 25 April 1996]. Kyiv, 1998. 432 p. (Rus).

Received 25.05.2016

A.V. Voloshko<sup>1</sup>, Doctor of Technical Science, Professor,  
Ya.S. Bederak<sup>2</sup>, Engineer,

<sup>1</sup> National Technical University of Ukraine «Kyiv Polytechnic Institute»,

37, Prospect Peremohy, Kyiv-56, 03056, Ukraine.  
phone +380 47 2392979, e-mail: ei@uch.net

<sup>2</sup> PJSC «AZOT»,

72, Pervomayskaya Str., Cherkassy, 18014, Ukraine.

## LOW VOLTAGE NETWORKS INSULATION MONITORING WITH TWO AND THREE VOLTMETER READOUTS METHODS

**Purpose.** In the paper there are described methods of two and three voltmeter readouts for insulation resistance periodic measurement in live DC and AC/DC IT networks. A new measuring method for AC/DC networks is proposed. Application of a novel algorithm for shortening of measurement cycle is explained. **Methodology.** All methods of two and three voltmeter readouts consist in connection of a resistor and measurement of mean value of network's fixed point-to-ground voltages. **Results.** A new algorithm implemented in KDZ-3 device enables determination of steady-state voltage of a DC network's pole much faster than in other exploited systems. **Originality.** In author's modification of two voltmeter readouts method, line-to-ground voltage mean value is measured at AC side of AC/DC network. This innovation has not been applied for implementation of periodic insulation monitoring in AC/DC IT networks yet. **Practical value.** The use of author's innovation will allow to execute measurements at AC side of AC/DC IT networks which might be necessary if rectifier's output circuits are unavailable. Shortening of measurement cycle duration of two or three voltmeter readouts method's is of great importance in networks with high capacitance. References 8, figures 7.

**Key words:** low voltage DC, AC/DC IT networks, insulation resistance, methods of two and three voltmeter readouts.

*Представлено применение методов контроля изоляции сетей низкого напряжения постоянного и двойного рода тока с помощью вольтметра и резистора. Приведены формулы для вычисления сопротивления изоляции методами двух и трех отсчетов вольтметра. Предложен новый способ двух отсчетов вольтметра для сетей двойного рода тока. Представлена модификация рассматриваемых методов, ограничивающая их основной недостаток – длительность переходного процесса.* Библ. 8, рис. 7.

**Ключевые слова:** сети низкого напряжения постоянного и двойного рода тока, сопротивление изоляции, метод двух и трех отсчетов вольтметра.

**Introduction.** Insulation monitoring is of great importance for safe and reliable operation of low voltage DC and AC/DC IT networks. Periodic measurement of insulation resistance is commonly performed there with use of resistor and voltmeter. These methods are referred to as two or three voltmeter readouts (readings) methods. Three voltmeter readouts method is commonly applied in automated insulation monitoring and fault location systems. Two voltmeter readouts method is simpler and produces smaller changes of conductor-to-ground voltages, but it does not enable to determine insulation resistances of single conductors.

**Goal of the paper.** Technical literature is short of detailed information on voltmeter readouts methods. Ways to limit the main shortcoming of these methods, i.e. long duration of transient process following connection of a resistor, have not been proposed yet. Therefore goal of the paper is to deliver a review of voltmeter readouts methods as well as to present an innovative algorithm for shortening duration of measurement. Also a new measuring procedure is proposed by author which expands capability of two voltmeter readouts method.

### Two voltmeter readouts method. DC networks.

Simplest method of insulation equivalent resistance determination  $R_i$  of DC networks exploits an additional resistor  $R_0$ . For this purpose steady-state voltages of a selected pole-to-ground are measured before and after connection of the resistor between this pole and ground (Fig. 1).

Network's insulation equivalent resistance  $R_i$  substituting resistors  $R_1, R_2$  connected in parallel is given by formula

$$R_i = R_0 \cdot \frac{(U_{21} - U_{22}) \cdot R_V}{U_{22} \cdot (R_0 + R_V) - U_{21} \cdot R_0}, \quad (1)$$

where  $U_{21}$  is voltage of pole (-) without resistor  $R_0$ ,

$U_{22}$  – voltage of pole (-) with resistor  $R_0$ . If voltmeter resistance  $R_V$  meets condition  $R_V \gg R_0$ , then simpler formula is valid

$$R_i = R_0 \cdot \frac{U_{21} - U_{22}}{U_{22}}. \quad (2)$$

Insulation resistances of single poles are

$$R_1 = R_i \cdot \frac{E}{U_{21}} \text{ and } R_2 = R_i \cdot \frac{E}{E - U_{21}},$$

but voltage of network source  $E$  must be known.

An indispensable condition for application of this method is constant value of  $E$ . This requirement is in force also for other methods of voltmeter readouts.

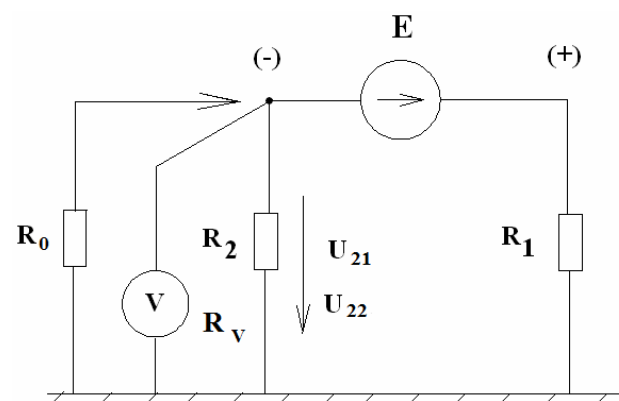


Fig. 1 Method of insulation equivalent resistance determination of DC network:  $E$  – voltage of network source,  $R_1, R_2$  – insulation resistances of pole (+) and (-),  $R_0$  – resistance of additional resistor,  $R_V$  – voltmeter resistance,  $U_{21}, U_{22}$  – voltages of pole (-) before and after connection of resistor  $R_0$

### AC/DC networks.

Two voltmeter readouts method can also be used in AC/DC IT system where diode rectifiers are fed by AC network (Fig. 2). This system integrates galvanically connected AC and DC circuits, both of them separated from ground (IT). Depending on location of voltage measurement two methods are available.

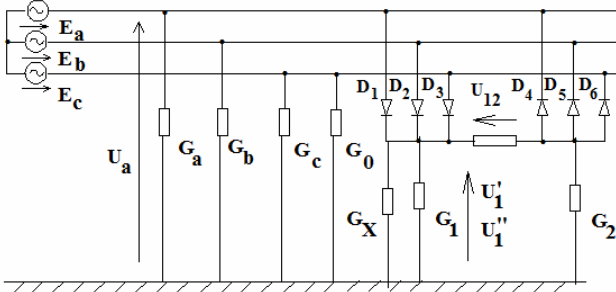


Fig. 2. AC/DC system equivalent scheme for determination of insulation resistance with use of additional conductances:  $E_a, E_b, E_c$  – source phase voltages,  $G_a, G_b, G_c$  – phase insulation conductances,  $G_0, G_X$  – additional conductances,  $U'_1, U''_1$  – positive pole voltages without and with conductance  $G_X$ ,  $U_a$  – phase «a» voltage

The first method exploits measurement of rectifier's selected pole-to-ground voltage. In this case (see Fig. 2 without  $G_0$ ) mean values of this voltage are measured in normal operation  $U'_1$  (without  $G_X$ ) and with  $G_X$  connected between this pole and ground  $U''_1$ . According to [3] these voltages are equal to

$$U'_1 = \frac{G_a + G_b + G_c + 2 \cdot G_2}{G_a + G_b + G_c + G_1 + G_2} \cdot \frac{U_{12}}{2},$$

$$U''_1 = \frac{G_a + G_b + G_c + 2 \cdot G_2}{G_a + G_b + G_c + G_1 + G_2 + G_X} \cdot \frac{U_{12}}{2}. \quad (3)$$

From equations (3) sought parameter  $R_i = \frac{1}{G_a + G_b + G_c + G_1 + G_2}$  (insulation equivalent resistance of the whole AC/DC system) is obtained

$$R_i = R_X \cdot \frac{U'_1 - U''_1}{U'_1}. \quad (4)$$

In the second method (proposed by author) [2] there is exploited characteristic feature of AC/DC networks, i.e. mean value of phase voltage at AC side may be different from zero according to formula

$$U_{a-mean} = \frac{G_1 - G_2}{G_a + G_b + G_c + G_1 + G_2} \cdot \frac{U_{12}}{2}. \quad (5)$$

AC side conductor-to-ground mean voltage is measured in two states: (1)  $U_{a1-mean}$  in normal working condition, (2)  $U_{a2-mean}$  with an additional resistor  $R_0 = 1/G_0$  connected between any conductor at AC side and ground. The sought parameter  $G_i$  can be calculated from formula

$$R_i = R_0 \cdot \frac{U_{a1-mean} - U_{a2-mean}}{U_{a2-mean}}, \quad (6)$$

which follows directly from (5).

If AC side-to-ground voltage has zero mean value (due to  $G_1 = G_2$ ), then one of  $G_1$  or  $G_2$  conductances should be changed by grounding artificially any selected

pole through a test conductance  $G_X$ . Then both steps of the procedure described above are executed, after which the test conductance  $G_X$  should be removed. The sought parameter  $R_i$  is given as

$$R_i = \frac{1}{\frac{1}{R_0} \cdot \frac{U_{a2-mean}}{U_{a1-mean} - U_{a2-mean}} - \frac{1}{R_X}}. \quad (7)$$

It should be noted that due to use of mean values of voltages, network-to-ground capacitances do not influence insulation measurement result. Therefore they are not shown at the drawing. It must be also underlined that formulas (2), (4) and (7) for two voltmeter readouts method in both types of monitored networks are identical.

### Three voltmeter readouts method.

#### DC networks.

Three voltmeter readouts method consists of successive measurement of three voltages with voltmeter with internal resistance  $R_V$  and connected in parallel additional resistor  $R_0$ . These steady-state voltages are measured between:  $U_{12}$  – poles of DC network;  $U_1$  – pole (+) and ground;  $U_2$  – pole (-) and ground (Fig. 3).

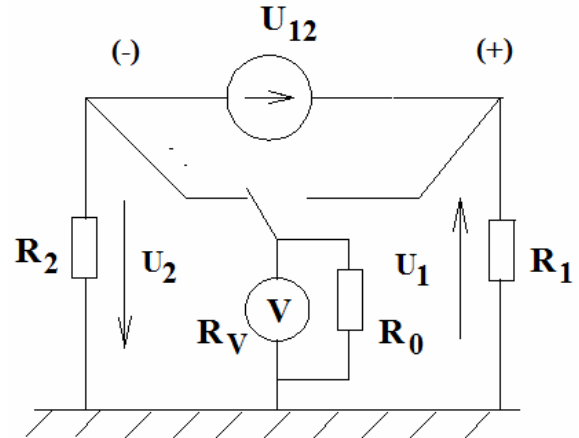


Fig. 3. Determination of DC network insulation resistance with three voltmeter readouts method:  $U_{12}$  – network source voltage,  $R_1, R_2$  – insulation resistance of pole (+) and (-),  $R_0$  – additional resistance,  $R_V$  – voltmeter resistance,  $U_1$  – pole (+) voltage with connected  $R_0$  and  $R_V$ ,  $U_2$  – pole (-) voltage with connected  $R_0$  and  $R_V$

Sought value of insulation equivalent resistance  $R_i$  is obtained from formula:

$$R_i = \frac{R_1 \cdot R_2}{R_1 + R_2} = \frac{R_0 \cdot R_V}{R_0 + R_V} \cdot \frac{U_{12} - U_1 - U_2}{U_1 + U_2}. \quad (8)$$

Resistances of single poles insulation  $R_1$  and  $R_2$  are:

$$R_1 = \frac{R_0 \cdot R_V}{R_0 + R_V} \cdot \frac{U_{12} - U_1 - U_2}{U_2}; \quad (9)$$

$$R_2 = \frac{R_0 \cdot R_V}{R_0 + R_V} \cdot \frac{U_{12} - U_1 - U_2}{U_1}. \quad (10)$$

It can be proved that formulas (8) – (10) are true also if voltages are measured not at the poles but at any two points of the battery situated at opposite sides of its «zero» point (i.e. point with zero potential against ground).

### AC/DC IT networks

In AC/DC IT networks three voltmeter readouts method is applied for determination of equivalent resistance of the whole system in the same way as in DC networks [4] (Fig. 3). Also in this case steady-state voltages are measured between:  $U_{12}$  – poles of DC network;  $U_1$  – pole (+) and ground;  $U_2$  – pole (–) and ground. Sought value of insulation equivalent resistance  $R_i$  is obtained from formula (8).

### Examples of commercial application of three voltmeter readouts method.

**DC networks insulation monitor (isometer) MD-04 type.** MD-04 device (manufactured by C&T Elmech, Poland) [5] (Fig. 4) is designated for periodic measurement of insulation resistance of DC networks with nominal voltage 24, 48, 60, 110 or 220 V. The device is fed by voltage of the monitored network. The measurement is executed periodically by connection of an additional resistor between ground and each pole in succession.



Fig. 4

Examples of waveforms of negative pole-to-ground voltage recorded during MD-04 monitor operation are shown in Fig. 5,*a,b*. It should be noted that in both cases steady-state voltages are equal because insulation resistances are the same. After each measurement cycle of both pole-to-ground voltages, a microprocessor system calculates insulation resistances which are displayed at the front panel. The isometer executes the measurement automatically immediately after connection to the network, periodically or after manual start. Measurement and calculation takes from 4 seconds to 2 minutes. In case of insulation deterioration an alarm LED is lit, then the measurement is repeated twice. If this result is confirmed, an output relay closes its contact. Information on the isometer status and insulation condition is issued also by RS485. Measurement error of MD-04 monitor does not exceed  $\pm 10\%$ .

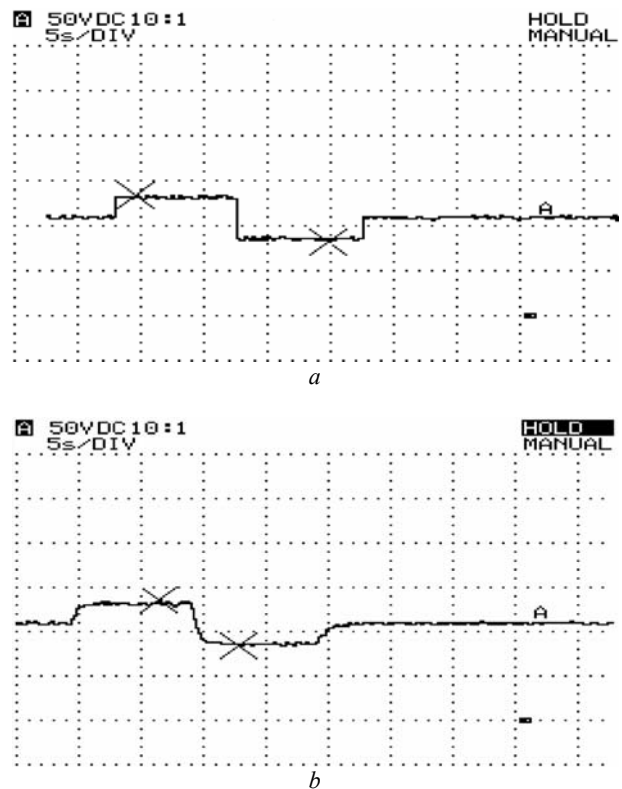


Fig. 5. Waveforms of negative pole-to-ground voltage recorded (from 85 to 130 V) during MD-04 monitor's operation: *a)*  $R_i=45$  k $\Omega$ ,  $C_i=0$   $\mu$ F, *b)*  $R_i=45$  k $\Omega$ ,  $C_i=20$   $\mu$ F

At Fig. 5,*b* attention should be turned to transient process duration about 2 s caused by network capacitance. Prolonged duration of this process (for high insulation capacitances and resistances it may reach even few tens of seconds) is the main shortcoming of all methods of voltmeter readouts. For its limitation a novel calculation algorithm has been implemented in insulation monitors KDZ-3 type (manufactured by ZPrAE, Poland) [6, 7]. It makes it possible to determine already at initial stage the final steady-state voltage of any pole. For this purpose voltages are measured at the initial moment  $y_0$  ( $t_0=0$ ) and in successive moments  $y_1$  ( $t_1$ ) and  $y_2$  ( $t_2$ ) (Fig. 6).

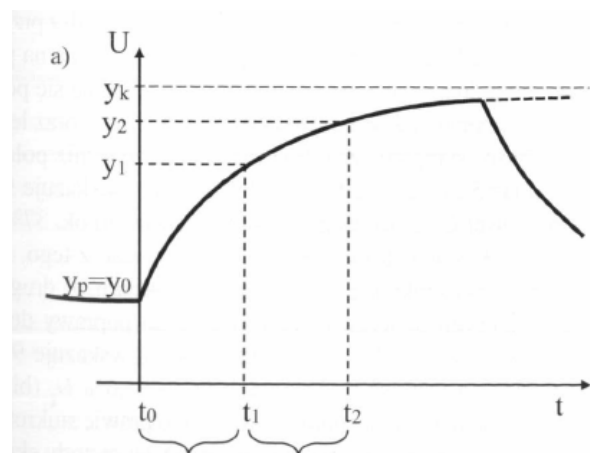


Fig. 6. Initial part of DC network pole voltage function following connection of an additional resistor to the other pole

The following formula for this voltage  $y(t)$  is assumed

$$y(t) = y_k - (y_k - y_0)e^{-\frac{t}{T}}, \quad (11)$$

where  $y_k$ ,  $T$  – unknown parameters.

From the following equations, assuming  $t_2=2t_1$

$$y_1 = y_k - (y_k - y_0)e^{-\frac{t_1}{T}};$$

$$y_2 = y_k - (y_k - y_0)e^{-\frac{t_2}{T}}, \quad (12)$$

the sought parameter – steady-state voltage  $y_k$  – is obtained

$$y_k = \frac{y_0 \cdot y_2 - y_1^2}{y_2 - 2 \cdot y_1 + y_0}. \quad (13)$$

In this way duration of measuring cycle of devices exploiting two or three voltmeter readout method can be shortened even by 90 %.

**DC networks insulation monitor RKI1 type.** RKI1 device (manufactured by «Cheboksary Electric Apparatus Plant», Russia) [8] (Fig. 7) is designated for insulation monitoring of 110 and 220 V auxiliary circuits. Its functions include measurement of DC network's voltage and its variation as well as insulation resistance (equivalent and for single poles). The device fulfills signaling of parameters values outside set threshold limits. Its internal resistance is 100 kΩ. Relative error of insulation resistance measurement does not exceed 1 %. Monitor can measure insulation resistance with two methods: a) three voltmeter readouts method, b) two voltmeter readouts method – insulation resistance is determined based on measured voltages of both poles against ground which are proportional to respective insulation resistances. Of course in any network there may be used only one monitor exploiting this method. This requirement relates also to monitor MD-04.



Fig. 7

### Conclusions.

1. Thanks to simplicity voltmeter readouts methods of insulation resistance measurement are commonly applied

### How to cite this article:

Olszowiec P. Low voltage networks insulation monitoring with two and three voltmeter readouts methods. *Electrical engineering & electromechanics*, 2016, no.5, pp. 64-67. doi: 10.20998/2074-272X.2016.5.11.

in DC and AC DC IT networks. Their alternative are techniques based on imposition of test signal from an auxiliary voltage source.

2. Application of two or three voltmeter readouts methods causes variation of conductor-to-ground voltages. However the same effect is caused by devices exploiting imposition of test signals.

3. There is presented a novel method of limiting operation time of devices exploiting two or three voltmeter readouts methods.

4. There is presented a modified method of two voltmeter readouts for AC/DC networks. Its novelty consists in measurement of mean value of phase voltage at AC side of diode rectifier.

### REFERENCES

- Ivanov E., Diachkov A. How to measure correctly insulation resistance of electric systems? *Electrical engineering news*, 2002, no.1(13). Available at: <http://www.news.elteh.ru/arh/2002/13/22.php> (Accessed 12 September 2015). (Rus).
- Olszowiec P. *Insulation Measurement and Supervision in Live AC and DC Unearthed Systems*. Lecture Notes in Electrical Engineering, 2nd edition. Springer, 2014. doi: 10.1007/978-3-642-29755-7.
- Olszowiec P. O wyznaczaniu napięć trójfazowych prostowników diodowych. *Wiadomości Elektrotechniczne*, 2015, vol.1, no.10, pp. 33-34. (Pol). doi: 10.15199/74.2015.10.8.
- Ivanov E., Diachkov A. How to measure correctly insulation resistance of electric systems? *Electrical engineering news*, 2002, no.2(14). Available at: <http://www.news.elteh.ru/arh/2002/14/26.php> (Accessed 12 September 2015). (Rus).
- Available at: <http://www.elmech.pl/spis-produktow-2> (Accessed 25 May 2016). (Pol).
- KDZ-3. *System kontroli i lokalizacji doziemien*. Available at: [www.zprae.pl/download.php?file=pub/File/KDZ-3.pdf](http://www.zprae.pl/download.php?file=pub/File/KDZ-3.pdf) (Accessed 10 July 2015). (Pol).
- Opara A. Zastosowanie ekstrapolacji nieliniowej w systemie pomiaru i lokalizacji doziemienia. *Wiadomości Elektrotechniczne*, 2016, vol.1, no.2, pp. 24-27. (Pol). doi: 10.15199/74.2016.2.5.
- Rele kontrolia tsepei postoiannogo toka RKI-1. Tekhnicheskoe rukovodstvo po ekspluatatsii* [The relay DC control circuits РКI-1. Technical Manual]. Available at: [http://srza.ru/uploads/catalog/srz\\_rki.pdf](http://srza.ru/uploads/catalog/srz_rki.pdf) (Accessed 22 September 2015). (Rus).

Received 13.08.2016

Piotr Olszowiec, MSc., Electrical Engineer,  
Elporem i Elpoautomatyka Spółka z o.o.,  
28-200 Staszow, ul. Wschodnia 10/51, Poland,  
phone +48 606 613976,  
e-mail: olpio@o2.pl

S.S. Rudenko

## REQUIREMENTS FOR DEVICES FOR VERTICAL ELECTRICAL SOUNDING OF SOIL AT DIAGNOSTICS OF GROUNDING DEVICES

*Purpose.* Creation the scientific requirements for technical characteristics of equipment for vertical electrical sounding based on the electrophysical characteristics of the soil of energy objects with the different voltage classes. *Methodology.* In work used statistical methods for the analysis database of results the soil sounding and for receiving distribution of largest size of the grounding system. To determine the required range of measurement and permissible value of circuit resistance applied the mathematical description of the electromagnetic field to calculate the apparent resistivity of the soil and the Wenner method of calculating the resistance of a vertical electrode. Also, in work used elements of probability theory to creation the stochastic correlation between device parameters and characteristics object of the research. *Results.* In the paper found that in the most severe cases (when the depth of sounding is the three maximal diagonal of grounding) at 99% energy objects in Ukraine the lower limit of resistance measurement for the respective classes of voltage must be no more than 1.3 milliohms to 35 kV, 0.6 mOhm to 110 kV, 0.5 milliohms to 150 kV, 0.1 mOhm for  $\geq 220$  kV. Also it proved that the measurement equipment for vertical electrical sounding when performing electromagnetic diagnostics of grounding system the power facilities Ukraine with 35-750 kV voltage class for all possible values of soil resistivity should be with limit of measurement from 0.1 mOhm to 7.2 kOhm and resistance measuring circuit to 66 kOhm. *Originality.* For the first time used a statistical approach to evaluate the optimal technical requirements for equipment the soils resistivity when performing diagnostics of grounding systems energy objects of Ukraine. The results obtained in this work, establish the probabilistic dependence of the technical characteristics of measuring equipment from the actual depth of sounding in Wenner's configuration (the distance between electrodes) and from the voltage class of object. *Practical value.* The obtained results allow depending on the specific parameters of the object optimally select the equipment. This technique allows you to create a range of equipments with optimal cost and overall dimensions depending on the region (considering to a significant spread of values of soil resistivity) and on the voltage class of investigated object. References 7, tables 6, figures 5.

*Key words:* vertical electrical sounding, grounding device, soil, energy object, technical requirements for equipment.

*На основе анализа статистической базы данных по зондированию грунта и диагностики состояния заземляющего устройства сформулированы требования и созданы рекомендации относительно выбора приборов для проведения вертикального электрического зондирования в зависимости от класса напряжения энергообъекта и доверительной вероятности. Доказана эффективность выбора приборов на основе оптимальных требований.* Библ. 7, табл. 6, рис. 5.

*Ключевые слова:* вертикальное электрическое зондирование, заземляющее устройство, грунт, энергообъект, технические требования к приборам.

**Problem definition.** The purpose of the vertical electrical sounding (VES) is to determine the parameters of the geoelectric structure – the electrophysical characteristics (EPC) of soil: the number of layers, their electrical resistivity (ER) and the power, by injecting an AC generator and measuring the voltage drop on a specific section of the ground surface [1-3]. The value of the spacing of the current and potential electrodes is caused by the type of installation and the required depth sensing. Apparatus, method and interpretation of VES means are well-developed, both theoretically and practically in the framework of the geological survey [4]. Indicated EPC are the initial data for the determination of normalized electrical parameters of the grounding device (GD) as at the design stage as well as during its operation [5]. Therefore, the determination of their maximum reliability is one of the most important tasks.

Devices for VES are characterized by electrical parameters, technological ones (stand-alone or utility power, the ability to connect to a PC, moisture), as well as dimensions and weight parameters. As part of the electromagnetic state diagnostics of the grounding device (EMD GD) during the VES basic parameters of measuring instruments are: accuracy class, measuring range, sensitivity, permissible value of the current and potential resistance circuit, the operating frequency. It is

also an important requirement for them is the portability and battery life, as the VES is carried out, as a rule, far away from the mains. The operating frequency is selected close to the industry, but differs from it in order to minimize the influence of electromagnetic field working electrical currents. During the VES in the implementation of EMD GD, the parameters of the instrument requirements (measurement limit, sensitivity, and the permissible value of the measuring circuit resistance), and in general the possibility of using a particular installation of VES are determined by the value of the ER and geometrical dimensions of the GD [1, 5] but in the literature clear requirements to instruments not available. Therefore, the development of technical requirements for appliances for VES depending on the ER of the soil and the required depth sensing is an urgent task. The development of these requirements it is proposed to implement on the basis of the analysis of the database of VES in different regions of Ukraine near the locations of power plants voltage class of 35 – 750 kV [5]. Availability of statistical data on the soil ER and GD sizes allow us to make a probabilistic assessment of the applicability of the instrument in their technical specifications it should be taken into account that the voltage class is crucial for electrical installations' geometrical sizes.

© S.S. Rudenko

**The goal of the paper** is the development of science-based requirements for specifications of equipment for VES in the framework of the EMD GD based on the grounds of the EPC of soils of energy objects of Ukraine of different voltage classes.

In the formation of the requirements for appliances for VES at EMD GD it is necessary to solve a number of tasks in the following sequence:

- to perform statistical analysis of ER of layers of soil in order to determine the probability that the value of the resistivity in one of the confidence intervals;
- to assess the required depth sensing;
- to carry put statistical analysis of GD sizes for different voltage classes;
- to determine the allowable values of the lower and upper limits of the measurement device;
- to define the permissible value of the resistance measuring circuit;
- to formulate a generalized technical requirements for devices.

**1. Statistical analysis of soil layers ER.** For the statistical analysis of the resistivity we used VES results database compiled for 7 years from 2007 to 2014 [6]. These data are shown in Table 1.

Table 1

	ER ratio			Layer ER $\rho_i, \Omega \cdot m$			ER power	
	$\rho_1/\rho_2$	$\rho_2/\rho_3$	$\rho_1/\rho_3$	$\rho_1$	$\rho_2$	$\rho_3$	$h_1, m$	$h_2, m$
Average	5.12	6.03	12.11	183.9	136.93	67.63	0.79	5.46
Median	2.75	2.29	4.31	75	29	18	0.45	4
Mode	5	0.5	2	200	15	30	0.2	10
Minimum	0.017	0.004	0.018	3.0	1.2	0.3	0.02	0.01
Maximum	83.3	416.7	625	8700	7000	9000	10	35
Sample	612	592	592	612	612	592	612	592

Analysis of the data presented in Table 1 [6] the minimum and maximum values of ER of various layers showed that VES devices for the diagnosis of the state of the memory must be capable of measuring the ER of 0.3 to 9000  $\Omega \cdot m$ .

Such a wide range of measurements, taking into account the large spread required probing depth (it varies from a few dozen to several hundred meters, depending on the GD size of the object), leads to an increase in the unit cost and large overall dimensions, as well as to the need for close venue VES network or mobile power source (e.g., a diesel generator). However, it should be noted that these values are the limit and cover 100 % of the soil and substations of all voltage classes of Ukraine. In order to assess the optimal requirements, use the histogram distribution EPC values given in Table 1 from [6]. Their analysis showed that when considering ER values as a single set of data and calculating a relative particular, are within  $\rho \in [3; 9000] \Omega \cdot m$  covers 99 % of the cases,  $\rho \in [3; 2000] \Omega \cdot m$  – 98% of cases, and  $\rho \in [5.5; 2000] \Omega \cdot m$  – 97 % which may allow to significantly reduce the required range of measured values. Common power (99 % of cases) lies within  $h_1 \in [0.1; 7.5] m$  and  $h_2 \in [0.5; 30] m$ .

## 2. Estimation of the required depth of sounding.

In [1, 7] that the memory size actually defines the required depth sensing. However, as the literature review,

carried out in [6], a clear correlation between the size of the memory and the required depth sensing is absent, and the dependence of the current electrodes separation was obtained by S.I. Kostruba only for installation of Burgsdorf in 1983:

$$L_C = K_{VES} \sqrt{S}, \quad (1)$$

where  $L_C$  is the distance between current electrodes, m;  $K_{VES}$  is the geometrical size ratio between the substation and the electrode spacing varying from 1 to 3 depending on the GD area ( $S$ ),  $m^2$ .

However, the literature has not shown a similar or some other relationship to other VES systems (in particular for the most common installation of Wenner).

In [1, 7] presented some data on the required depth sensing obtained by studying the dependence of the resistance of the GD of its area. From the analysis of these works should be concluded on the need to determine the structure of the soil, at least, at a depth of about  $\sqrt{S}$  at the ER decrease with increasing depth, while increasing the ER of the underlying layers – need information about the structure of the soil at a depth of a few  $\sqrt{S}$ .

In addition, an important practical issue is the depth of the installation, i.e. dependence of the depth sensing the magnitude of a particular installation spacing current (or potential) electrodes. Probing depth different settings VES studied more than eighty years since the 30s of the last century, and the matter has undergone three major stages of development: in the 30s they engaged K. Schlumberger, in 1970 – Roy and Apparo and the last stage of the research which began in the late 80s from the work by Barker and lasting until now [3]. The main methods of estimating the depth at the moment are: the dependence of the current density on the depth of the derivative of the current density on the depth Merrick function and the use of formulas by Dar-Zarrouk. This current density is taken to decrease its value up to 50-80 %, and their extremes are taken according to the derivative of the current density on the depth and Merrick function. According to the data given in the works of geophysical prospecting depth for installation of Schlumberger (Wenner installation is actually a special case) in a fraction of the spacing of current electrodes varies from  $1/10 L_C$  to  $1/2.5 L_C$  while in the literature [3] there are cases where the depth is reduced to  $1/200 L_C$  under the influence and relations of macroanisotropy of ER layers.

So, in works devoted to carrying out VES for the design or diagnose memory, there are ambiguous information about the desired depth sensing which should be determined by the GD size and soil ER. In the frame of this work will take the assumption, the traditional practice of VES for the design and GD diagnostic: the probing depth setting Wenner is one-third the value of the current spacing of the electrodes (ie, inter-electrode distance between the two nearest electrodes  $L_e$ ). Given that the issue required depth sensing still does not have a unique solution, and in the practice of EMD GD for storage of measurement and touch voltage resistance is used the distance  $(1.5 - 3) D$ , where the  $D$  is the longest diagonal of the GD then consider the required probing depth of

between one and three  $D$ . Therefore, is fair to the Wenner installation expression is fair:

$$L_e = K_{VES}D, \quad (2)$$

where  $K_{VES}$  ranges from 1 to 3.

Here, the expression (1) to determine the distance between the current electrodes, respectively, will be:

$$L_C = 3K_{VES}D. \quad (3)$$

**3. Statistical analysis of GD sizes for different voltage classes.** The size of the memory, as indicated earlier, defines the required depth sensing EMD during EMD GD. Fig. 1 shows a histogram of the percentage distribution  $f$  of the greatest diagonal  $D$  to 963 electrical substations, diagnostics of memory which was conducted between 1999 and 2015.

From the analysis of Fig. 1 shows that 58 % of the highest value storage diagonal lies within 10-100 m, i.e. spacing value in the application of current electrodes Wenner installation according to (3) is 90 – 900 m (with the coefficient of spacing  $K_{VES} = 3$ ) and can be realized in practice.

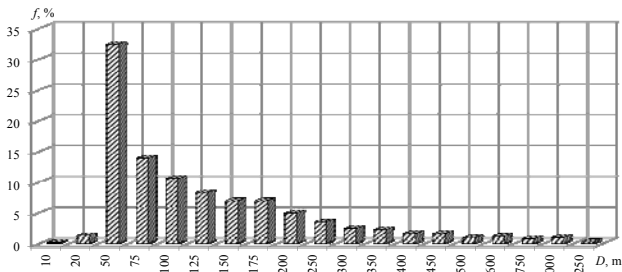


Fig. 1. The probability density of the largest diagonal values in the GD of energy objects of Ukraine

Fig. 2 – 5 shows the histograms of the percentage distribution of the length of the largest diagonal  $f$  for different voltage classes.

Based on the histograms shown in Fig. 2–4, in Table 2 presents data on the maximum size of the GD diagonals for the confidence interval with a confidence level  $\gamma$  equal to 50 %, 80 %, 90 % and 99 % of the patients of power corresponding to the voltage class. For example, this means that 80% of substations voltage class  $U = 110$  kV have maximum diagonal GD length  $D \leq 160$  m and  $D \leq 250$  m for 99% of the specified voltage class substations.

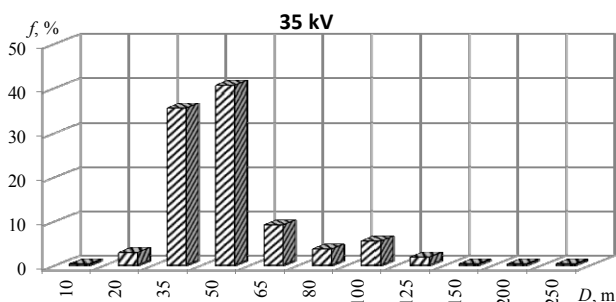


Fig. 2. The probability density of the maximum GD size of substation 35 kV

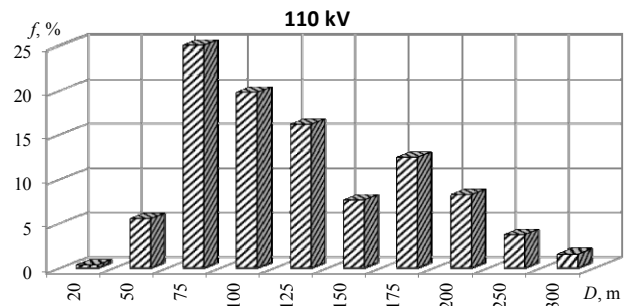


Fig. 3. The probability density of the maximum GD size of substation 110 kV

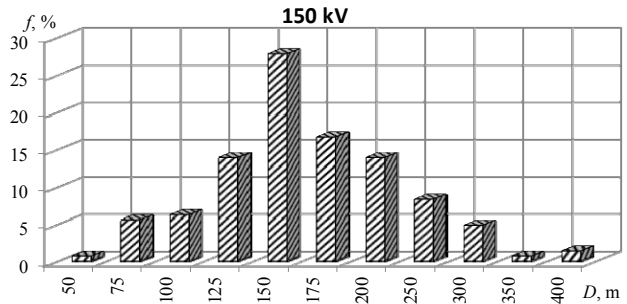


Fig. 4. The probability density of the maximum GD size of substation 150 kV

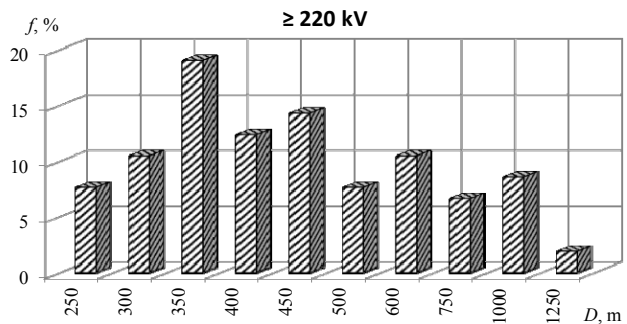


Fig. 5. The probability density of the maximum GD size of substation 220 kV and more

Table 2

Voltage class $U, \text{ kV}$	Maximal GD size $D, \text{ m}$			
	$\gamma = 50 \%$	$\gamma = 80 \%$	$\gamma = 90 \%$	$\gamma = 99 \%$
35	40	50	80	125
110	100	160	185	250
150	140	180	220	350
$\geq 220$	400	600	800	1250

So, these values indicate a large variation of maximum GD diagonal of power to different voltage class but at the same time allow us to estimate the permissible value of the lower limit of measurement at the level of trust to the appropriate voltage class.

**4. Determination of permissible values of the lower and upper limits of the measurement of the device.** The value of the apparent ER will always be in the range between the minimum and the maximum value of resistivity geoelectric layer structure, so to determine the technical requirements for appliances for VES by Wenner installation and their probabilistic estimation of use defined previously [6] statistics data of EPC. From the expression for apparent ER of the Wenner installation and

the distance between the electrodes, as measured by the limit value of  $R_{lim}$  resistance can be written as:

$$R_{lim} = \frac{\rho}{2\pi L_e}, \quad (4)$$

where  $\rho$  is the apparent ER value.

To determine the lower limit of measurement using the minimum value of the ER of the first layer taken from Table 1 and the electrode spacing  $L_e$  calculated by the formula (2), where the length of the largest GD diagonal  $D$  from the Table 2 with the appropriate level of trust.

Table 3 shows the values of the lower limit of measurement device  $R_{l,lim}$  at  $K_{VES} = 1-3$ . The values obtained show that, for example, during the VES on probing depth equal to one diagonal of a energy object ( $K_{VES} = 1$ ) for 90 % of energy objects of lass of 110 kV the device must have the lower measuring limit of no more than 2.6 m $\Omega$ .

So, these data allow us to estimate the applicability of the instrument for carrying out VES on its lower measuring limit of energy object for different voltage classes based on three variables taken electrode spacing.

Table 3

Confidence level $\gamma, \%$	Electrode spacing $L_e$	Lower measuring limit of the device $R_{l,lim}, m\Omega$ for classes of voltage:			
		$U=35$ kV	$U=110$ kV	$U=150$ kV	$U \geq 220$ kV
50 %	3D	4	1.6	1.1	0.4
	2D	6	2.4	1.7	0.6
	D	11.9	4.8	3.4	1.2
80 %	3D	3.2	1	0.9	0.3
	2D	4.8	1.5	1.3	0.4
	D	9.5	3	2.7	0.8
90 %	3D	2	0.9	0.7	0.2
	2D	3	1.3	1.1	0.3
	D	6	2.6	2.2	0.6
99 %	3D	1.3	0.6	0.5	0.1
	2D	1.9	1	0.7	0.2
	D	3.8	1.9	1.4	0.4

To determine the upper limit of measurement and resistance measurement electrodes specify multiple confidence levels (95%, 99.9% and 100%) and consider the corresponding values of the resistivity of the first layer:

- 600  $\Omega \cdot m$  (confidence interval covers up to 95%  $\rho_1$  values);
- 2000  $\Omega \cdot m$  (confidence interval covers up to 99.9 %  $\rho_1$  values);
- 9000  $\Omega \cdot m$  (confidence interval covers 100%  $\rho_1$  values)

To determine the upper limit of measurement should consider the lowest value of distance between electrodes  $L_e$ , which is determined by the condition  $L_e \geq 3t$  and  $L_e \geq 6r_0$ , where  $t$  and  $r_0$  are the immersion depth and radius of the electrode, respectively. Generally, in the practice of EMD GD  $L_{min}$  is 0.2 m. The results of

calculation using (2), with the ER value and the specified confidence levels are shown in Table 4.

Obtained results establish a probabilistic dependence for the upper and lower limits of the measuring devices for VES at EMD GD energy objects of Ukraine, and a substantial increase shown in Table 3, 4 limits (that are usually associated with a significant increase in capacity and device cost) in most cases can be not justified.

Table 4

Soil ER $\rho_{max}, \Omega \cdot m$	Confidence level $\gamma, \%$	Lower limit of the measurement of the device $R_{up,lim}, \Omega$
600	95.0	480
2000	99.9	1600
9000	100.0	7170

**5. Determination of the permissible resistance value measuring device circuit.** When finding an acceptable resistance to current and potential circuits consider the electrode radius  $r_0$  plunged vertically into the soil to depth  $t$ . Since the limit value is the maximum possible resistance of the electrode, the assessment should be performed for the maximum value of the ER of a homogeneous soil, wherein the electrode is known [7] has a resistance of:

$$R_e = \frac{\rho}{2\pi t} \ln \frac{2t}{r_0}, \quad (5)$$

In carrying out VES in the frame of EMD GD by the author together with employees of the Scientific-&-Research Planning-&-Design Institute «Lightning» NTU «KhPI» electrodes are used on a radius of 4 mm to 10 mm, which are clogged in the measuring process to a depth of 50 to 500 mm.

Calculation results of the measurement electrode resistance for ER and confidence intervals from Table 4 are shown in Table 5.

Table 5

Soil ER, $\rho, \Omega \cdot m$	Confidence level $\gamma, \%$	Electrode immersion depth $t, m$	Measuring electrode resistance $R_e, \Omega$ :	
			at $r_0 = 4$ mm	at $r_0 = 10$ mm
600	95.0	0.05	6150	4400
		0.1	3740	2870
		0.2	2200	1770
		0.3	1600	1310
		0.5	1060	880
2000	99.9	0.05	20500	14660
		0.1	12460	9540
		0.2	7330	5880
		0.3	5320	4350
		0.5	3520	2940
9000	100.0	0.05	92220	65970
		0.1	56040	42920
		0.2	32990	26420
		0.3	23930	19550
		0.5	15820	13200

The data obtained allow to formulate the requirements for permissible resistance measuring circuit devices for VES, as well as take into account the diameter of the measuring electrodes and the depth of their dives.

**7. The formulation of generalized technical requirements for devices.** Assessing the characteristics of the device, it is possible to draw a conclusion about the applicability of it with a certain probability based on the longest diagonal of the memory and the voltage of a power class. To do this, move on to the confidence level  $\gamma$  confidence probability  $P$  (the male probability).  $P$  is obtained based on the properties of the probability of the occurrence of three independent events, and is determined according to the expression (6):

$$P = P_{l.lim} \cdot P_{up.lim} \cdot P_C, \quad (6)$$

where  $P_{l.lim}$  is the confidence level based on the Table 3;  $P_{up.lim}$  is the confidence level based on the Table 4;  $P_C$  is the confidence level based on the Table 5.

Table 6 shows the generalized probabilistic requirements for device performance for VES. When this is taken into account that in practice during VES measuring electrodes immersion depth  $t$  on average is 0.2 m and the resistance  $R_c$  of the measuring circuit is equal to twice the resistance  $R_e$  of the electrode from Table 5.

Table 6

Voltage class $U$ , kV	$R_c$ , k $\Omega$	$R_{up.lim}$ , k $\Omega$	$R_{l.lim}$ , m $\Omega$		
			$L_e = D$	$L_e = 2D$	$L_e = 3D$
At confidence probability $P = 0.791$					
35	15	1.6	9.5	4.8	3.2
110			3.0	1.5	1.0
150			2.7	1.3	0.9
$\geq 220$			0.8	0.4	0.3
At confidence probability $P = 0.899$					
35	66	6.4	6.0	3.0	1.3
110			2.6	1.3	0.6
150			2.2	1.1	0.5
$\geq 220$			0.6	0.3	0.1
At confidence probability $P = 0.99$					
35	66	7.2	3.8	1.9	1.3
110			1.9	1.0	0.6
150			1.4	0.7	0.5
$\geq 220$			0.4	0.2	0.1

Consider the example of the use of Table 6 in selecting the device for carrying out VES for substation of the voltage class:

1)  $U = 35$  kV. As initial data we set:

- the value of the electrode distance equal to three GD diagonals ( $L_e = 3D$ );
- confidence level  $P = 0.99$ .

Consequently, for the substations of 35 kV voltage class with the given parameters of the instrument must have a measuring range from 1.3 m $\Omega$  to 7.2 k $\Omega$  and allow the resistance of current and potential circuits up to 66 k $\Omega$ .

2)  $U = 150$  kV. As initial data we set:

- the value of the electrode distance equal to two GD diagonals ( $L_e = 2D$ );
- confidence level  $P = 0.899$ .

Consequently, for the substations of 150 kV voltage class with the given parameters of the instrument must have a measuring range from 1.1 m $\Omega$  to 6.4 k $\Omega$  and allow the resistance of current and potential circuits up to 66 k $\Omega$ .

### Conclusions.

In the paper for the first time a statistical approach for estimating the optimal specifications for devices for the purpose of VES EMD GD of energy objects of Ukraine is used. Obtained earlier statistics on soil resistivity allowed to divide the significant range resistivity values into the range of confidence intervals characterized by a confidence level of engulfing.

To estimate the required depth of sounding, in the paper the statistical distribution of length of the largest GD diagonal by voltage classes is analyzed. Dependencies of lower limit value on the voltage class of devices and the level of confidence desired value are determined based on the required depth of sounding and statistics on the largest GD diagonal of existing energy objects of Ukraine, and the upper limit value – based on the statistical distribution of the ER for the appropriate level of confidence.

The results obtained in this work establish a probabilistic link between the technical characteristics of the device, the actual depth of sounding by Wenner installation (interelectrode distance) and the voltage class of the object. This allows the device to select optimally the device depending on the particular characteristics of the object, as an incorrect choice of device leads to the impossibility of full measurement or a significant increase in cost and weight and size characteristics of the device. It is found that the device for VES in the frame of EMD GD state of energy objects of Ukraine to encompass all classes of voltage and the possible values of soil ER should have the limit of measurement from 0.1 m $\Omega$  to 7.2 k $\Omega$  and allow the resistance of the measurement circuit to 66 k $\Omega$ .

### REFERENCES

1. Averbukh M.A. Zabusov V.V., Pantelev V.I. *Sistemnyi podkhod k otsenke zazemliayushchikh setei elektroustanovok severnykh promyshlennykh kompleksov* [The systematic approach to the evaluation of grounding grids electrical installations of northern industrial complexes]. Krasnoyarsk, Siberian Federal University Publ., 2009. 164 p. (Rus).
2. Hördt A. *Praktikumsunterlagen Angewandte Geophysik und Geoelektrik*. Technische Universität Braunschweig Institut für Geophysik und extraterrestrische Physik, 2006. 11 p. (Ger).
3. Shevnin V.A., Kolesnikov W.P. Rating depth VES for the uniform and layered medium. *Electronic Journal «GEORazrez»*, 2011, no.1(8), pp. 1-9. Available at: [http://www.georazrez.ru/download/2011/08/Shevnin-Otchenka\\_glubinnosti\\_VEZ.pdf](http://www.georazrez.ru/download/2011/08/Shevnin-Otchenka_glubinnosti_VEZ.pdf) (Accessed 10 November 2013). (Rus).
4. Kolesnikov V.P. *Osnovy interpretatsii elektricheskikh zondirovaniy* [Fundamentals of electrical sounding interpretation]. Moscow, Nauchnyi mir Publ., 2007. 248 p. (Rus).

5. Koliushko G.M., Koliushko D.G., Rudenko S.S. On the problem of increasing computation accuracy for rated parameters of active electrical installation ground grids. *Electrical engineering & electromechanics*, 2014, no.4, pp. 65-70. (Rus). doi: **10.20998/2074-272X.2014.4.13**.

6. Koliushko D.G., Rudenko S.S., Koliushko G.M. Analysis of electrophysical characteristics of grounds in the vicinity electrical substation of Ukraine. *Electrical engineering & electromechanics*, 2015, no.3, pp. 67-72. (Rus). doi: **10.20998/2074-272X.2015.3.10**.

7. Borisov R.K., Gorshkov A.V., Zharkov Y.V. *Zazemliaiushchie ustroystva elektroustanovok (trebovaniia normativnykh dokumentov, raschet, projektirovanie, konstruksii,*

*sooruzhenie): spravochnik* [The grounding system of electrical installations (regulatory requirements, calculation, design, construction: Handbook]. Moscow, Publishing House MEI, 2013. 360 p. (Rus).

*Received 02.09.2016*

*S.S. Rudenko, Postgraduate Student, Research Associate, National Technical University «Kharkiv Polytechnic Institute», 21, Kyrpychova Str., Kharkiv, 61002, Ukraine.  
e-mail: nio5\_molniya@ukr.net*

*How to cite this article:*

Rudenko S.S. Requirements for devices for vertical electrical sounding of soil at diagnostics of grounding devices. *Electrical engineering & electromechanics*, 2016, no.5, pp. 68-73. doi: 10.20998/2074-272X.2016.5.12.